TAMPEREEN TEKNILLINEN YLIOPISTO
TAMPERE UNIVERSITY OF TECHNOLOGY

Han He

New Additive Manufacturing Solutions and Novel Materials for UHF RFID Tag Antennas and Interconnections

Julkaisu 1550 • Publication 1550

Tampere 2018

Tampereen teknillinen yliopisto. Julkaisu 1550
Tampere University of Technology. Publication 1550

Han He

New Additive Manufacturing Solutions and Novel Materials for UHF RFID Tag Antennas and Interconnections

Thesis for the degree of Doctor of Science in Technology to be presented with due permission for public examination and criticism in Sähkötalo Building, Auditorium SA203, at Tampere University of Technology, on the 1st of June 2018, at 12 noon.

Tampereen teknillinen yliopisto - Tampere University of Technology
Tampere 2018

Doctoral candidate:	Han He Wireless Identification and Sensing Systems Research Group The Faculty of Biomedical Sciences and Engineering Tampere University of Technology Finland
Supervisor:	Johanna Virkki, Adj. Prof. Wireless Identification and Sensing Systems Research Group The Faculty of Biomedical Sciences and Engineering Tampere University of Technology Finland
Instructor:	Leena Ukkonen, Prof. Wireless Identification and Sensing Systems Research Group The Faculty of Biomedical Sciences and Engineering Tampere University of Technology Finland
Pre-examiners:	Maurizio Bozzi, Prof. Department of Electrical, computer and biomedical enginnering University of Pavia Italy Steve Beeby, Prof. Department of Electronics and Computer Science University of Southampton United Kingdom
Opponent:	Ville Viikari, Associate Prof. Department of Electronics and Nanoengineering Aalto University Finland

ISBN 978-952-15-4150-6 (printed)
ISBN 978-952-15-4162-9 (PDF)
ISSN 1459-2045

New Additive Manufacturing Solutions and Novel Materials for UHF RFID Tag Antennas and Interconnections

Han He

Abstract

In the recent years, radio-frequency identification (RFID) technology has been widely integrated into application in modern society including as a successor to the barcode in the retail supply chain, remote monitoring, automatic detection, and smart healthcare. Looking ahead to the future, our lives will be surrounded by small, embedded and wireless electronic devices that provide information about everything for everybody in real time. At the core of this vision lie two key concepts: ubiquitous sensing and the Internet of Things. RFID technology is seen as one of the most prominent technologies of today for the implementation of these future concepts.

This thesis investigates the possibilities of additive manufacturing (AM) methods, mainly inkjet printing and 3D direct write (DW) dispensing, for establishing passive ultra high frequency (UHF) RFID tags on novel eco-friendly substrates, such as paper, cardboard, wood, and textile. The selected conductive inks in this study are nanoparticle silver ink, graphene ink, and stretchable silver ink.

The antenna-integrated circuit (IC) interconnection is also important in this study, as it influences the wireless performance of RFID tags by changing the impedance matching between IC and antenna. Thus, RFID tags with various IC attachment methods were evaluated to achieve better wireless performance and to simplify the fabrication procedure. In addition, considering the actual use situations, the possibilities of RFID tags used in harsh environment, such as in high moisture conditions and under repeated mechanical stress, are very essential in this study.

Most of the established tags in the thesis show excellent performance and achieve the requirements of a number of modern RFID applications, such as supply chain, wearable biomedical sensing, and environment monitoring. Especially promising are the stretchable 3D DW dispensed silver tags, which have a peak read range of around 10 meters. When integrated into textile substrates, these tags have countless applications in wearable wireless platforms. Moreover, environment-friendly graphene inks show great potential to replace the high cost metallic inks in the future, as graphene tags showed excellent wireless performance in this study. In terms of reliability, by using a stretchable silver conductor, 3D DW dispensed RFID tags with embroidered antenna-IC interconnections achieve high reliability during actual use situations of clothing-integrated wireless components, including stretching, bending and immersing.

The results of this thesis create new paths for the production of environment-friendly electronics. They are especially useful for the RFID sector, as well as clothing-integrated electronics, wireless sensor networks (WSN), and packaging industries.

Preface

This study was carried out at Wireless Identification and Sensing Systems (WISE) Research Group at BioMediTech Institute and Faculty of Biomedical Sciences and Engineering at Tampere University of Technology (TUT) during the years 2016 – 2018. The research was funded by the Finnish Funding Agency for Technology and Innovation (TEKES) and the Academy of Finland. The work is also supported by Nokia Foundation. The financial support is gratefully acknowledged.

I would like to thank my supervisor, Adjunct Prof. Johanna Virkki, for her support and guidance throughout my work. I also wish to sincerely thank my instructor, Prof. Leena Ukkonen, for her support. I would like to express my sincere gratitude to Prof. Hiroshi Nishikawa at Osaka University and Prof. Liquan Chen at the Southeast University, for their support during my visiting at Osaka and Nanjing. I would like to acknowledge all my present and past co-workers in WISE lab, and also all co-authors of publications.

I wish to thank all my friends for their support and encouragements. I would like to thank my lover Chen Xiaochen for all the support, kindness and encouragement during this thesis. Most of all, I wish to thank all my parents for their unconditional love and constant support.

Tampere, January 2018

He Han

Contents

List of Symbols and Abbreviations

2D Two-Dimensional

3D Three-Dimensional

AM Additive Manufacturing

CIJ Continuous Inkjet

DOD Drop on Demand

DW Direct Writing

HF High Frequency

IC Integrated Circuit

ID Identification

IoT Internet of Things

LF Low Frequency

RF Radio Frequency

RFID Radio Frequency Identification

SEM Scanning Electron Microscopy

UHF Ultra-High Frequency

WSN Wireless Sensor Networks

PC Polycarbonate

PET Polyethylene Terephthalate

PI Polyimide

List of Publications

I. H. He, L. Sydänheimo, J. Virkki, and L. Ukkonen, “Experimental Study on Inkjet-Printed Passive UHF RFID Tags on Versatile Paper-Based Substrates’’, International Journal of Antennas and Propagation, Vol. 2016, Article ID 9265159, 8 pages, 2016, doi:10.1155/2016/9265159.

II. H. He, J. Tajima, L. Sydänheimo, H. Nishikawa, L. Ukkonen, and J. Virkki, “Inkjet-Printed Antenna-Electronics Interconnections in Passive UHF RFID Tags’’, in Proceedings of International Microwave Symposium, 4-9 June 2017, Honolulu, HI, USA, pp. 598-601.

III. H. He, M. Akbari, X. Chen, A. Nommeots-Nomm, L. Chen, L. Ukkonen, and J. Virkki, “Fabrication and Performance Evaluation of 3D–Printed Graphene Passive UHF RFID Tags on Cardboard’’, in Proceedings of Progress in Electromagnetics Research Symposium, 22-25 May 2017, St Petersburg, Russia, pp. 1-5.

IV. H. He, M. Akbari, L. Ukkonen, and J. Virkki, “Fabrication and Evaluation of 3D-Printed Heat and Photonic Cured Graphene RFID Tags on Veneer’’, in Proceedings of Applied Computational Electromagnetics Society Symposium, 1-4 August 2017, Suzhou, China, pp. 1-2.

V. H. He, M. Akbari, L. Sydänheimo, L. Ukkonen, and J. Virkki, “3D-Printed Graphene Antennas and Interconnections for Textile RFID Tags: Fabrication and Reliability towards Humidity’’, International Journal of Antennas and Propagation, Vol. 2017, Article ID 1386017, 5 pages, 2017, doi:10.1155/2017/1386017.

VI. H. He, M. Akbari, L. Sydänheimo, L. Ukkonen, and J. Virkki, “3D-Printed Graphene and Stretchable Antennas for Wearable RFID Applications’’, in Proceedings of International Symposium on Antennas and Propagation, 30 Octorber-2 November 2017, Phuket, Thailand, pp. 1-2.

VII. H. He, X. Chen, L. Ukkonen, and J. Virkki, “Textile-Integrated Three-Dimensional Printed and Embroidered Structures for Wearable Wireless Platforms’’, Textile Research Journal, published online, doi: https://doi.org/10.1177/0040517517750649.

1 Introduction

Over the past 50 years, the Internet has rapidly developed from the small intranet to the worldwide pervasive network, which can include billions of users. Nowadays, the small electronic devices embedded on physical things, extend the application of internet to everything surround us, which is called the Internet of things (IoT) [Bal17, Atz10, Gub13].

In the IoT paradigm, most of physical objects in daily life, e.g. vehicles and home appliances, as well as people, can be connected by the internet and identify themselves to other devices. RFID technology, in which information and communication systems are invisibly embedded in the environment around us, is one of the key technology of the IoT.

An RFID system contains three parts: a host, an RFID reader, and an RFID tag. An RFID tag is composed of an antenna and an application-specific integrated circuit. In the recent years, RFID tags has been widely integrated into application in modern society including as a successor to the barcode in the retail supply chain, remote monitoring, automatic detection, and smart healthcare. Thus, in this thesis novel materials and manufacturing methods for RFID tag antennas were studied, in order to achieve better wireless performance and lower cost. In addition, various types of IC attachement methods were utilized to simplify the fabrication of RFID tags and to improve the reliability of antenna-IC interconnections.

This study was mainly experimental, most of all exploring the possibilities of very eco-friendly substrate materials: paper, cardboard, wood, and textile. Novel AM solutions, including inkjet printing and 3D DW dispensing, were utilized in the study. The possibilities of three kinds of conductive inks: nanoparticle silver ink, graphene ink, and stretchable silver ink, were also studied for manufacturing passive RFID tags.

Nowadays, one of the main issues, which obstruct the RFID technology aquiring a wide range of commercial usage in identification applications, is the cost [Wan06]. Even though the prices for UHF RFID tags are not very high at the moment, beginning from few cents of Euro upwards, they do not

achieve the requirement of extremely low-cost products e. g. in the retail trade. However, cost reduction is not the main objective in the thesis. Briefly, the cost of antenna manufacturing can be decreased during two phases of tag fabrication process. Firstly, the cost can be reduced by replacing the high cost metallic ink with environment-friendly carbon-based ink. For instance, the price of Harmia nanoparticle silver ink is $7.46/g, while the cost of an inkjet printable graphene ink from Haydale Ltd. is only $0.57/g. In addition, novel IC attachment step, such as printed antenna-IC interconnections [Bjö15], can be selected to simplify the procedure as well as reduce the material cost by avoiding the usage of metallic epoxy glue. However, the exact value of the cost reduction can not be calculated in the thesis.

Moreover, considering the environment and human health, it is necessary to avoid the harmful effect from metallic ink and electronics wastage. Renewable materials and minimal need of toxic or harmful materials and chemicals is extremely desirable in future electronics [Jun15]. Thus, finding environment-friendly materials to replace the traditional harmful materials is essential [Vir15]. In this study, RFID tags were fabricated on biodegradable green substrates, such as normal copy paper and packaging cardboard, to replace the high-cost, unrenewable, traditional polymer substrate materials, including polyesters, polycarbonate (PC), Polyethylene Terephthalate (PET), and Polyimide (PI).

The possibilities of RFID tags used in harsh environments, such as in high moisture conditions and under repeated mechanical stress, are very essential to exploit the application area of RFID tags, especially for wearable RFID technology. Thus, enhancing the reliability of RFID tags was been an important and interesting topic recently [Akb16b, Chen17].

In the thesis, the achieved results show that AM methods on a number of environment-friendly substrates using conductive inks are very promising enablers of the future RFID technology. Especially, the high-performance 3D DW dispensed tags are a very interesting approach for the future green high-volume electronics manufacturing for identification and sensing applications. However, inkjet printing is also a good consideration when high-precision printing work is required and it works well with selected green substrates. Considering the environmental issues, it can be concluded that carbon-based inks, e.g. graphene, have great potential to replace the high-cost and harmful metallic inks with 3D DW dispensing. In this thesis, novel manufaturing solutions for antenna-IC interconnections were established. Also, the first reliabilty studies of RFID tags with various IC attachment methods were completed in this thesis. Based on the achieved results, the developed solutions enable more effective fabrication of eco-friendly RFID tags, especialy a combination of embroidering and 3D DW dispensing, which can achieve high read range (more than 3 meters) also in harsh environments.

The future of RFID require tagged items to report more information related to the state of the real-world objects, such as temperature, humidity, and pressure. There is thus an obvious trend to integrate RFID technology with WSN, which could be utilized widely in health monitoring, crack detection, and food quality evaluation. In this thesis, the success of fabricating green passive RFID tags, using both environment-friendly inks (e.g. graphene) and substrate materials (e.g. paper and wood), opens new doors for versatile RFID-based wireless solutions.

1.1 Objectives and scope of the thesis

The main objectives of my research are to establish new types of green passive RFID tags and to study effective additive fabrication methods and novel materials, mainly inkjet printing and 3D DW dispensing of the nanoparticle silver ink, the stretchable silver conductor and the graphene ink, to fabricate them. The objectives of the thesis are presented in detail in the following:

- To manufacture RFID components directly on environmentally friendly substrates by using additive manufacturing methods and novel conductive materials.
- To optimize the additive manufacturing methods and the use of materials to achieve simple, and fast production of wireless platforms.
- To develop antenna-IC attachment methods that enable better wireless performance and simplify the fabrication procedure.
- To examine, analyse, and improve the wireless performance and reliability of these novel green RFID components.

1.2 Structure of the thesis

This thesis outlines the work done in seven publications, which is divided into five chapters. The structure of thesis is shown in Figure 1. Chapter 1 provide a brief introduction about the aim, results, and structure of thesis, followed by author's contributions. In chapter 2, basic knowledge of RFID technology and RFID measurement methods are explained. Chapter 3 represents the properties of utilized substrate materials as well as conductive inks. Chapter 4 presents AM methods for RFID tag antennas, which are utilized in this study. Chapter 4 introduces several IC attachment methods, together with the reliability study of RFID tags using these methods. Chapter 5 concludes the thesis results and presents my ideas for future research directions of passive UHF RFID technology.

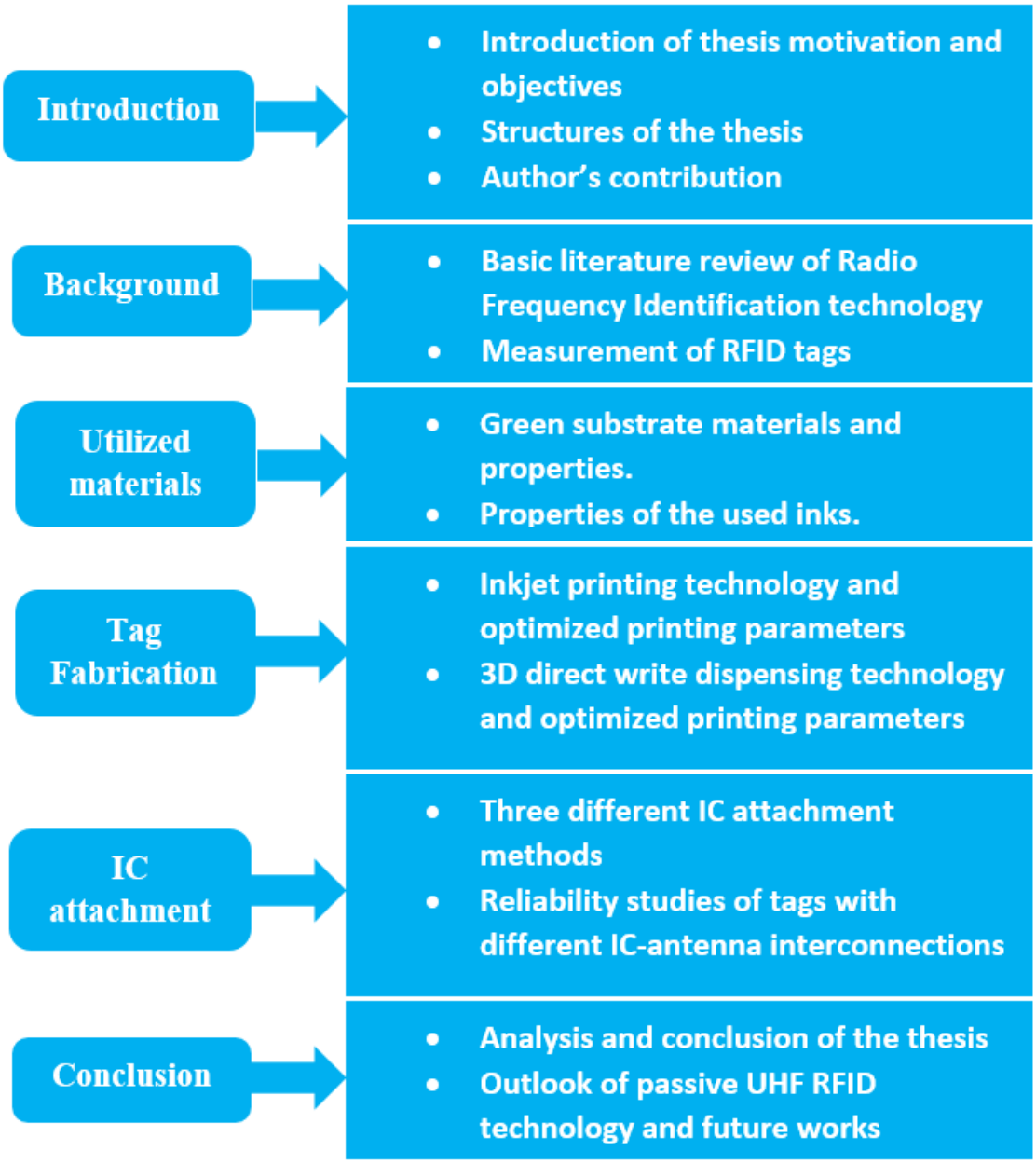

Figure 1. Structure of the thesis

1.3 Author's contribution

This thesis includes scientific outputs of seven publications. These publications are a result of collaboration. The contribution of the author is as follows:

Publication I, The author was the main contributor to this paper including: ink pre-treatments, fabrication, and the measurement. The results were analyzed by the author. The manuscript was written by author and revised with the co-authors.

Publication II, The author was the main contributor to this paper, including all fabrication steps and wireless measurements. The SEM pictures were made by Johanna Virkki in Osaka University. The author wrote the manuscript. The results were analyzed by the author. The manuscript was revised and improved with the co-authors.

Publication III, The author was the main contributor to this paper. The fabrication was done with the help of Mitra Akbari. The author completed all the measurements. The results were analyzed by the author. The author wrote the manuscript. The manuscript was revised and improved with the co-authors.

Publication IV, The author was the main contributor to this paper. The fabrication was completed with the help of Mitra Akbari. The author completed all the measurements. The results were analyzed by the author. The author wrote the manuscript. The manuscript was revised and improved with the co-authors.

Publication V, The author was the main contributor to this paper, including all fabrication steps and wireless measurements. The results were analyzed by the author. The author wrote the manuscript. The manuscript was revised and improved with the co-authors.

Publication VI, The author was the main contributor to this paper, including all fabrication steps and wireless measurements. The results were analyzed by the author. The author wrote the manuscript. The manuscript was revised and improved with the co-authors.

Publication VII, The author was the main contributor to this paper. The fabrication was done by the author. The measurement was completed with the help of Xiaochen Chen. The results were analyzed by the author. The author wrote the manuscript. The manuscript was revised and improved with the co-authors.

2 Basics of RFID Technology

Radio-frequency identification (RFID) is an automated identification method that utilizes radio communication to identify physical objects. It is advantageous over traditional optical automated identification methods, like barcode systems, in various ways: RFID technology does not require a clear line of sight to sense the devices, it can identify different objects simultaneously, it can operate in harsh or dirty environments, identification information can be updated and classified, and RFID can be automatically operated without large human labor [Wyl06]. Thanks to these features, RFID has been implemented in numerous applications such as people and animals tracking [Fry05, Vou10], access control [Rie07], toll collection [Kam10], supply chain management [Mää16], and logistics applications [Pen06].

Every RFID system consists of three main components: A tag, a reader and a host computer. A tag, which primarily includes an antenna and an integrated circuit, is attached as a label to the object to be identified. The IC stores the identification information in its memory unit. ICs can be either read-only or read-write. Read-only IC has the information stored when manufactured and cannot be altered. Read-write IC allows the user to add or write over its original information. A reader is a radio transceiver that transmits and receives signal to communicate with the tag. The host computer is connected to the reader to control the reader and process the communication data. A general configuration of a RFID system is shown in Figure 2 [Dob08].

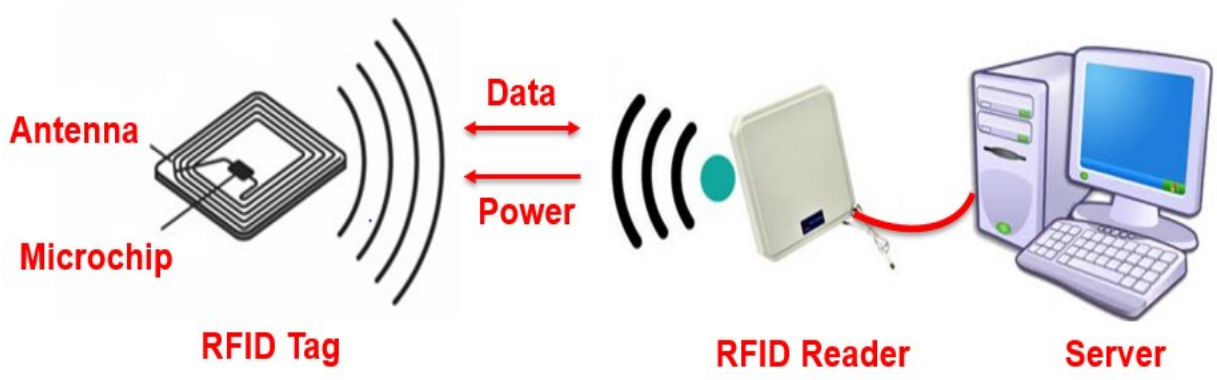

Figure 2. RFID system configuration.

When a RFID tag enters the interrogation zone of a reader, the data stored in the tag IC, e.g. manufacture data, serial numbers, and date of production, can be detected by the reader. After that, the host computer which connects to the reader, would process the data for different purposes. To describe the RFID system in an understandable way, the master-slave principle is illustrated in Figure 3. Without the electromagnetic wave from the reader, the (passive) tag is inactive, therefore, we consider the reader as a master and tag as a slave. In addition, there is also master-slave relationship between the reader and the host application. As a master, the host always sends commands and controls the reader after processing the identification information [Kar10].

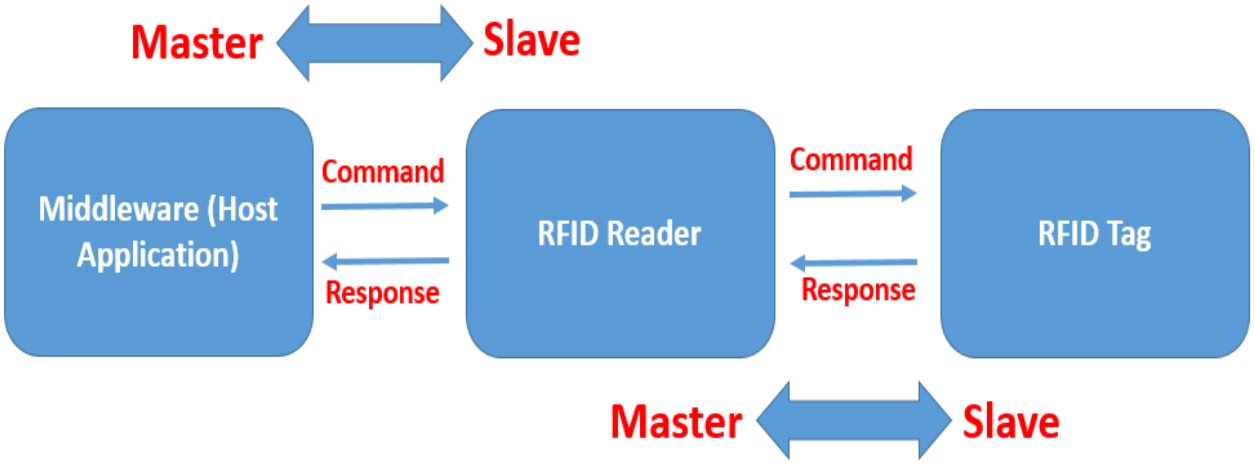

Figure 3. The master-slave principle.

2.1 Classification of RFID systems

RFID systems are typically categorized based on energy source of the tag and operation frequency band.

2.1.1 Active, semi-passive, and passive RFID tags

The tags in RFID systems can be divided as active, semi-passive and passive tags. An active tag contains its own power supply, usually an on-board battery, to provide power for the IC and transmitting data to the reader. For transmitting, it synthesizes a carrier signal by using a local oscillator and crystal reference. Then the tag is able to communicate with different frequency channels in the specified frequency band. This can reduce the interference with other tags nearby. Active tag can start the communication first without being interrogated by the reader. The operational range of an active tag is significantly greater, several kilometers in some case, due to its high transmitting power. However, it suffers from high cost, extra size, and additional maintenance for the battery [Dod08].

In semi-passive systems the tag has a battery, but it is used only to power up the IC, but the transmission module works in a passive way, utilizing the modulated backscattering principle. Like active tags, semi-passive tags suffer from additional cost, size, maintenance requirement, although they also have higher read range than passive tags [Dod08].

A passive tag is free from a local power source or its own radio transmitter. It fully relies on reader radio signal to power the tag circuitry and to send information back to the reader. The reader has to initialize the radio communication. The tag antenna receives the radio signal and induces a radio frequency voltage, which can ‘wake up’ the IC and generate the backscattered wave to the reader. Moreover, to modulate the backscattered wave with the tag information, a switchable transistor, which acts as a load to vary the input impedance, is utilized [Dod08]. The backscatter modulation principle is illustrated in Figure 4. Without any local batteries nor any conventional transmitters, the tag circuit can be extremely simple and cost is significantly reduced. Though the read range is less than that of an active tag, it still meets the requirement of many applications [Dod08].

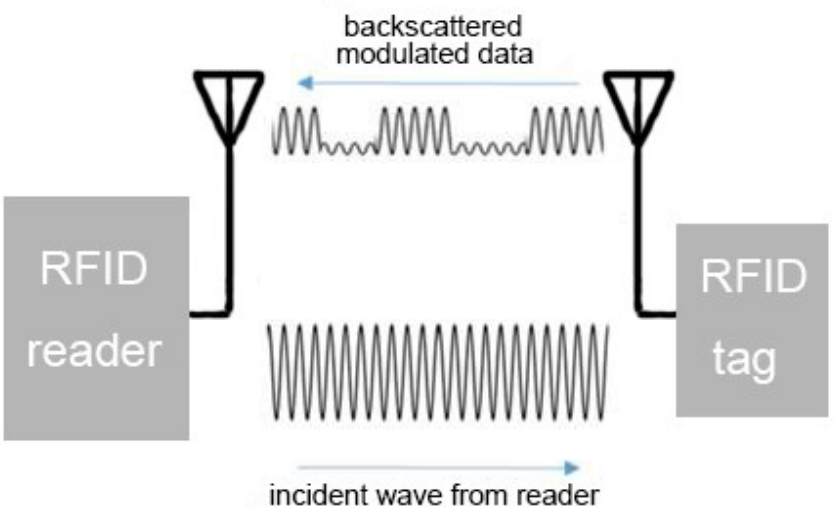

Figure 4. The backscatter modulation principle of passive RFID technology.

Passive UHF RFID tags combine the advantages of passive tags and UHF RFID systems. This simplicity leads to favorable features like light weight, compact size, long lifetime (without battery maintenance or placement). The UHF frequency also enables these tags to have longer read range than low-frequency (LF) and high-frequency (HF) tags, up to tens of meters. The small wavelength leads to reduced size of the antennas.

2.1.2 Operation frequency bands

RFID systems operate in radio frequencies. The operation frequencies vary from 100 kHz to over 5 GHz. The frequency is restricted in a narrow band for a certain RFID system. Typical frequency bands are: 125/134 kHz, 13.56 MHz, 860-960 MHz, and 2.4-2.45 GHz. The 125/134 kHz systems operate in LF band, hence they are referred to as LF systems. Readers and tags, which operate at 13.56 MHz, are called HF systems. The 860-960 MHz and 2.4-2.45 GHz bands both belong to ultra-high-frequency (UHF) band. For the convenience of distinguishing these two, readers operate in 860-960 MHz are characterized as UHF systems and 2.4-2.45 GHz systems are known as microwave systems.

Electromagnetic waves travel in vacuum at the speed of light, $c = 3*10^8$ m/s. The wavelength of an electromagnetic wave with frequency f in vacuum, λ is defined as: $\lambda = c/f$. The wavelengths in RFID systems typically range from 2000 m to 12 cm. The antenna sizes are usually about 0.01-1 m. In LF systems and HF systems, the wavelength is much larger than the antenna size. The reader antenna and tag antenna are inductively coupled. On the other hand, in UHF systems and microwave systems, the antennas are radiatively coupled. In inductively coupled systems, the available energy

from the reader antenna concentrates in the near field of the antenna, a very close region near the antenna. In radiatively coupled system, the reader and tag communicate in the far field. One significant difference between these two is that an inductively coupled system has a small read zone with read range comparable to the antenna size, while the radiative read zone is larger, complex and discontinuous. UHF and microwave tags also provide higher data rate than LF and HF tags. More details of RFID tags working in different frequency ranges are concluded in Table 1.

Table 1. Frequency ranges of different RFID systems with the detailed information [Cha07, Dob05, Fen11, Fin03, Rid09].

Frequency range	read range	Advantages	Disadvantages	Applications
LF	typically smaller than 0.5 meters	Tolerant to metals and water; No restrictions of frequency use.	Low data transmission rate; Affected by electrical noise.	Animal tracking, Identifying metal objects.
HF	Approximately 1 m	Quite tolerant to metals, water and electrical noise; Possibility to read multiple tags simultaneously; Faster data transmission than in LF.	Worldwide use of the 13.56 MHz frequency; Limited range; Water and metals tolerance not as good as with LF.	Credit cards, Access control cards, Passports.
UHF	typically 4 – 5 m	Long range High data transmission rate; Possibility to read multiple tags simultaneously; Low-cost manufacturing.	Absorbed by water; Reflected by metals; Interference with other applications	Supply chain, IoT
Microwave	Approximately 1 m	Very high data transmission rate; Possibility to read many tags simultaneously; Very small size.	Greatly absorbed by water; Greatly reflected by metals.	Environment monitoring, Electronic toll collection.

2.2 Applications of passive UHF RFID

Nowadays, passive UHF RFID systems have a wide range of applications, including supply chain management, access control, human tracking, and remote monitoring, due to the following benefits:

• Passive RFID does not require line-of-sight access to read the tag.

• Passive RFID tags do not need on-board battery, which reduces the weight and enhances the lifetime.

• The read range of a passive UHF RFID is larger than that of a bar code reader.

• Readers can simultaneously communicate with multiple RFID tags. A reader collects detail information in one pass, without having to scan each product.

• RFID tags can store more data than traditional tags, such as bar codes.

2.2.1 Supply chain management

The main application area of Passive UHF RFID technology is supply chain management. Passive UHF RFID tags are utilized to track products from the factory to warehouse stock and point of sale [Ang05]. Integrating tags into the cargos could enable manufacturers or retailers, delivery confirmation, and product information. The placement of shipped cargos during shipment can be achieved with no discrepancies and zero errors, by utilizing RFID technology. Thus, the efficiency and reliability of the entire supply chain is improved further [Wei05, Mic05, Kar03].

In Figure 5, Shenzhen Hopeland Technologies CO. Ltd provides an example of RFID-based supply chain management [Hop18]. Tags are attached on products during the manufacturing process, which could store all the related information of corresponding products. After that, products are shipped to the warehouse. When items are moved in or out of the warehouse, the read-write equipment registers it and forwards the data to the backend system. This allows the management center to manage the vast amounts of products going into and leaving the storage, recognize cargo and help with placement of the cargo in the warehouse [Hop18]. Finally, when products embedded with RFID tags enter a distribution center, the stored information in tags could be used to put products in proper places, sort them quickly and efficiently, and dispatch the cartons to the retailing centers in less time with improved accuracy [Hop18].

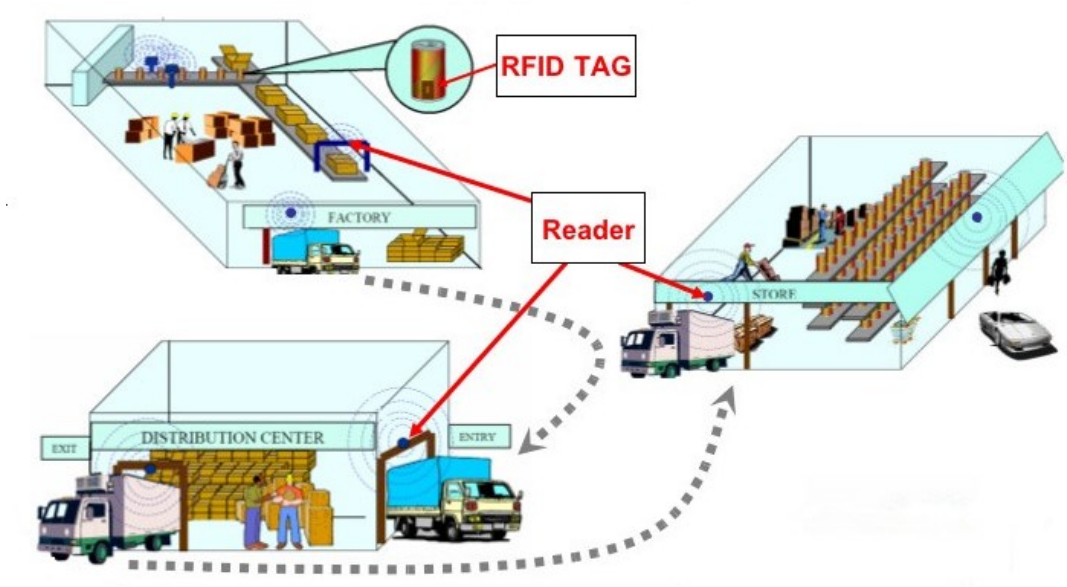

Figure 5. An example of passive UHF RFID in supply chain management [Hop18].

2.2.2 Smart homes

Passive UHF tags combined with ambient sensors, could improve the quality of home life by assisting human's daily activities and taking care of the safe living environments. For instance, sensor tags with sensors for the temperature, humidity or gas monitoring, which are integrated into floors, walls, and windows, can monitor the temperature, humidity or gas in the home. RFID readers, which are located on walls or doors of monitored rooms, can connect to the mobile devices. These tags would be used to minimize energy consumption [Dow09a]; to provide early warnings of possible structural damages, e.g. water damages or to warn about the presence of toxic gases [Dow09b]. Another crucial feature of pervasive computing is its ability to monitor, track and identify activities performed by humans in different environments. Features such as these are enabled by UHF RFID based sensor tags [Koc07] [Bue09]. For example, in [Bue09], everyday objects, such as coffee machine, TV, telephone, and book, are instrumented with UHF RFID tags and accelerometers. RFID readers along the walls can detect when the objects are used by examining this sensor data, and daily activities are then inferred from the traces of object.

2.2.3 Human tracking

Human tracking, especially for the elder or the disabled, is also an interesting application area of passive RFID technology. In recent research, wear tag-embedded bracelets or wristbands were utilized to monitor attendance and to locate lost children in school [Lin10], the reader then forwards the information to the control center through a pocket switched network. In addition, wearable RFID tags, together with the fixed RFID readers, are able to track the position and ensure the safety of the

patients [Naj11, Per12b]. Therefore, wearable RFID technology plays an important role in this application.

As shown in Figure 6, the company Borda Technology has designed a RFID-based patient tracking system for hospital and health center [Bor18]. Firstly, wearable RFID Tags are given to all patients, which include personal information of corresponding individuals. Then, RFID Readers are installed at all essential points, such as rooms, stairways and corridors. Thus, the location of every patient could be detected. Last, the location of all patients can be monitored by mobile devices real time. Medical staff could arrive on time to help the patients when needed.

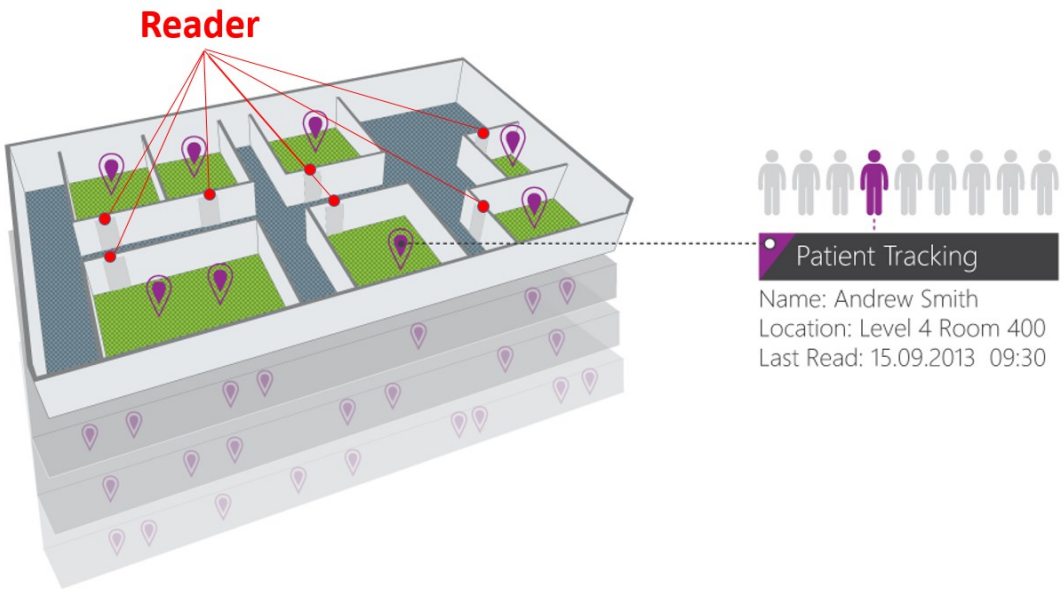

Figure 6. A RFID-based real-time patient tracking system [Bor18].

2.2.4 Remote sensing and monitoring for healthcare

RFID tags can be utilized as wearable sensors around human body, which has attracted lots of interests from international researchers recently. Sensors are placed on human body, e.g. wrist, neck, finger, and breast, to monitor physiological conditions of objectives, and help patients to maintain their health through biofeedback phenomena such as temperature analysis, sweating rate, breathing, heart rate, among others [Ame14].

Passive UHF RFID tags, with external temperature sensor, can be utilized for sensing applications. For example, in [Age16], two conductive fabric electrodes with interconnects were connected to an RFID heart rate detection circuit, which used an on-off keying modulation scheme, to receive and transmit heart rate data. [Ame14] represents a wearable RFID system to remote monitor the situation of people, which is shown in Figure 7. The system is capable to detect and report the presence or

the absence of the user in the bed, his jerky movements and his motion patterns, accidental falls, prolonged absence from the bed, prolonged periods of inactivity and interactions with nearby objects (glass, urinal, medicine, etc.).

Furthermore, RFID tag antennas can be used as sensing elements directly instead of external sensors. An epidermal passive strain sensor using UHF RFID tags is presented in [Rak14], which intends to detect eyebrow or neck skin stretch to offer the possibility of allowing paraplegic patients to control wheelchairs. [Mer16] shows two types of wearable RFID sensors on human body to achieve sweat rate measurements. In [Lon15], a RFID-based wearable strain sensor was designed, which has the potential to monitor the movement of healing limbs and chest movements (breathing).

Figure 7. A wearable RFID system for remote monitoring [Ame14].

2.3 RFID measurements

For RFID technology, there are many parameters that can be measured to evaluate the wireless performance of RFID tags, such as read range of tags and antenna radiation pattern. In the thesis, all tags were tested in an anechoic measurement chamber by using Voyantic Tagformance RFID measurement system, which includes an RFID reader with an adjustable transmission frequency (0.8…1 GHz) and output power (up to 30 dBm), and provides the recording of the backscattered signal strength (down to −80 dBm) from the tag under test. Figure 8 shows Voyantic Tagformance RFID measurement system and the chamber.

One important parameter, but by no means not the only, that describes the performance of an RFID tag is the read range. The read range is the maximum distance that the reader can successfully detect the tag. The maximal distance between the tag and the reader antenna in an environment without reflections or external disturbances is the theoretical read range of a tag [Publications I–VII].

Power transfer between antenna and IC is best described by a power transmission coefficient (PTC) τ [Rao05, Vir13a]. This describes the power which is delivered to the load and reflected back to the reader [Vir13a]. Realized gain G_r can be analyzed using the path-loss measurement data from the measurement unit, which is also useful in antenna design [Vir13a]:

$$G_r = \frac{P_{IC}}{L_{fwd} * P_{TS}} \tag{1}$$

where P_{IC} is the tag IC sensitivity, and P_{TS} and L_{fwd} are the measured threshold power and forward losses, respectively. After that, the H-plane and E-plane realized gains can be plotted as radiation patterns.

Threshold power is an important parameter of an RFID system, it is the minimum power needed to activate the tag IC [Bjö09]. Threshold power of an arbitrary tag can be expressed as:

$$P_{TS} = \frac{P_{IC}}{G_{tx} G_{tag} \tau (\frac{\lambda}{4\pi d})^2 \left|\rho_{tx} \cdot \rho_{tag}\right|^2} \tag{2}$$

where P_{IC} is the sensitivity of the RFID IC, G_{tx} and G_{tag} are the gains of the reader and tag antenna, τ is the PTC, λ is the wavelength of the signal from the reader, d is the distance between the tag and the reader antenna, ρ_{tx} and ρ_{tag} are the unit electric field vectors of the transmitter antenna and tag antenna.

In addition, the sensitivity of the tag could be presented in equation (3) [Bal05, Der07, Rao05].

$$P_{tag} = P_{tx} G_{tx} G_{tag} (\frac{\lambda}{4\pi d}) \tag{3}$$

where P_{tag} is the power received by the tag antenna, P_{tx} is the power transmitted by the reader antenna. During the measurement of theoretical read range, P_{tag} is assumed to be the threshold value P_{TS}.

Finally, theoretical read range d_{Tag}, presented in equation (4), can be obtained from equation (3) using the Friis' equation [Bal05, Der07, Rao05].

$$d_{Tag} = \frac{\lambda}{4\pi} \sqrt{\frac{P_{tx} G_{tx} G_{tag} \tau}{P_{TS}}} \tag{4}$$

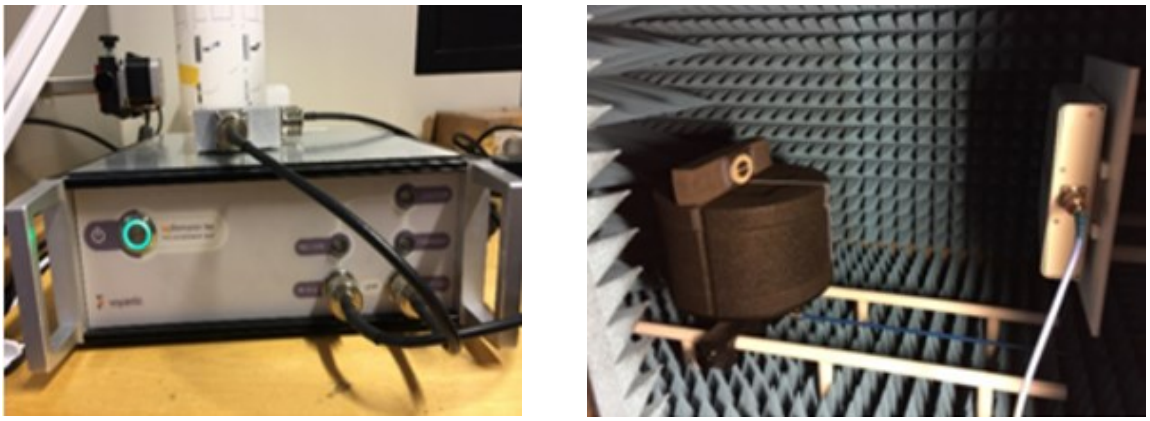

Figure 8. Voyantic Tagformance RFID measurement system (left) and the anechoic chamber (right).

3 Materials

3.1 Substrate materials

To extend the commercial usage of the passive RFID technology, it is essential to reduce the cost of RFID tags. Thus, the substrate material of RFID tag is always required to be inexpensive and easily available in large quantities [Per12a]. Furthermore, the substrate material should be environment-friendly which can be easily biodegraded after its life cycle. According to these requirements, paper, cardboard, wood and textile are selected in the study [Publications I–VII].

In general, the electrical properties of substrate, including loss tangent and relative permittivity, could affect the electrical performance of a tag to some extent [Kel12, Vir12a, Vir13b]. However, in this study, the electrical properties of the substrates are good enough for the application area in the thesis. Hence, the wireless performance of RFID tags is mainly affected by the electrical properties of antenna materials. To achieve better wireless performance of the RFID tag, manufacturing parameters should be optimized in advance according to the electrical properties of the utilized materials [Publications I–VII].

Furthermore, the roughness of substrate surface and porosity of substrate material have a significant impact on electrical performance of RFID tags [Vir12a]. The conductive ink can be absorbed into a porous material, which lead to the uneven deposited ink layer on the substrate [Vir12a, Vir13b]. Examples of ink absorbing substrate materials used in this study include cardboard, textile and wood veneer. A cross section is shown in Figure 9 to illustrate the absorption of the stretchable ink on a cotton textile.

Thus, the main constraint of the substrates utilized in this thesis is the roughness of the surface. Inkjet printing requires substrate with smooth and coated surface. While 3D DW dispensing can be operated on rougher materials. Curing temperature is not a restriction when select substrate in this

study. The highest curing temperature utilized in the thesis is 150 °C, which is tolerable for all the substrates.

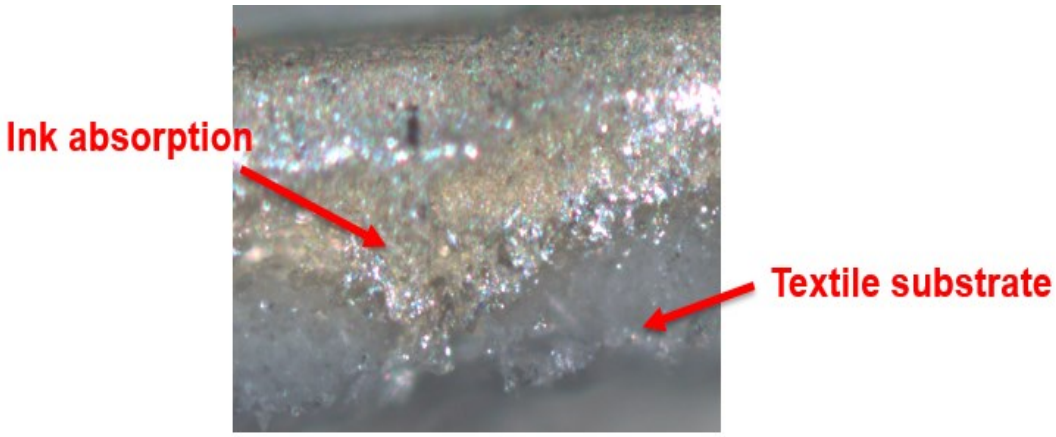

Figure 9. Ink absorption of the textile substrate.

3.1.1 Polyimide film

Kapton, which is a flexible polyimide film from Dupont, is used as the substrate in the thesis for AM. It has already proven as a substrate of choice for RFID applications based on past experience [Riz17]. Compared to the traditional Polyethylene terephthalate (PET) film, it has higher heat resistance, which makes it suitable for heat curing during the manufacturing process.

3.1.2 Cardboard and paper

Paper, which has a wide range of usage in daily life and industry, is an interesting substrate material for ultra-low-cost printed electronics [Ami12, Rid09]. Due to its low-cost, biodegradability and light-weight, paper is well suited to AM [Ami12, Kim15, Ore11, Rid09]. There are various types of paper, according to a number of parameters, such as density, thickness, coating, and texture. These parameters, especially the coating materials, could affect the performance of paper as a substrate in AM [Rid09]. A proper coating, which can make the surface of the paper smooth, even, and water-resistant, is a potential solution for the ink absorption problem [Vya09].

In general, cardboard has same properties as paper. However, compared to paper, cardboard usually has a rougher surface even with the same coating, which increases the difficulty.

3.1.3 Wood

Wood is a potential alternate as a substrate material in passive UHF RFID technology [Vir12b]. The benefits of the wood veneer, including environment-friendly, good durability, and low cost, make it popular in many RFID application areas, e.g. product packaging and retail. However, wood is not an

ideal choice for inkjet printing, mainly due to its porous and rough surface. The deposited inks on wood could be easily absorbed, hindering the nanoparticles to form conductive traces. Thus, three-dimensional (3D) DW dispensing, which could generate high-volume ink flow, was selected in this study to manufacture RFID tags on wood veneer [Publication IV]. More details will be presented in the following chapters.

3.1.4 Textile

As a comfortable, warm, and reassuring material which could protect human skin from the environment, textile is the first and most natural interface for the body during the whole life. Clothing usually covers more than 80% of the skin, thus, textile material can be seen as the most appropriate interface to implement new sensorial and interactive functions. Functions like sensing, transmission, and energy generation are implementable through textile technology. Based on recent research results, textile becomes a potential substrate material for wearable RFID technology which could be integrated with clothing easily, due to the flexibility, stretchability and stability [Cha13, Whi14, Publication VII].

3.2 Conductive inks

AM methods with conductive ink has attracted lots of interest recently. Metallic nanoparticle (NP) inks, which can provide high conductivity printed ink layer, have been widely utilized recently with inkjet printing technology [publication I, II]. Gold (Au) and silver (Ag) are the conventional choices to form nanoparticle inks, while copper (Cu) and nickel (Ni) nanoparticles inks are also available. Silver has the highest conductivity among metals and the silver oxide is also conductive. The main drawback of silver ink is the high price, which limits its potential in mass production. Copper ink attracts tremendous interests due to its relatively high conductivity (slightly less than silver, higher than gold) and its low cost. The main limitation is that copper ink is easily oxidized in ambient environment and copper oxide is an insulator.

In order to reduce the cost of materials, which could reach the requirement by RFID industry, other printable inks were studied to replace more expensive NP inks. The stretchable silver ink, which is suitable for 3D DW dispensing, could be an alternative [Publication VI, VII].

Moreover, let us consider the harmful effect from metallic particles to human body and environment. The novel carbon-based material, such as graphene, was studied in the thesis [Publication III-VI]. Graphene is an environmentally friendly and low-cost material with great electrical and mechanical properties. It can be used in AM [Kop15, Hua15, Akb16a] and it has the capacity to integrate with versatile materials, including porous substrates, such as cardboard and fabrics [Akb16a].

Finally, curing is applied to establish a conductive trace or antenna on a substrate. This is realized by removing the solvents and dispersing agents from the ink, allowing the conductive particles to conduct by direct physical contact. Neck formation between the particles take place due to Ostwald ripening and surface-to-volume ratio reduction [Per08]. The curing process is a key step in printed electronics. It affects the mechanical and electrical properties. The time consumed by the curing process directly decides the whole inkjet printing manufacture time as deposition time is less flexible.

There are different ways to eliminate the dispersing agents and the solvents. Thermal curing in an oven is the most conventional method, which was mostly utilized in the thesis. The curing parameters are specified by the ink properties, which will be introduced in the following contents.

3.2.1 Silver nanoparticle ink

Basically, nanoparticle inks consist of two fundamental parts: the liquid element and the dispersed or dissolved element. The liquid element, such as a kind of organic solvent, can decide the basic ink properties. The dispersed element, e.g. metal particles, is utilized for realizing the specific function. The diameter of particles in nanoparticle conductive inks is very small, generally from 1 nm to 100 nm. Due to the particle size, this ink has several advantages, such as ease of dispersal in many solvents, high purity and high metal loading [Cal01]. Usually, high conductivity metal such as gold, silver and copper are selected in nanoparticle inks. Compared to silver or gold NP inks, copper NP inks have significantly lower cost [Ryu11, Par14]. However, copper ink is easily oxidezed in ambient environment and copper oxide is an insulator. Thus, silver nanoparticle ink is selected in this study.

The size of inkjet printer nozzles is extremely small, thus, avoid blocking of nozzles, the diameter of particles should be small enough which is no more than 1-5 percent of the nozzle size [Cal01]. Thus, nanoparticle ink should be a proper choice of inkjet printing technology.

Harima NPS-JL silver Nanoparticle ink was utilized in the study for inkjet printing on paper and cardboard. The properties of the used NP ink are shown in Table 2.

Table 2. Properties of Harima silver Nanoparticle ink [Har18].

Ink	Ag NPS-JL NanoPaste®
Solid content (wt%)	52-57
Particle size (nm)	5-12
Average particle size (nm)	7
Resistivity (μΩ·cm)	4-6
Viscosity (mPa·s)	11.5 (measured at 20°C and 60 rpm)
Recommended thermal curing	120-150 °C for 60 minutes

Recently, the usage of nanoparticle inks attract a number of discussions, especially for the harmful effect of NPs to humans and environment [Saj15]. The current knowledge of these issues about NPs is seriously incomplete, which indicates that NPs and related products must be further studied before they are widely used in industry [Saj15]. Due to the extremely small size, there are several consideration of NPs, such as high surface-to-volume ratio, which increases toxicity [Saj15]. In addition, their penetration ability to human or animal tissue, or into plants, increases [Saj15]. It has been found that NPs with diameter less than 35 nm can penetrate the blood-brain barrier, NPs smaller than 40 nm can enter the nuclei of cells, and NPs smaller than 100 nm, e.g. the silver NPs used in the thesis, can enter into cells [Saj15]. Besides the particle size, other properties, such as shape and material of NPs, should be considered in terms of toxic effects of NPs [Saj15].

3.2.2 Stretchable silver ink

The growing interest towards wireless body area networks (WBAN) which will enable future body-centric wireless communication and sensing applications, has created a huge demand for textile-integrated electronics. The research and development work around WBAN technologies is currently very active [Van14, Zhe14, Ken09, Man12]. One key technology in this interesting area is wearable RFID technology, requires the antennas to be an integral part of clothing, and to endure repeated mechanical stress. This leads to the challenge of implementing stretchable and bendable antennas.

A stretchable silver conductor (DuPont PE872) was selected as antenna material in the study. The stretchable silver ink has larger conductive particles than NP inks. This makes it unsuitable for inkjet printing, because they would not come out of the nozzles of a print head. However, it is very suitable

e.g. to brush-painting, 3D DW dispensing and screen printing, or in general, to processes where the ink is not dispensed through small nozzles. The properties of this stretchable silver ink are shown in Table 3.

Table 3. Properties of DuPont PE872 stretchable silver ink [Dup18].

Ink	DuPont PE872
Solids (%) @ 150°C	60-65
Dried Print Thickness (microns)	8-12
Density (g/cc)	2.0
Viscosity (PaS), 10rpm, 25°C	50-80
Recommended thermal curing	100-160 °C for 2-10 minutes

3.2.3 Graphene ink

Graphene, as a 2-dimensional crystalline allotrope of carbon with low resistivity (10−6 Ω·cm) and high stability, has attracted many researchers and industrial sectors to adopt it as an alternative to traditional metallic elements for printed electronics, interconnects, and semiconductor applications. Better manufacturability and higher reproducibility of graphene have also made it a prominent competitor over carbon nanotubes (CNTs) in electronic applications. Favorable features of graphene, e.g., transparency and stretchability, also make graphene interconnects applicable in light emitting diodes (LEDs) for applications such as information displays and biomedical systems [Goo12].

As an environmentally friendly and low-cost conductive material, graphene has the capacity to integrate with challenging substrate materials, such as soft and stretchable textiles [Hua15, Akb16b]. For those reasons, and because of graphene's great electrical and mechanical properties, graphene-based conductive inks were utilized in this study [publications I-III], by replacing traditional inks with metallic components. A water-based graphene ink (HDPlas® IGSC02002) (Haydale Ltd., UK) was selected in this study using 3D DW dispensing. The properties of the used inks are in Table 4.

Table 4. Properties of the graphene ink (HDPlas® IGSC02002) [Goo18].

Ink	Graphene ink (HDPlas® IGSC02002)
Solids (%)	40
Thickness (microns)	13 micron wet emulsion, 7 micron dried
Coverage Area (cm^2/g)	550
Viscosity (PaS)	5.5
Sheet Resistvity	12 Ω/sq. (normalized to 25 microns)
Recommended thermal curing	60°C and above for 30 minutes

4 Additive Antenna Manufacturing Techniques

Basically, the manufacturing methods of RFID antennas are classified in two categories, which are subtractive manufacturing method and AM method. The principle of subtractive manufacturing is to remove the conductive materials from the redundant areas of the substrate. The typical subtractive manufacturing method is etching. On the contrary, the conductive materials is deposited only on desired areas during AM. Thus, due to the less wastage of the conductive material compared to etching [Hal11] or other subtractive manufacturing methods, AM was selected in the study for RFID tag antenna fabrication.

One of the most significant applications of printing technologies is in printable electronics. The printing technologies such as inkjet printing and 3D printing are mold-free technologies along with low amount of consumed materials; they provide cost-effective and rapid manufacturing process.

4.1 Antenna patterns

Two different antenna patterns were optimized for AM in this thesis. The geometry dimension of the dipole antenna for inkjet printing is shown in Figure 10, which was previously utilized in [Vir12a]. The aim frequency of the antenna design is 915 MHz, but the antenna can achieve satisfied performance in broadband (850MHz to 1000MHz). In addition, the antenna design for 3D DW dispensing is shown in Figure 11, which was based on a design in [Bjö14]. This design has input impedance same as of used RFID IC input impedance.

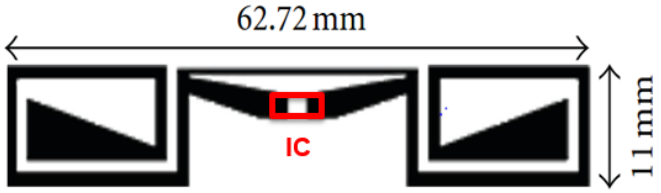

Figure 10. The antenna pattern for inkjet printing.

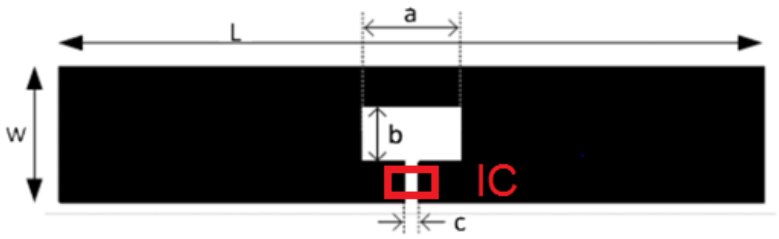

a (mm)	b (mm)	c (mm)	L (mm)	W (mm)
14.3	8.125	2	100	20

Figure 11. The antenna pattern for 3D DW dispensing.

4.2 Inkjet printing

Inkjet printing is a non-contact material deposition technology for manufacturing UHF RFID tags in recent years. Its additive nature allows it to provide fast, precise, and low-cost production on various novel substrates, such as papers, cardboard and polyimide film [Kim13, Mor12b].

Inkjet technology is classified as continuous inkjet (CIJ) and drop-on-demand (DoD) [Moh02]. In a CIJ system, an external electric field is applied to a continuous stream with electrostatic charge. The external electric field determines the droplet to land on the substrate or to be recycled. CIJ is a fast method with high drop velocity. However, low print resolution, extensive maintenance, and the risk of contamination during the ink recirculation limit the usage of CIJ technology [Der08].

A DoD printer contains nozzles that jet individual droplets when needed. The droplet generation is based on piezoelectric, thermal, electrostatic or acoustic elements. The most common modes are thermal and piezoelectric. In a thermal DoD system, ink is heated and vaporized. Ink vaporization produces bubbles that generate pressure to jet the droplets. This is widely used in conventional desktop printers. Piezoelectric mode is used for inkjet printing conductive nanoparticle inks because the high temperature in thermal mode will lead to ink curing [Sir03]. Piezoelectric inkjet print head is controlled by applying voltage pulses to the piezoelectric crystal to cause physical deformation to

allow the droplet to be jetted. The voltage amplitude and shape can be set accurately to allow high print accuracy. The print head is driven by electric precision motor to move in one direction while the platen that holds the substrate can move in a perpendicular direction such that the two-dimensional layout can be printed. The principle of the DoD printer is shown in Figure 12.

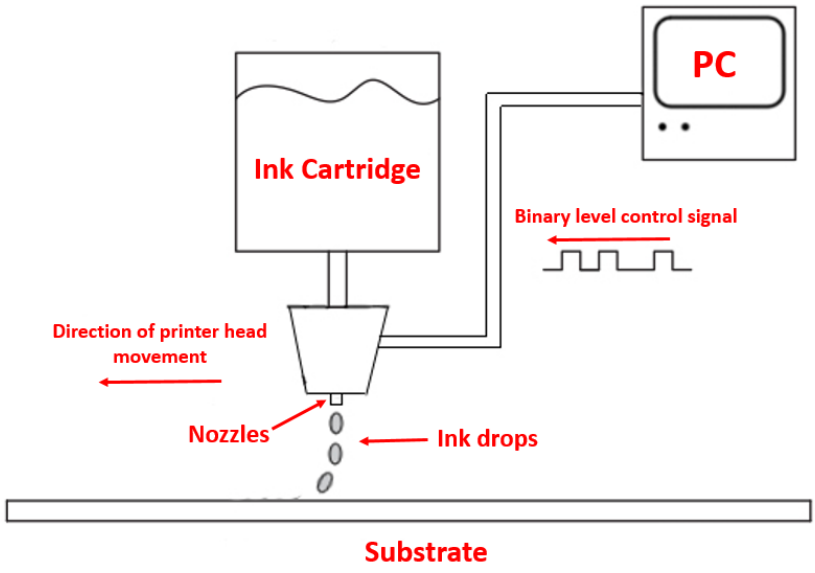

Figure 12. The principle of DoD inkjet.

Fujifilm Dimatix DMP-2831 material inkjet printer [Fuj18] with a platen area of 210 mm * 310 mm was selected for inkjet printing study [Publication I, II]. The printer is shown in Figure 13. The material printer is mounted with a 10 pL volume cartridge that has a print head with 16 nozzles. From 1 to 16 nozzles can be selected for jetting the droplets. The pulse voltage applied to each nozzle can vary from 18V to 35V. The print head height can be adjusted according to the substrate thickness. Temperatures for the platen and cartridge can be controlled between 40℃ to 60℃ and 28℃ to 35℃, respectively. Pattern resolution ranges from 100 dot-per-inch (dpi) to 5080 dpi to fit different droplet spacing from 254 µm to 5 µm. These printing parameters are critical to control the ink flow from the print head.

Figure 13. Fujifilm Dimatix DMP-2831 material inkjet printer.

Generally, the drop form is determined by jetting pulse shape and the jetting voltage of the nozzles could control the drop rate. With too high drop speed, too much ink would be deposited which will spread on substrate and destroy the shape of the designed pattern. When drop speed is slow, there could be insufficient ink to form ink layer with high conductivity [Lim13]. Substrate temperature could control the drying speed of deposited inks on the substrate while cartridge temperature can influence the viscosity of the ink, which can further change the quality of the ink flow [Kan11, Shi13].

Inkjet printing needs low viscosity liquid phase ink materials [Par07, Vir13a]. The inkjet inks should fulfil at least the following properties: have a very low viscosity, where no component separation occurs during high acceleration, and electrically conductive structures are possible to make with them [Fal11]. In the case of inks in inkjet printing, the electrical conductivity is achieved via conductive particles in a liquid, and to achieve the minimal component separation the particles should be as small as possible [Fal11]. The inks are printed through nozzles on a substrate, and after ink drying a conductive line is established. Printed particles do not form uniform, conductive material. Therefore directly after printing the conductive line is not conducting [Fal11]. The inkjet printed pattern comes conductive via curing; the conductive metal particles are sintered with each other establishing an electrically conductive connection between conductive particles [Par07].

One drawback with inkjet printing of RFID tags is that one printing layer produces very thin conductive layer. In addition, the very thin layer does not withstand e.g. the chip attachment process very well. Hence, multiple inkjet printed layers are needed for a good result [Publication I, Vya09]. In addition, with multiple inkjet printed layers also multiple curing rounds are needed [Publication I, Vya09]. This slows the process significantly.

Inkjet printing on two types of papers (a coated one and an uncoated one) and a coated cardboard, together with Harima NPS-JL silver Nanoparticle ink, was studied in the thesis [Publication I]. Printing

parameters, including the jetting frequency, the jetting voltage, the temperature of the ink cartridge, as well as the pattern resolution, have to be optimized based on the ink and the substrate before printing. The pattern resolution is one of the most important parameters: printing with too high resolution can cause bulging and too low resolution results in isolated drops. Generally, the printing resolution is decided by droplet spacing. Thus, ink droplets on every substrate should be measured firstly to ensure the appropriate droplet spacing, which is usually equal to the radius of the drop. Silver nanoparticle ink droplets on the coated paper, as an example, are shown in Figure 14. In addition, Table 5 represents the optimized printing parameters of inkjet printing using silver nanoparticle ink.

The inkjet printed pattern on the uncoated paper shows no conductivity, the surface of the four-layer printed pattern is mostly black and no coherent metallic trace formed after curing, which is shown in Figure 15(a). Due to the absorption of the deposited ink by the uncoated substrate, there are insufficient metallic particles at the surface to form a conductive pattern.

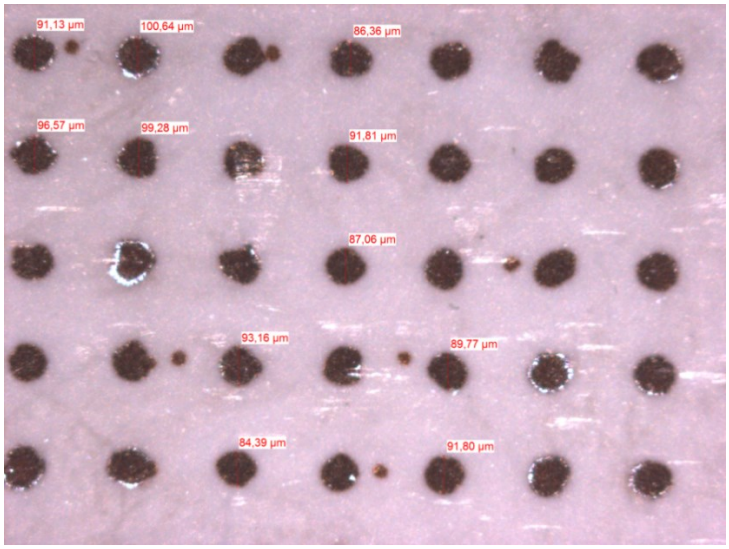

Figure 14. Silver nanoparticle ink droplets on the coated paper [Publication I].

Table 5. Optimized inkjet printing parameters.

Parameter	
Cartridge temperature (°C)	40
Platen temperature (°C)	50
Jetting voltage (V)	28
Jetting frequency (kHz)	23
Curing time (minutes)	60
Curing temperature (°C)	150
Printing resolution (dpi) (coated paper and cardboard)	635
Printing resolution (dpi) (uncoated paper)	508

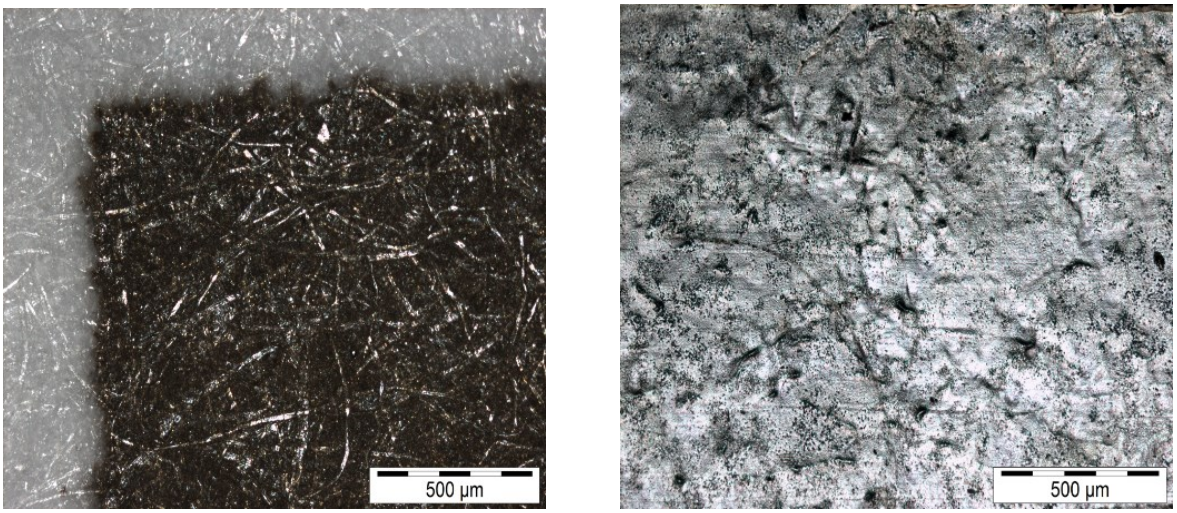

(a) (b)

Figure 15. The surface of: (a) inkjet printed pattern on the uncoated paper substrate, (b) inkjet printed pattern on the coated paper substrate [Publication I].

The coated paper was found to be a suitable substrate for inkjet printing. The surface of an inkjet-printed tag on this paper is totally metallic although there are some small black holes and thin gaps,

as shown in Figure 15(b). To better understand the connection of the deposited ink layer and the coated paper substrate, the scanning electron microscopy (SEM) picture (Figure 16) is utilized to show the cross-section of an inkjet printed RFID tag. It indicates that proper coating could protect the paper substrate from ink absorption problem successfully.

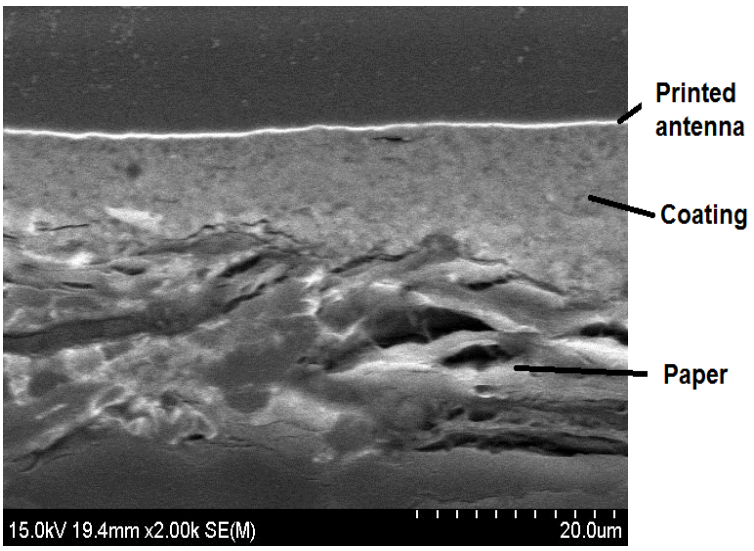

Figure 16. Cross-section of the inkjet-printed antenna on coated paper from SEM [Publication I].

Based on the results of inkjet-printed tags on the coated paper, more layers lead to longer read ranges, since more ink was deposited on the paper to form a thicker conductive pattern, which has lower losses and better radiation efficiency. However, judging from the wireless performance of tags on the coated cardboard, when more layers are printed, the read range decreases inversely. Thus, depositing multiple layers directly does not always correspond to a higher read range and the optimized number of layers for antennas on each substrate material needs to be studied separately.

4.3 3D direct write dispensing

DW represents technologies which have ability to generate two-dimensional (2D) or 3D structures on any kinds of flexible or rigid surfaces with planer or conformal complex geometry. The DW technologies require no masks or tooling [Li15, Cao15, Lew04, Mor09]. The most common structures using DW technologies are in passive or active electronic components such as conductors, insulators, antennas, batteries, etc [Li15, Cao15]. In the AM community, definition of DW typically consists of manufacturing technologies to write or print structures or electronics directly from a computer file with feature resolution below 50 μm [Gib15].

Due to the small size of inkjet printing nozzles, the deposited ink flow is quite limited. Thus, for substrates which have rough surface and obvious ink absorption, e.g. textile and wood veneer, inkjet printing is not a reasonable choice. Instead, 3D DW dispensing could be a better way to manufacture RFID tags on these substrates [Cao 15, Publication III-VII].

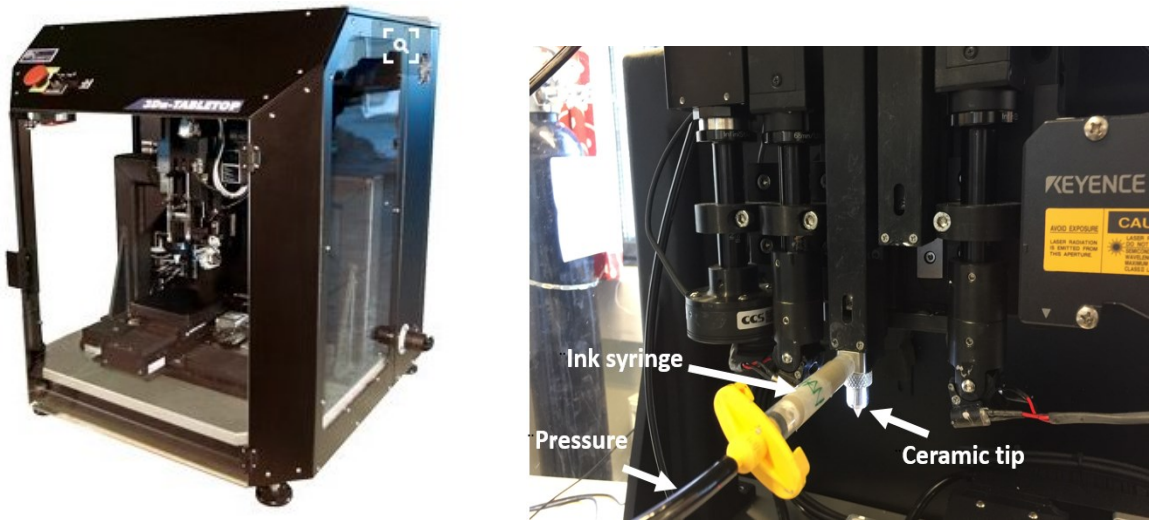

Figure 17. nScrypt 3D DW system with an ink syringe and a ceramic nozzle tip.

As shown in Figure 17, nScrypt 3D DW system was used in the study, which equipped with a deposition system and a ceramic nozzle tip. Firstly, the printing spacing and angle can be defined when designing the printed pattern, by a built-in software. After that, during the dispensing process, the air pressure from a positive pressure pump is applied to the system, which pushes the ink into the main valve body, and finally through the ceramic nozzle tip. The nozzle of DW systems is generally equipped with X-Y-Z motion control system and a scanning system, which guarantee the depositing accuracy during the printing. The example of printing scaffolds is shown in Figure 18. The parameters of the utilized ceramic nozzle plays an important role in 3D DW dispensing, which can determine the shape and size of the deposited ink flow. By adjusting the air pressure from the pump, start and stop point of the ink flow, the deposition speed, and the size of the ceramic nozzles, the ink flow could be controlled precisely. A wide spread variety of inks can be used in nozzle DW system such as solders, metallic or ceramic based inks, adhesives and epoxies. The viscosities of acceptable inks depend on many parameters, especially the size of the printing nozzles, printing temperature and feeding pressure. Larger nozzles, higher temperature, and higher pressure will allow inks with higher viscosities. However, the exact range of acceptable viscosities is hard to provide. The example applications are to manufacture scaffolds and microfluidic networks. [Gib15, Lew04, The03]. The utilized printing parameters of DW dispensing for both graphene ink and stretchable silver ink are shown in Table 6.

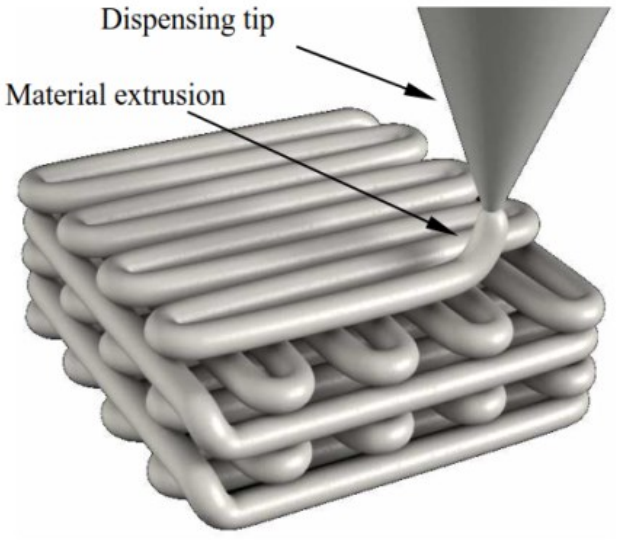

Figure 18. Schematic illustration of direct writing [Gib15, Li07].

Table 6. Optimized parameters of 3D direct write dispensing.

Parameter	
Material feed pressure	16.9 Psi
Printing spacing	125 μm
Printing angle	0°
Inner/outer diameter of tip	125/175 μm
Number of printed layers	1

Publication III shows DW dispensed graphene-based RFID tags on cardboard packaging substrates: one has a rough, non-colored surface, while the other is smooth and colored white. The tag antennas were heated in an oven at 60 ℃ for 30 minutes. The peak read range of the tag on the smooth cardboard was around 3.8 meters, while the tag on rough cardboard has slightly shorter read range of 3.2 meters. In conclusion, the performance of graphene-based tags on the smooth cardboard is slightly better than tags on the rough one. It is probably due to the rough cardboard without any coating has more ink absorption than the smooth one.

In publication IV, graphene-based RFID tags were fabricated by 3D DW dispenser on wood veneer. The tag antennas were cured in an oven at 60 ℃ for 30 minutes, which leads to a peak read range of 4.5 meters.

Publication VI compared the performance of DW dispensed RFID tags using graphene ink and stretchable silver ink on a 100% cotton textile substrate. Firstly, magnifications of finished antennas are shown in Figure 19. As can be seen, both inks had good adherence to the textile substrate. The peak read ranges of tags with graphene ink and stretchable ink were 4.8 meters and 10.9 meters, respectively. Based on the results, the performance of RFID tags with stretchable silver ink is much better than graphene-based tags. However, graphene-based tags, which have a peak read range of around 5 meters, also achieve the requirements of many RFID applications.

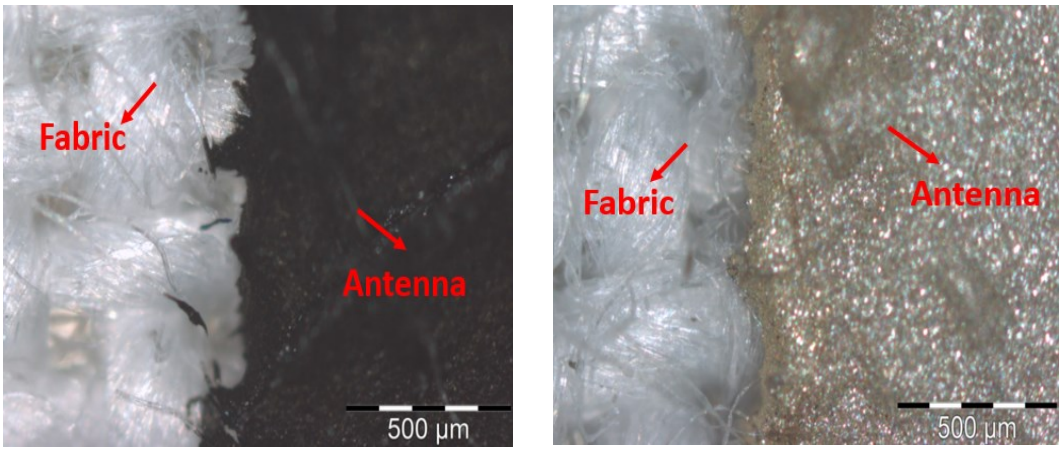

Figure 19. The surface of RFID tags using the graphene ink (left) and stretchable silver ink (right) [Publication VI].

5 IC Attachment and Reliability Studies

IC is a critical component of the RFID tag. Nowadays, the IC could store more information than just the simple ID code of the chip. The IC can have additional read-only memory (ROM) and/or read-write memory (R/W), which the reader can interact with. The ROM can contain for instance additional details connected to the item the tag is attached on. This information is typically something that does not need to be read every interrogation time of the tag, but this information is available when needed [Wan06]. The R/W memory can typically be used e.g. for storing time stamps or needed history data, for instance item's previous owners [Wan06].

In this study, the used packaged RFID IC is NXP UCODE G2iL series IC [NXP14], which is shown in Figure 20. The chip has 128 bit electronic product code (EPC) memory, 64 bit tag identifier code (ID), and a low wake-up power of 15.8 µW (-18 dBm) [NXP14]. Tag ID includes a 32 bit factory locked unique serial number assigned by the IC manufacturer [NXP14]. The IC is mounted on a plastic strap with two copper pads on both sides by the manufacturer, which simplifies the IC attachment process in laboratory by hand [Dea10]. Thus, the attachment between the strap and the fabric, which was carried out by the author, has more significant effect on the tag performance in the thesis.

During the AM process, the most commonly used IC attachment approach is to glue the IC on the antenna directly with e.g. conductive epoxy. In this study two component Circuit Works Conductive Epoxy CW2400 is used for joining the copper pads of IC on the antenna pattern area. In addition, other methods are also studied to simplify the attachment procedure, decrease the materials cost, and improve the reliability of the interconnections between antenna and IC. Furthermore, the reliability of antenna-IC interconnections is an interesting topic, which will be described in details next.

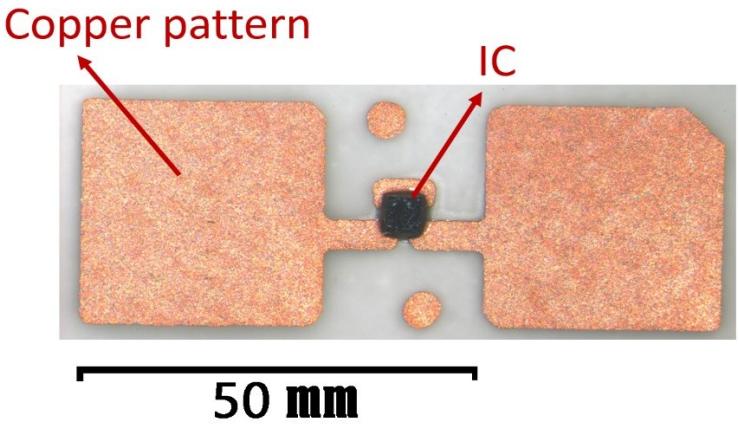

Figure 20. NXP UCODE G2iL series IC.

5.1 IC attachment methods

In this study, three different methods were studied for the antenna-microchip interconnection: The first method was a commonly used way, where the IC is attached on top of the printed and cured antenna with conductive silver epoxy (Circuit Works CW2400). This method has been used, e.g., in [Wan15, Che17, Mor12a]. It is proved that this epoxy glue shows good conductivity and establishes a well-working electric interconnection between antenna and IC. However, some challenges have been reported, such as reliability problems under mechanical stress and continuous washing [Wan15, Che17].

In the second method, the antenna was deposited on top of the IC strap pads, and thus the antenna-IC interconnection was cured together with the antenna. Before printing, a reference point on the fabric substrate needs to be set in order to determine the position of the antenna. Then, IC strap is placed on the exact position on the substrate, and the antenna is deposited on the substrate and on the IC strap copper pads. The strap does not need to attach to the fabric tightly. After printing, the deposited inks will connect the copper pads to the substrate very well. This recently invented approach skips one process step, and thus saves significant amounts of time and costs. This type of IC attachment method has showed high conductivity in the thesis, where graphene ink and non-stretchable silver ink [Bjö15] have been used to fabricate RFID tags.

In the third method, embroidery technique was utilized for attaching the IC on the printed antenna pattern. The IC strap copper pads were embroidered on the fabricated antenna using Husqvarna Viking embroidery machine and conductive yarn (Shieldex multifilament thread 110f34 dtex 2-ply HC). The DC linear resistivity of the thread is 500 ± 100 Ω/m, and the diameter is approximately 0.16 mm. We attached the IC strap copper pads to the 3D-printed antennas by embroidering a cross over

them with conductive yarn. As an example, Figure 21 shows 3D DW dispensed RFID tags with stretchable silver ink using these IC attachment methods and corresponding magnifications of the antenna-IC interconnections [Publication VII].

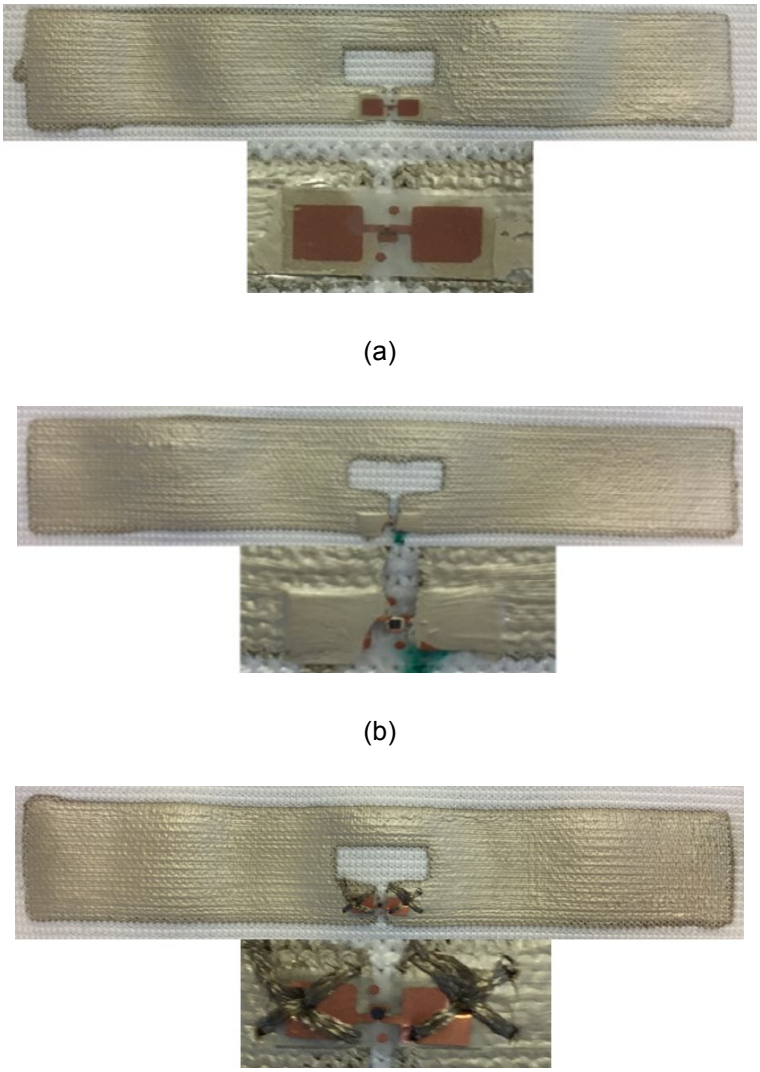

(a)

(b)

(c)

Figure 21. RFID tags and magnifications of the antenna-IC interconnections: (a) epoxy-glued joint, (b) 3D-printed joint, (c) embroidered joint [Publication VII].

5.1.1 Inkjet printing results for IC-antenna interconnections studies

In publication II, inkjet printed tags using Harima NPS-JL silver nanoparticle ink were studied to compare epoxy-glued and printed antenna-IC interconnections. The assembled tags with the inkjet-printed antenna-IC interconnections on paper and polyimide substrates are shown in Figure 22. As

a result, for each substrate, tags with both types of IC interconnections have similar wireless performance. Thus, the inkjet-printed electric interconnection can be considered to be a good replacement for the epoxy-glued one.

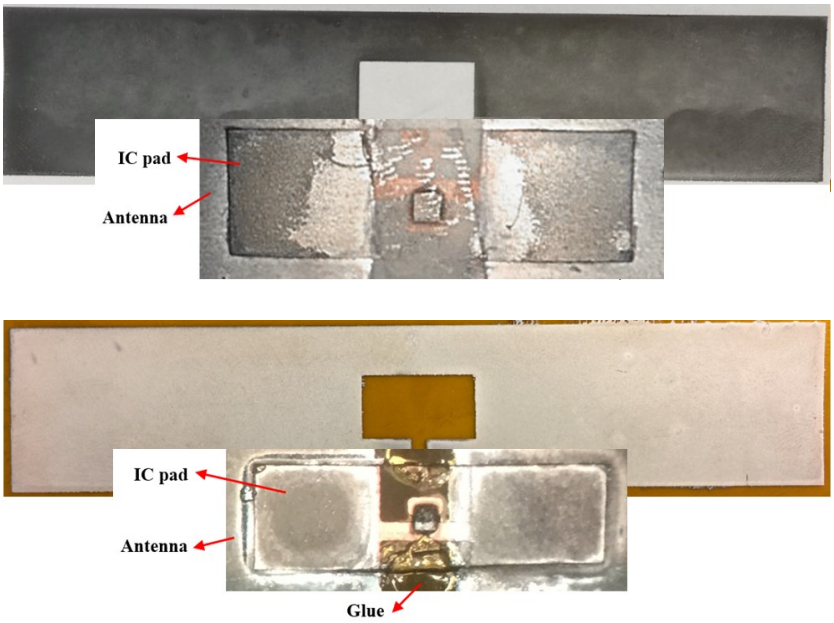

Figure 22. Manufactured tag and the magnification of the antenna-IC interconnection on paper (top) and on polyimide film (bottom) [Publication II].

5.1.2 3D DW dispensing results for IC-antenna interconnections studies

Graphene-based RFID tags on a cotton substrate using 3D DW dispenser were studied in [publication V]. Assembled tags and magnifications of the antenna-IC interconnections are shown in Figure 23. The wireless measurement results confirm that graphene RFID tags with printed antenna-IC interconnections achieve peak read ranges of 5.2 meters, which makes them superior to graphene tags with epoxy-glued ICs. The reliability study of these tags will be introduced in the following section.

Figure 23. Ready passive UHF RFID tags with epoxy-glued antenna-IC interconnections (top) and 3D DW dispensed antenna-IC interconnections (bottom) [Publication V].

[Publication VII] represents 3D DW dispensed RFID tags on an elastic textile using stretchable silver ink. As presented in Figure 21, all previously mentioned IC attachment methods were compared in this work. As a result, all these tags show similar wireless performance. The peak read ranges of the tags with epoxy-glued joint, DW dispensed joint, and embroidered joint were 8.8 meters, 9.6 meters, and 8.1 meters, respectively. These results are very promising when compared to earlier reported RFID tag results: The performance is similar or superior to 3D-printed silver and copper RFID tags, respectively [Bjö15], and significantly superior to 3D-printed graphene RFID tags on textile substrates. Further, none of these previously reported 3D-printed RFID components has been stretchable. More details will also be presented next.

5.2 Reliability studies

Passive RFID technology, which could be integrated into clothes, is one of the key technologies in this interesting area. During actual use, these wearable wireless components have to endure many kinds on environmental stresses, such as harsh weather conditions and continuous washing [Par16, Nay15, Wan15]. Also mechanical stresses, including stretching and bending, are always involved in wearable applications, and cause challenges for the design and manufacturing of wireless components [Wan15, Chen17]. One major reliability challenge lies in the electric and mechanical interconnections of wearable platforms [Nay15, Chen17]. Thus, as a potential selection for wearable RFID technology, the RFID tags using different IC attachment methods were evaluated in high moisture conditions, as well as during and after cycling bending and stretching [Publication VII].

5.2.1 Stretching test

As for the stretching test, the performance of the tags was studied by stretching them from the initial length of 100 mm to 105 mm, 110 mm, and 115 mm. The stretching was done by attaching the tags

to the foam structure with tape. The components were measured during each elongation. In Publication VII, 3D DW dispensing together with stretchable silver conductor were utilized to manufacture RFID tags on a stretchable fabric. After that, the wireless performance and reliability of tags using different IC attachment methods were evaluated. Firstly, simple printed lines with dimension of 60 mm x 10 mm were studied, instead of fully printed antennas, to understand the ink properties during reliability test. The impact of stretching on the resistances of the printed lines was studied by stretching them from the initial length of 60 mm to 80 mm. The resistance measurements in this study were done using a Fluke 115 multimeter. The measurement probes were placed in the opposite corners of the printed lines, along longitudinal direction (60 mm). The resistance results during strain are shown in Table 7. Then, as described in Table 8, the resistances of the printed lines were measured after 10, 20, 50, and 100 stretching cycles, where the lines were stretched from 60 mm to 80 mm and back. The frequency of the stretching cycles was 10 times / minute. The resistances were measured immediately after the stretching cycles.

The surface of a printed pattern before and during stretching is shown in Figure 24. As can be seen, the ink layer had a good adherence to the fabric substrate before stretching. During stretching, there are some small cracks, which leads to the increase of the resistance, as presented Table 7. The increased resistances in Table 8, on the other hand, are caused by these small cracks not fully returning to their initial smooth structure immediately after strain.

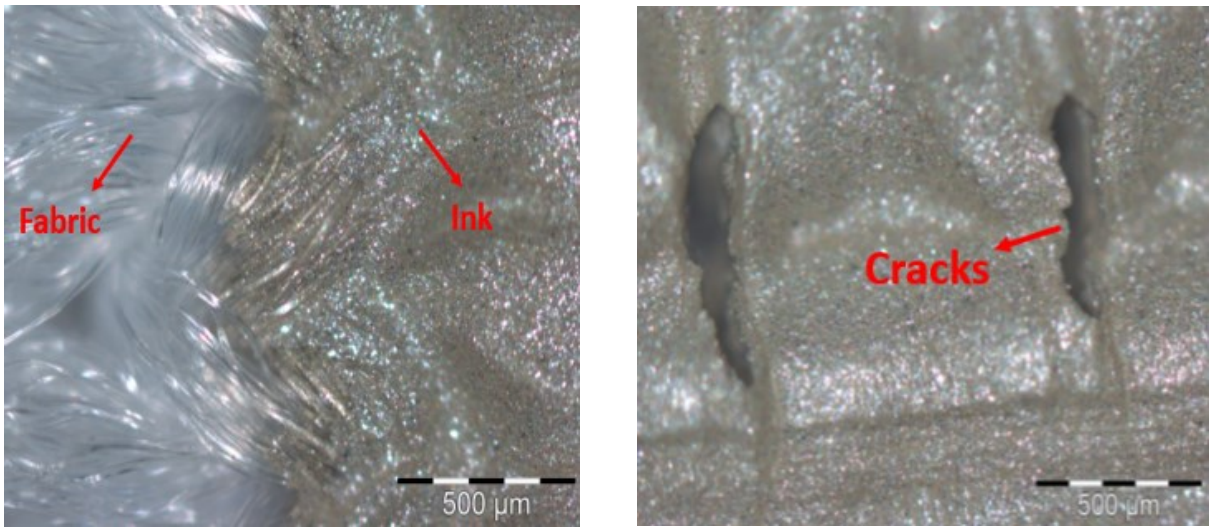

Figure 24. Optical microscopic image of a 3D-printed line before stretching (left) and during stretching (right) [Publication VII].

Table 7. The resistance of the printed line during various strain positions.

Length (mm)	Resistance (Ω)
60 (initial)	0.7
70	9.2
80	21.5

Table 8. The resistance of the printed line after stretching cycles.

Stretching cycles	Resistance (Ω)
initial	0.7
10	2.3
20	5.5
50	22.4
100	66.7
After 1 week recovery	1.9

After that, the reliability of DW dispensed RFID tags, with three different methods for IC attachment, were evaluated. The tags with epoxy-glued IC attachment and 3D-printed IC attachment were not stretchable, since the antenna-IC interconnections of these tags were easily broken. See Figure 25 for broken IC attachments. The attainable read ranges of the tags with embroidered antenna-IC interconnections under incremental strains from 0 % to 15 % are presented in Figure 26(a). In addition, Figure 26(b) shows the attainable read ranges in a non-stretched state after 20, 50, and 100 stretching cycles, where the tags were stretched from 100 mm to 115 mm each time. The frequency of the stretching cycles was 10 times / minute. After all stretching cycles, the tags recovered in room conditions for 5 days, and the performance was measured again.

As a result, tags with embroidered antenna-IC joints experienced a slight downward shift in the frequency of the peak read range when stretched increasingly. It is noticeable that the peak read range value was only slightly effected by the harsh strain, and the tags showed excellent read ranges of over 6 meters throughout the global UHF frequency band, even when stretched from 100 mm to 115 mm. Moreover, after a 100 stretching cycles (stretched from 100 mm to 115 mm each time), the peak read range was still around 7 meters. It can be seen that the reduction in the performance of the non-stretched state tag also declined with the number of stretching cycles. After recovered 5 days in room conditions, the read range returned to 8 meters, which is only 0.8 meters less than the

initial performance. After stretching, the surface of the conductor layer had serious cracks, which affected the antenna resistance and thus decreased the RFID tag read range. However, a few days recovery on an office table, the conductor layer revised back from elongation. The cracks were smaller although there is a permanent change in the conductive layer structure. Thus, the read range of the tag increases after 5-day recovery. Thus, the tag with embroidered antenna-IC interconnections is quite reliable during the stretching test.

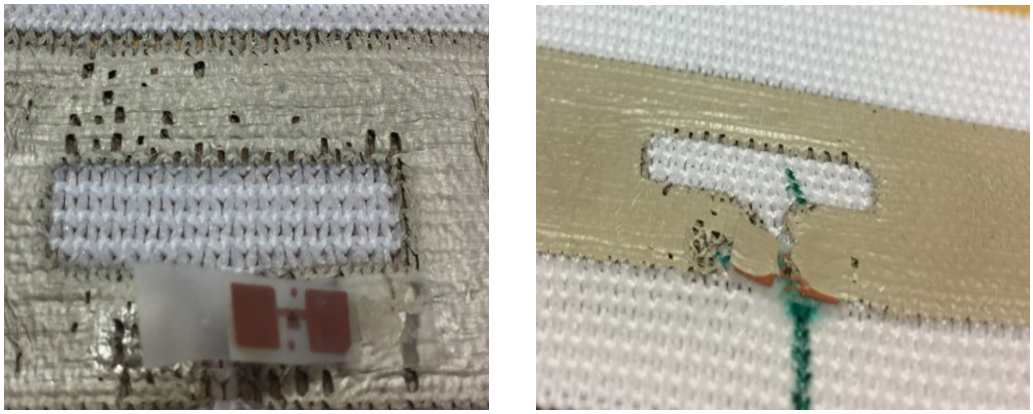

Figure 25. Broken antenna-IC interconnections of epoxy-glued joint (left) and 3D-printed joint (right) [Publication VII].

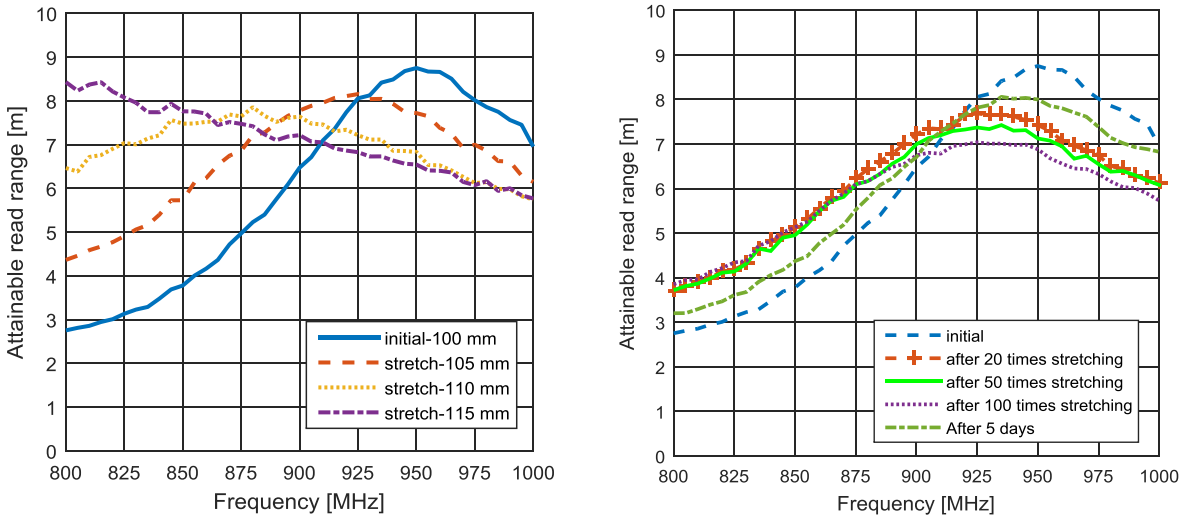

Figure 26. Attainable read ranges of a tag with an embroidered antenna-IC joint: (a) during various elongations, (b) after multiple stretching cycles (stretched from 100 mm to 115 mm each time) [Publication VII].

5.2.2 Immersing test

During the immersing test, the tags were placed in tap water (pH = 6.5-7) and wirelessly measured immediately after one-minute dipping. After that, these tags were left in room conditions to dry and are measured again after 1 hour, 1 day, and finally 1 week, when they were total dry. As mentioned before, publication V shows the 3D DW dispensed tags with different IC attachment methods on a 100% cotton fabric. Due to the properties of the graphene ink, DW dispensed tags shows insufficient elasticity and flexibility. Thus, only immersing test were applied in the study. Figure 27 represents the results of the immersing test for tags with both IC attachment. It indicates that the effect of humidity on the tags with the epoxy-glued ICs is more significant, most probably due to the moisture absorption of the glue itself, and the effect of that to the antenna-IC impedance matching.

In publication VII, it is concluded that humidity has no effect on conductivity of the line pattern. In addition to the tag performance, the read ranges of all types of tags decrease after 1 minute in water. The absorbed moisture affects the dielectric constant and loss tangent of the fabric substrate, which affects the performance of the antenna, as well as the antenna-IC impedance matching, and thus the wireless performance of the tags. After drying for one hour in room conditions, the read ranges of all types of tags have increased close to normal, but there is still a significant shift in the peak frequency range, caused by the absorbed moisture. When the tags are dry again, the wireless responses of all types of tags have returned to the initial performance. Thus, the humidity did not have a permanent effect on the performance of these tags.

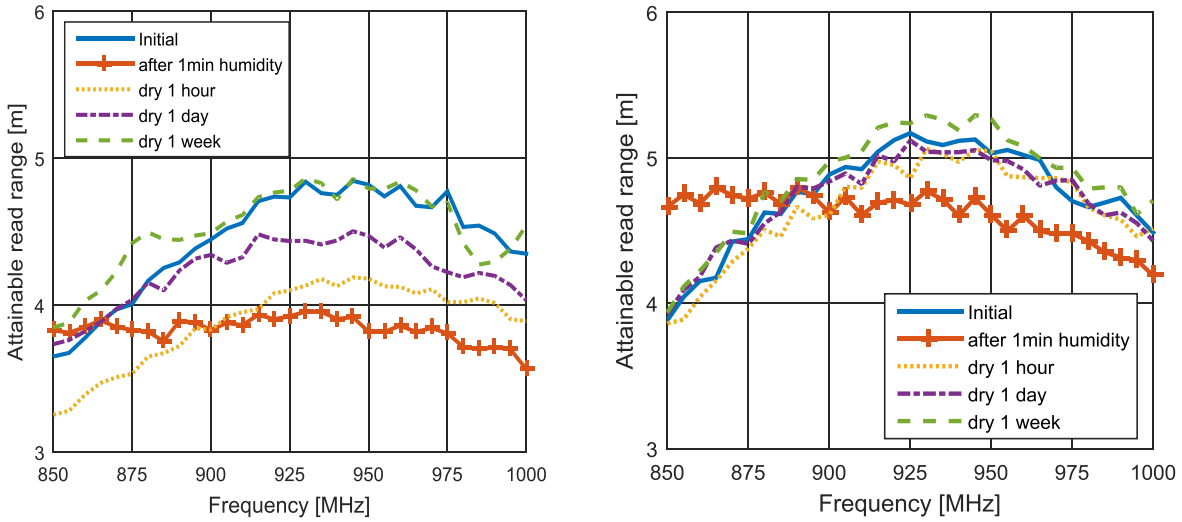

Figure 27. Read ranges of graphene RFID tags before and after high humidity conditions: (a) epoxy-glued IC attachment, (b) printed IC attachment [Publication V].

5.2.3 Bending test

In the bending test, the tags were bent over a 30 mm thick structure in Y-direction. The wireless performance was measured at different steps: before bending, when bent, and in a non-bended state after up to 100 bending cycles. The frequency of the bending cycles was 10 times / minute. This thesis provides the first step of the bending test, while all the measurements were operated in an anechoic chamber. Thus, the bending reliability was not evaluated on human body. The main purpose of the test is to study the performance of tag antennas after the structure change. Next, bending tests on human body with a larger amount of samples will be carried out for reliability evaluation.

In Publication VII, the results present that the read ranges of all types of tags decrease about 2 meters during bending, but when measured in the non-bended state, the performance of these tags is stable even after a 100 times of bending. In conclusion, multiple bending cycles did not affect all kinds of tags obviously.

6 Discussion and Conclusions

In the future, our lives will be surrounded by invisible embedded electronic devices, which can gather information about their environment and forward it to other devices and people. Everything will be identifiable, traceable and in some cases able to communicate with each other. RFID, along with other wireless sensing technologies, offering low-cost and high-effective communication, is a potential solution for wireless communication and the IoT.

The main obstacle of passive UHF RFID is the cost of the tags. In order to achieve the omnipresent worldwide usage of RFID, the tag fabrication costs should be as low as possible. In addition, the harmful effect of RFID tags to environment and human body should be minimized. Finally, the reliability of RFID tags in harsh environments should be improved for the long-term usage.

In this thesis, different AM methods, including inkjet printing and 3D DW dispensing, are utilized for depositing conductive inks on versatile eco-friendly substrates. The possibilities of selected conductive inks, such as nanoparticle silver ink, graphene ink, and stretchable silver ink, are studied for manufacturing UHF passive RFID tags on environment-friendly substrates: paper, cardboard, wood, and textile. The general fabrication process of passive RFID tags is illustrated in Figure 29.

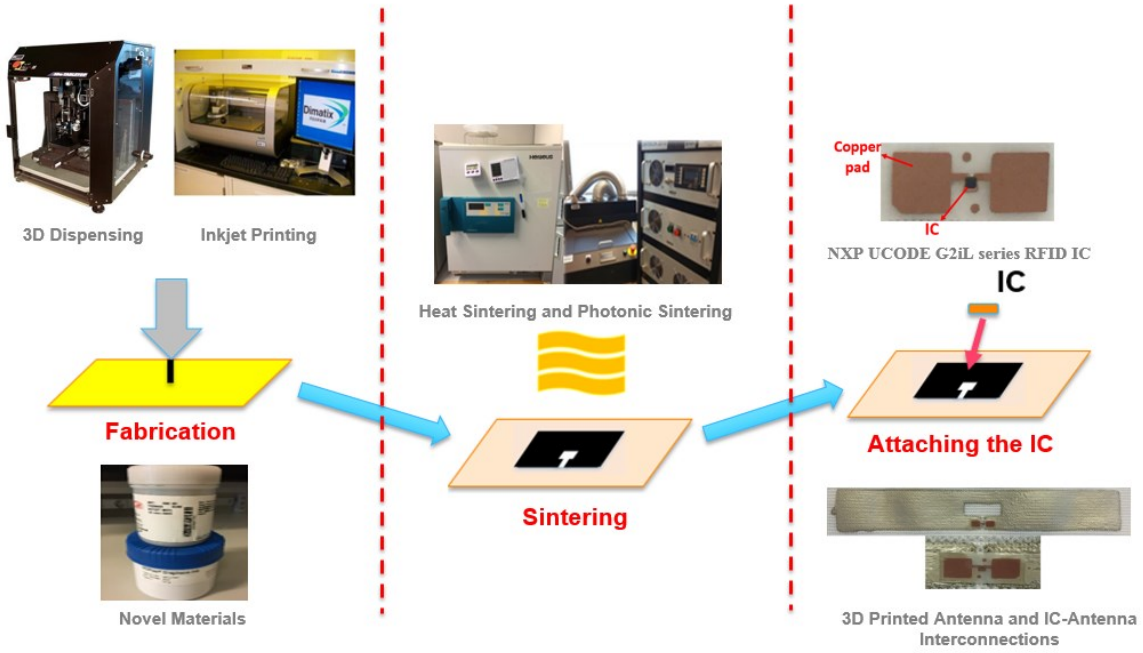

Figure 29. The illustration of the whole RFID tag fabrication process.

6.1 Discussion

Most of the passive UHF tags in this thesis show longer read ranges than 4 meters, which exceed the requirements of a number of modern RFID applications, such as patient tracking, smart logistics and supply chain, human sensing and monitoring, as well as indoor positioning. To the best of our knowledge, this thesis provides the first presentation of 3D DW dispensed graphene RFID tags [Publication III]. The previously reported graphene-based RFID tags from other research works are mainly fabricated by inkjet printing and screen printing [Kop15, Sin17, Ara16].

In addition, the reliability of RFID tags with versatile antenna-IC interconnections were firstly studied in this work [Publication VII]. Previous works mainly focus on the reliability of RFID tag antennas [Akb16b, Wan15, Sca12, Saa12]. However, in this thesis, the antenna-IC interconnections were proved to be one of the most significant factors affecting the wireless performance of RFID tags in harsh environments. Novel IC attachment methods, thus, were studied to improve the efficiency and reliability of RFID tags. The cost and time of RFID tag fabrication can be significantly reduced by depositing the antenna on IC directly, which also supports the mass production of RFID tags. The 3D DW dispensed RFID tags with embroidered antenna-IC interconnections on textile substrate achieve excellent reliability during actual use situations, including stretching, bending and immersing.

Thus, textile-based RFID tags, which are able to be integrated into clothing easily, can be the future choice of the wearable electronics industry.

6.2 Conclusions

In the thesis, main conclusions are listed below:

- AM in UHF RFID tag fabrication is a very good choice when considering environmentally friendly, affordable, high-volume manufacturing. Inkjet-printed tag on product packaging materials, such as paper, cardboard, and wood veneer, is essential to products identification and tracking due to its small size and long read range. In addition, 3D DW dispensed tag on textile substrate, which can be easily integrated into clothes, has potential to solve the tracking and remote monitoring of elder and patient.
- Although the established graphene-based RFID tags do not perform in the same high level as the tags using metallic inks, graphene-based materials are still essential for replacing the harmful and high cost metallic inks in the fabrication of IOT and sensing networks, and these prototypes can be considered a promising starting point.
- Novel antenna-IC connection methods are important to improve the tag performance. Tag with printed IC attachment, which skips one process step and thus saves significant amounts of time and costs, enables better wireless performance and simplify the fabrication procedure.
- Furthermore, when thinking about the reliability aspects, tag with embroidered IC attachment shows best performance. The immersing test represents that the tag can be utilized under the water, but more test should be carried out to evaluate the washing possibility of these tags. Previous results approved that electrotextile-based tags could survive even after 15 washing cycles [Wan15]. Bending and stretching test indicates that these tags are wearable during sports, dancing and other activities.

6.3 Short summaries of the results from the publications

In the subsequent paragraphs, the main results of the publications of this thesis are summarized.

Publication I, entitled ” Experimental Study on Inkjet-Printed Passive UHF RFID Tags on Versatile Paper-Based Substrates”, studied the possibilities of inkjet printing together with nanoparticle silver ink on various paper-based substrates. For every substrate, the printing parameters were optimized to achieve the best wireless performance. It was discovered that the performance of inkjet-printed

tags on coated substrates is significant better than on uncoated substrates, which have porous surface. Generally, more printing layers could lead to better conductivity of the deposited pattern, which improve the wireless performance of RFID tags correspondingly. However, for some substrate materials, depositing multiple layers directly does not always correspond to a higher read range. When superabundant layers are deposited, inks will spread on the substrate and destroy the shape of the designed pattern.

Publication II, entitled ” Inkjet-Printed Antenna-Electronics Interconnections in Passive UHF RFID Tags”, studied further research on inkjet printing technology with nanoparticle silver inks. In addition, in order to simplify the manufacturing process, a new IC attachment method was studied. The tag antenna is printed on top of the IC fixture directly, to replace the traditional process, i.e., the IC attachment with conductive glue. Both types of tags show satisfied performance on paper and polyimide film. Thus, inkjet-printed antenna-electronics interconnections can be considered to be promising replacements for the epoxy-glued ones in passive UHF RFID applications, and also in other wireless applications.

Publication III, entitled ” Fabrication and Performance Evaluation of 3D–Printed Graphene Passive UHF RFID Tags on Cardboard”, studied the fabrication and wireless performance of 3D-printed graphene-based passive UHF RFID tags on two different cardboard packaging substrates. Based on the results, 3D DW dispensed environment-friendly graphene antennas have great potential to replace the significantly more expensive silver-based RFID antennas.

In publications IV-VI, 3D DW dispensed RFID tags using graphene ink were studied on wood veneer and textile. The achieved read range results were compared to previously published results using the same antenna geometry and conductive ink, where the graphene tag antennas were fabricated by doctor-blading on a cardboard [Akb16a] and fabric [Akb16b] substrates. The antennas presented here show superior performance compared to the earlier results. The results achieved in this study strongly support the 3D printing of graphene-based wireless electronics. Publication V indicates that graphene-based tags with dispensed antenna-IC interconnections have slightly superior read ranges, compared to RFID tags with epoxy-glued antenna-IC interconnections. In addition, those graphene-based tags have ability to work in high humidity conditions.

Publication VII, entitled “Inkjet-Printed Antenna-Electronics Interconnections in Passive UHF RFID Tags”, studied the possibility of 3D DW dispensing on a stretchable textile substrate for RFID tag fabrication. For IC attachment, conductive epoxy glue, DW dispensing, and embroidery were used, in order to find the most reliable methods to embed wireless platforms into textiles. The results represent that tags with embroidered antenna-IC attachment on a DW dispensed antenna has the best reliability in continuous strain, as they were the only ones withstanding harsh stretching. The combi-

nation of 3D DW dispensing and embroidery is a promising fabrication approach for solving the current reliability challenges in RFID antenna-IC interconnections and for taking the next steps in establishment of textile-integrated identification and sensing platforms.

6.4 Future work

The future work will focus on the textile-based wearable RFID tags, which could be utilized around human body for the purposes of healthcare and wellbeing, such as activities monitoring, moisture and temperature sensing, as well as patient identification and tracking. Thus, the antenna design should be firstly optimized to work near the human body, which has a significant influence to the antenna performance. After that, the performance of the tags need to be measured in actual use situations, attached on the human body, in normal office or healthcare environment. Further, off-the-shelf RFID readers will be utilized in the future work to enhance the mobility of RFID system. Considering the environment issues, stretchable metallic inks should be replaced by eco-friendly inks. Thus, carbon-based inks, which have good stretchability and flexibility, will be studied in the next work. Finally, to reduce the cost of RFID tags further, chipless tags, which provides different methods of storing identification information without chip, will be studied in the future. By eliminating the use of silicon IC chips, chipless RFID tags can offer more competitive price than normal silicon IC based tags. Besides, chipless tags possess longer communication range since they do not necessitate the use of transistors as silicon based tags that require a threshold voltage to power up IC circuits. The versatile expertise about manufacturing solutions and novel materials achieved in this thesis is a significant prerequisite of future chipless RFID studies.

References

[Age16] Agezo, S., Zhang, Y., Ye, Z., Chopra, S., Vora, S., and Kurzweg, T. P., “Battery-free RFID heart rate monitoring system”, in Proceedings of IEEE Wireless Health, 25-27 October 2016, Bethesda, MD, USA, pp. 136-142.

[Akb16a] Akbari, M., Virkki, J., Sydänheimo, L., and Ukkonen, L., “The possibilities of graphene-based passive RFID tags in high humidity conditions”, in Proceedings of IEEE International Symposium on Antennas and Propagation (APSURSI), 26 June-1 July 2016, Fajardo, Puerto Rico, pp. 1269-1270.

[Akb16b] Akbari, M., Virkki, J., Sydänheimo, L., and Ukkonen, L., “Toward graphene-based passive UHF RFID textile tags: A Reliability Study”, IEEE Transactions on Device and Materials Reliability, vol. 16, pp. 429–431, 2016.

[Akb17] Akbari, M., He, H., Juuti, J., Tentzeris, M. M., Virkki, J., and Ukkonen, L., "3D printed and photonically cured graphene UHF RFID tags on textile, wood, and cardboard substrates", International Journal of Antennas and Propagation, vol. 2017, Article ID 7327398, pp. 1-8, 2017.

[Ame14] Amendola, S., Lodato, R., Manzari, S., Occhiuzzi, C., and Marrocco, G., "RFID technology for IoT-based personal healthcare in smart spaces", IEEE Internet of Things Journal, Vol. 1, pp. 144-152, 2014.

[Ami12] Amin, Y., Chen, Q., Zheng, L. R., and Tenhunen, H., “Design and fabrication of wideband archimedean spiral antenna based ultra-low cost “green” modules for RFID sensing and wireless applications”, Progress In Electromagnetics Research, Vol. 130, pp. 241–256, 2012.

[Ang05] Angeles, R., “RFID technologies: supply-chain applications and implementation issues”, Information systems management, Vol. 22, pp. 51-65, 2005.

[Ara16] Arapov, K., Jaakkola, K., Ermolov, V., Bex, G., Rubingh, E., Haque, S., ... and Friedrich, H., “Graphene screen-printed radio-frequency identification devices on flexible substrates”, Physica Status Solidi (RRL)-Rapid Research Letters, Vol.10, pp. 812-818, 2016.

[Atz10] Atzori, L., Iera, A., and Morabito, G., “The internet of things: A survey”, Computer networks, Vol. 54, pp. 2787-2805, 2010.

[Bal05] Balanis, C. A., “Antenna theory”, 3rd Edition, John Wiley & Sons, Hoboken, NJ, USA, 2005.

[Bal17] Balsamo, D., Merrett, G. V., Zaghari, B., Wei, Y., Ramchurn, S., Stein, S., ... and Beeby, S., “Wearable and autonomous computing for future smart cities: open challenges”, in Proceedings of 25th International Conference on Software, Telecommunications and Computer Networks, 21 - 23 September 2017, Split, Croatia, pp. 1-5.

[Bjö09] Björninen, T., Merilampi, S., Ukkonen, L., Sydänheimo, L., and Ruuskanen, P., "The effect of fabrication method on passive UHF RFID tag performance”, International Journal of Antennas and Propagation, vol. 2009, Article ID 920947, pp. 1-8, 2009.

[Bjö14] Björninen, T., Virkki, J., Sydänheimo, L., and Ukkonen, L., “Impact of recurrent stretching on the performance of electro-textile UHF RFID tags”, in Proceedings of the 5th Electronics System-integration Technology Conference (ESTC), 16-18 September 2014, Helsinki, Finland, pp. 1 – 5.

[Bjö15] Björninen, T., Virkki, J., Sydänheimo, L., and Ukkonen, L., “Possibilities of 3D direct write dispensing for textile UHF RFID tag manufacturing”, In Proceedings of IEEE International Symposium on Antennas and Propagation & USNC/URSI National Radio Science Meeting, 19-24 July 2015, Vancouver, BC, Canada, pp. 1316–1317.

[Bor18] Borda, RFID real-time tracking, [Accessed on 02.01.2018], Available at: http://www.bordatech.com/.

[Bue09] Buettner, M., Prasad, R., Philipose, M., and Wetherall, D., "Recognizing daily activities with RFID-based sensors", in Proceedings of the 11th international conference on Ubiquitous computing, 30 September–03 October 2009, Orlando, Florida, USA, pp.51-60.

[Cal01] Calvert, P., “Inkjet printing for materials and devices”, Chemistry of Materials, Vol. 13, pp. 3299-3305, 2001.

[Can07] Cangialosi, A., Monaly, J.E., and Yang, S.C., "Leveraging RFID in hospitals: Patient life cycle and mobility perspectives", IEEE Communications Magazine, Vol. 45, pp. 18-23, 2007.

[Cao15] Cao, Z., Shi, J. J., Torah, R. N., Tudor, M. J., and Beeby, S. P., “All dispenser printed flexible 3D structured thermoelectric generators”, Journal of Physics: Conference Series, Vol. 660, No. 1, pp. 1-5, 2015.

[Cha07] Chawla, V., and Ha, D. S., “An overview of passive RFID”, IEEE Communications Magazine, Vol. 45, No. 9, pp. 11–17, 2007.

[Cha13] Chauraya, A., Whittow, W. G., Vardaxoglou, J. Y. C., Li, Y., Torah, R., Yang, K., ... and Tudor, J., “Inkjet printed dipole antennas on textiles for wearable communications”, IET microwaves, antennas & propagation, Vol. 7, pp. 760-767, 2013.

[Che17] Chen, X., Liu, A., Wei, Z., Ukkonen, L., and Virkki, J., "Experimental study on strain reliability of embroidered passive UHF RFID textile tag antennas and interconnections", Journal of Engineering, vol. 2017, Article ID 8493405, pp. 1-7, 2017.

[Dea10] Deavours, D., and Dobkin, D., “UHF Passive RFID Tag Antennas”, in book: Guha, D., Antar, M. M., (ed.), Microstrip and Printed Antennas: New Trends, Techniques, and Applications, John Wiley & Sons Ltd, Chichester, UK, pp. 263–303, 2010.

[Der07] Derbek, V., Steger, C., Weiss, R., Preishuber-Pflügl, J., and Pistauer, M., “A UHF measurement and evaluation test system”, Elektrotechnik & Informationstechnik, Vol. 124, No. 11, pp. 384–390, 2007.

[Der08] Derby, B., “Bioprinting: inkjet printing proteins and hybrid cell-containing materials and structures”, Journal of Materials Chemistry, Vol. 18, pp. 5717-5721, 2008.

[Dob05] Dobkin, D. M., and Weigand, S. M., “Environmental effects on RFID tag antennas”, in Proceedings of the IEEE MTT-S International Microwave Symposium, 12–17 June 2005, Long Beach, CA, USA, pp. 135–138.

[Dob08] Dobkin, D. M., “The RF in RFID: UHF RFID in practice”, 2nd Edition, Newnes, 2012.

[Dup18] Dupont, PE872 stretchable silver conductor, [Accessed on 02.01.2018], Available at: http://www.dupont.com/content/dam/dupont/products-and-services/electronic-and-electrical-materials/documents/prodlib/PE873.pdf

[Dow09a] Dowling, J., Tentzeris, M., and Beckett, N., "RFID-enabled temperature sensing devices: A major step forward for energy efficiency in home and industrial applications?", in Proceedings of IEEE MTT-S International Microwave Workshop on

Wireless Sensing, Local Positioning, and RFID, 24-25 September 2009, Cavtat, Croatia, pp. 24-25.

[Dow09b] Dowling, J., and Tentzeris, M., ""Smart house" and "smart-energy" applications of low-power RFID-based wireless sensors", in Proceedings of Asia Pacific Microwave Conference, 7-10 December 2009, Singapore, pp. 2412-2415.

[Fal11] Falat, T., Felba, J., Platek, B., Piasecki, T., Moscicki, A., and Smolarek, A., "Low-temperature, photonic approach to sintering the ink-jet printed conductive microstructures containing nano sized silver particles", in Proceedings of the 18th European Conference on Microelectronics and Packaging (EMPC), 12-15 September 2011, Brighton, UK, pp. 1-4.

[Fen11] Fennani, B., Hamam, H., and Dahmane, A. O., "RFID overview", in Proceedings of the International Conference on Microelectronics (ICM), 19-22 December 2011, Hammamet, Tunisia, pp. 1-5.

[Fin03] Finkenzeller, K., "RFID handbook: fundamentals and applications in contactless smart cards and identification", 2nd Edition, John Wiley & Sons Ltd, Chichester, UK, 2003.

[Fry05] Fry, E. A., and Lenert, L. A., "MASCAL: RFID tracking of patients, staff and equipment to enhance hospital response to mass casualty events", In Proceedings of AMIA Annual Symposium, 22-26 October, 2005, Washington, USA, pp. 261-265.

[Fuj18] Fujifilm, Dimatix materials printer DMP-2831, [Accessed on 02.01.2018], Available at: http://www.fujifilmusa.com/shared/bin/DMP-2831_Datasheet_05-13.pdf

[Gib15] Gibson, I., Rosen, D., and Stucker, B., "Additive manufacturing technologies: 3D printing, rapid prototyping, and direct digital manufacturing", Second Edition, New York: Springer, 2015.

[Goo12] Goosey, M., "A short introduction to graphene and its potential interconnect applications", Circuit World, Vol. 38, pp. 83-86, 2012.

[Goo18] Goodfellow USA, Screen printable functionalized graphene ink, [Accessed on 02.01.2018], Availabe at: http://www.goodfellowusa.com/news-article/screen-printable-functionalized-graphene-ink/.

[Gub13] Gubbi, J., Buyya, R., Marusic, S., & Palaniswami, M., “Internet of Things (IoT): A vision, architectural elements, and future directions”, Future generation computer systems, Vol. 29, pp. 1645-1660, 2013.

[Hal11] Halonen, E., Pynttäri, V., Lilja, J., Sillanpää, H., Mäntysalo, M., Heikkinen, J., Mäkinen, R., Kaija, T., and Salonen, P., “Environmental protection of inkjet-printed Ag conductors”, Microelectronics Engineering, Vol. 88, No.9, pp. 2970–2976, 2011.

[Hal13] Halonen E., “Integration of inkjet-printing and processing into manufacturing for flexible electronics[M] “, Tampereen teknillinen yliopisto, 2013.

[Har18] Harima Chemicals Group, Harima NPS-JL datasheet, [Accessed on 02.01.2018], Available at: https://www.harima.co.jp/en/products/electronics/pdf/brochure16e_23.pdf.

[Hop18] Hopeland Technologies CO. Ltd., RFID in supply chain management, [Accessed on 02.01.2018], Available at: http://www.hopelandrfid.com/blog/rfid-in-supply-chain-management_b34.

[Hua15] Huang, X., Leng, T., and Zhang, X., et al., “Binder-free highly conductive graphene laminate for low cost printed radio frequency applications”, Applied Physics Letters, vol. 106, no. 20, Article ID 203105, pp. 1-4, 2015.

[Jun15] Jung, Y. H., Chang, T.-H., Zhang, H., Yao, C., Zheng, Q., Yang, V. W., Mi, H., Kim, M., Cho, S. J., Park, D.-W., Jiang, H., Lee, J., Qui, Y., Zhou, W., Cai, Z., Gong, S., and Ma, Z., “High-performance green flexible electronics based on biodegradable cellulose nanofibril paper”, Nature Communications, Vol. 6, Article ID 7170, pp. 1-11, 2015.

[Kam10] Kamarulazizi, K., and Ismail, W., “Electronic toll collection system using passive rfid technology”, Journal of Theoretical & Applied Information Technology, Vol.22, pp. 70-76, 2010.

[Kan11] Kang, J. S., Ryu, J., Kim, H. S., and Hahn, H. T., “Sintering of inkjet-printed silver nanoparticles at room temperature using intense pulsed light”, Journal of Electronic Materials, Vol. 40, No. 11, pp. 2268–2277, 2011.

[Kar03] Kärkkäinen, M., “Increasing efficiency in the supply chain for short shelf life goods using RFID tagging”, International Journal of Retail & Distribution Management, Vol. 31, pp. 529-536, 2003.

[Kar10] Karmakar, N. C., (Ed.)., “Handbook of smart antennas for RFID systems”, New Jersey: Wiley, 2010.

[Kel12] Kellomäki, T., Virkki, J., Merilampi, S., and Ukkonen, L., “Towards washable wearable antennas: a comparison of coating materials for screen-printed textile-based UHF RFID tags”, International Journal of Antennas and Propagation, vol. 2012, Article ID 476570, pp. 1-11, 2012.

[Ken09] Kennedy T, Fink P, Chu A, Champagne N, Gregory Y, Lin G and Khayat M., ”Body-worn E-textile antennas: the good, the low-mass, and the conformal”, IEEE Transactions on Antennas and Propagation, Vol. 57, pp. 910–918, 2009.

[Kim13] Kim, S., Riccardo, M., Bozzi, M., Nikolaou, S., and Tentzeris, M. M., “Inkjet-printed wearable microwave components for biomedical applications”, in Proceedings of 7th European Conference on Antennas and Propagation (EuCAP), 8-12 April 2013, Gothenburg, Sweden, pp. 1926-1929.

[Kim15] Kim, S., Kawahara, Y., Georgiadis, A., Collado, A., and Tenzeris, M. M., “Low-cost inkjet-printed fully passive RFID tags for calibration-free capacitive/haptic sensor applications”, IEEE Sensors Journal, Vol. 15, No. 6, pp. 3135–3145, 2015.

[Koc07] Koch, J., Wettach, J., Bloch, E., and Berns, K., "Indoor localisation of humans, objects, and mobile robots with RFID infrastructure", in Proceedings of 7th International Conference on Hybrid Intelligent Systems, 17-19 September 2007, Kaiserlautern, Germany, pp. 271-276.

[Kop15] Kopyt, P. et al., “Graphene-based dipole antenna for a UHF RFID tag", IEEE Transactions on Antennas and Propagation, vol. 64, no. 7, pp. 2862-2868, 2015.

[Lew04] Lewis, J. A. and Gratson, G. M., “Direct writing in three dimensions,” Materials Today, vol. 7, no. 7 – 8, pp. 32 – 39, 2004.

[Li07] Li, B., Roy, T. D., Smith, C. M., Clark, P. A., and Church, K. H., “A robust true direct print technology for tissue engineering”, in Proceedings of ASME 2007 International Manufacturing Science and Engineering Conference, 15–18 October 2007, pp. 103–108, Atlanta, Georgia, USA.

[li15] Li, Y., Torah, R., Beeby, S., and Tudor, “Fully direct-write dispenser printed dipole antenna on woven polyester cotton fabric for wearable electronics applications”, Electronics Letters, Vol. 51, pp. 1306-1308, 2015.

[Lim13] Lim, S., Joyce, M., Fleming, P. D., and Aijazi, A. T., “Inkjet printing and sintering of nano-copper ink”, Journal of Science and Technology, Vol. 57, No. 5, pp. 505061–505067, 2013.

[Lin10] Lin, X., Lu, R., Kwan, D., and Shen, X. S., “REACT: An RFID-based privacy-preserving children tracking scheme for large amusement parks”, Computer Networks, Vol. 54, pp. 2744-2755, 2010.

[Lon15] Long, F., Zhang, X. D., Björninen, T., Virkki, J., Sydänheimo, L., Chan, Y. C., and Ukkonen, L., “Implementation and wireless readout of passive UHF RFID strain sensor tags based on electro-textile antennas”, In Proceedings of 9th European Conference on Antennas and Propagation, 13-17 April 2015, Lisbon, Portugal, pp. 1-5.

[Mää11] Määttänen, K., Nummela, J., Ukkonen, L., and Sydänheimo, L., “Utilizing UHF RFID in supply chains: examples from similarities in paper and cell phone industries”, International Journal of Latest Trends in Computing, Vol. 2, No. 3, pp. 398-405, 2011.

[Man12] Manzari, S., Occhiuzzi, C., and Marrocco, G., “Feasibility of body-centric systems using passive textile RFID tags”, IEEE Antennas and Propagation Magazine, Vol. 54, pp. 49-62, 2012.

[Mer16] Merilampi, S., He, H., Sydänheimo, L., Ukkonen, L., and Virkki, J., “The possibilities of passive UHF RFID textile tags as comfortable wearable sweat rate sensors”, In Proceedings of Progress in Electromagnetic Research Symposium (PIERS), 8-11 August 2016, Shanghai, China, pp. 3984-3987.

[Mic05] Michael, K., and McCathie, L., “The pros and cons of RFID in supply chain management”, In Proceedings of International Conference on Mobile Business, 11–13 July 2005, Sydney, NSW, Australia, pp. 623-629.

[Moh02] Mohebi, M. M., and Evans, J. R., “A drop-on-demand inkjet printer for combinatorial libraries and functionally graded ceramics”, Journal of combinatorial chemistry, Vol. 4, pp 267-274, 2002.

[Mor09] Mortara, L., Hughes, J., Ramsundar, P. S., Livesey, F., and Probert, D. R., “Proposed classification scheme for direct writing technologies”, Rapid Prototyping Journal, vol. 15, no. 4, pp. 299 – 309, 2009.

[Mor12a] Moradi, E., Bjorninen, T., Ukkonen, L., and Rahmat-Samii, Y., “Effects of sewing pattern on the performance of embroidered dipole-type RFID tag antennas”, IEEE Antennas and Wireless Propagation Letters, Vol. 11, pp. 1482–1485, 2012.

[Mor12b] Moro, R., Bozzi, M., Kim, S., and Tentzeris, M., “Novel inkjet-printed substrate integrated waveguide (SIW) structures on low-cost materials for wearable applications”, in Proceedings of 42nd European Microwave Conference (EuMC), 29 October-1 November 2012, pp. 72-75.

[Naj11] Najera, P., Javier, L., and Rodrigo, R., "Real-time location and inpatient care systems based on passive RFID", Journal of Network and Computer Applications, Vol. 34, pp. 980-989, 2011.

[Nay15] Nayak, R., Singh, A., Padhye, R., and Wang, L., “RFID in textile and clothing manufacturing: technology and challenges”, Fashion and Textiles, Vol. 2, pp. 1-16, 2015.

[NXP14] NXP Semiconductors, NXP UCODE G2iL and G2iL+ datasheet, [Accessed on 02.01.2018], Available at: https://www.nxp.com/products/identification-and-security/smart-label-and-tag-ics/ucode/ucode-g2il-and-g2il-plus:SL3S1203_1213.

[Ore11] Orecchini, G., Alimenti, F., Palazzari, V., Rida, A., Tenzeris, M. M., and Roselli, L., “Design and fabrication of ultralow cost radio frequency identification antennas and tags exploiting paper substrates and inkjet printing technology”, IET Microwaves, Antennas & Propagation, Vol. 5, No. 8, pp. 993–1001, 2011.

[Par07] Park, B.K., Kim, D., Jeong, S., Moon, J., and Kim, J.S., “Direct writing of copper conductive patterns by ink-jet printing”, Thin Solid Films, Vol. 515, No. 19, pp. 7706–7711, 2007.

[Par14] Park, S.-H., and Kim, H.-S., “Flash light sintering of nickel nanoparticles for printed electronics”, Thin Solid Films, Vol. 550, pp. 575–581, 2014.

[Par16] Patron D, et al., “On the use of knitted antennas and inductively coupled RFID tags for wearable applications”, IEEE Trans. Biomed. Circuits Syst., Vol. 10, No. 6, pp. 1047-1057, 2016.

[Pen06] Penttilä, K., Keskilammi, M., Sydänheimo, L., and Kivikoski, M., “Radio frequency technology for automated manufacturing and logistics control. Part 2: RFID antenna utilisation in industrial applications”, The International Journal of Advanced Manufacturing Technology, Vol. 31, pp.116-124, 2006.

[Per08] Perelaer, J., de Laat, A. W., Hendriks, C. E., and Schubert, U. S., “Inkjet-printed silver tracks: low temperature curing and thermal stability investigation”, Journal of Materials Chemistry, Vol. 18, pp. 3209-3215, 2008.

[Per12a] Perelaer, J., Abbel, R., Wünscher, S., Jani, R., van Lammeren, T., and Schubert, U. S., “Roll-to-roll compatible sintering of inkjet printed features by photonic and microwave exposure: from non-conductive ink to 40% bulk silver conductivity in less than 15 seconds”, Advanced Materials, Vol. 24, No. 19, pp. 2620–2625, 2012.

[Per12b] Pérez, M. M., Cabrero-Canosa, M., Hermida, J. V., García, L. C., Gómez, D. L., González, G. V., & Herranz, I. M., “Application of RFID technology in patient tracking and medication traceability in emergency care”, Journal of medical systems, Vol. 36, pp. 3983-3993, 2012.

[Rak14] Rakibet, O.O., Rumens, C.V., Batchelor, J.C., and Holder, S.J., “Epidermal passive RFID strain sensor for assisted technologies." IEEE Antennas and Wireless Propagation Letters, Vol. 13, pp. 814-817, 2014.

[Rao05] Rao, K. V. S., Nikitin, P. V., and Lam, S. F., “Impedance matching concepts in RFID transponder design”, in Proceedings of the 4th IEEE Workshop on Automatic Identification Advanced Technologies (AutoID'05), 17-18 October 2005, Buffalo, NY, USA, pp. 39–42.

[Rid09] Rida, A., Yang, L., Vyas, R., and Tenzeris, M. M., “Conductive inkjet-printed antennas on flexible low-cost paper-based substrates for rfid and wsn applications”, IEEE Antennas and Propagation Magazine, Vol. 51, No. 3, pp. 13–23, 2009.

[Rie07] Rieback, M. R., Crispo, B., and Tanenbaum, A. S., “Keep on blockin’ in the free world: Personal access control for low-cost RFID tags”, Security Protocols, Springer Berlin Heidelberg, Vol. 4631, pp. 51-50, 2007.

[Riz17] Rizwan, M., et al. "Possibilities of fabricating copper-based RFID tags with photonic-sintered inkjet printing and thermal transfer printing", IEEE Antennas and Wireless Propagation Letters, Vol. 16, pp. 1828–1831, 2017.

[Ros15] Rose, D.P., et al., "Adhesive RFID sensor patch for monitoring of sweat electrolytes", IEEE Transactions on Biomedical Engineering, Vol. 62, pp. 1457-1465, 2015.

[Ryu11] Ryu, J., Kim, H.-S., and Hahn, T., “Reactive sintering of copper nanoparticles using intense pulsed light for printed electronics”, Journal of Electronic Materials, Vol. 40, No, 1, pp. 42–50, 2011.

[Saa12] Saarinen, K., and Frisk, L., “Reliability of UHF RFID tags in humid environments”, In Proceedings of 14th Electronics Packaging Technology Conference (EPTC), 05-07 December 2012, Singapore, pp. 180-184.

[Saj15] Sajid, M., Ilyas, M., Basheer, C., Tariq, M., Daud, M., Baig, N., and Shehzad, F., “Impact of nanoparticles on human and environment: review of toxicity factors, exposures, control strategies, and future prospects”, Environmental Science and Pollution Research, Vol. 22, No. 6, pp. 4122–4143, 2015.

[Sca12] Scarpello, M. L., Kazani, I., Hertleer, C., Rogier, H., and Ginste, D. V., “Stability and efficiency of screen-printed wearable and washable antennas”, IEEE Antennas Wireless Propag. Lett., vol. 11, pp. 838–841, 2012.

[Sha14] Shao, S., Kiourti, A., Burkholder, R., and Volakis, JL., “Flexible and stretchable UHF RFID tag antennas for automotive tire sensing”, In Proceedings of 8th Europe Conference on Antennas Propagation (EuCAP), 6-11 April 2014, The Hague, Netherlands, pp. 2908-2910.

[Shi13] Shin, K.-Y., Lee, M., Kang, H., Kang, K., Hwang, J. Y., Kim, J.-M., Lee, and S.-H., “Characterization of inkjet-printed silver pattern for application to printed circuit board (PCB)”, Journal of Electrical Engineering &Technology, Vol. 8, No. 3, pp. 603–609, 2013.

[Sin17] Singh, R., Singh, E., and Nalwa, H. S., “Inkjet printed nanomaterial based flexible radio frequency identification (RFID) tag sensors for the internet of nanothings”, RSC Advances, Vol.7, pp. 48597-48630, 2017.

[Sir03] Sirringhaus, H., and Shimoda, T., “Inkjet printing of functional materials”, MRS bulletin, Vol. 28, pp. 802-806, 2003.

[The03] Therriault, D., White, S. R., and Lewis, J. A., “Chaotic mixing in three-dimensional microvascular networks fabricated by direct-write assembly”, Nature Materials, vol. 2, pp. 265 – 271, 2003.

[Van14] Van-Daele, P., Moerman, I., and Demeester, P., “Wireless body area networks: status and opportunities”, in Proceedings of General Assembly and Scientific Symposium (URSI GASS), 16-23 August 2014, Beijing, China, pp. 1-4.

[Vir12a] Virtanen, J., Virkki, J., Elsherbeni, A. Z., Sydänheimo, L., and Ukkonen, L., “A selective ink deposition method for the cost-performance optimization of inkjet-printed UHF RFID tag antennas”, International Journal of Antennas and Propagation, vol. 2012, Article ID 801014, pp. 1-9, 2012.

[Vir12b] Virtanen, J., Virkki, J., Ukkonen, L., and Sydänheimo, L., “Inkjet-printed UHF RFID tags on renewable materials”, Advances in Internet of Things, Vol. 2, pp. 79-85, 2012.

[Vir13a] Virtanen, J., Virkki, J., Sydänheimo, L., Tenzeris, M., and Ukkonen, L., ”Automated identification of plywood using embedded inkjet-printed passive UHF RFID tags”, IEEE Transactions on Automation Science and Engineering, Vol. 10, No. 3, pp. 796–806, 2013.

[Vir13b] Virkki, J., Björninen, T., Merilampi, S., Sydänheimo, L., and Ukkonen, L., “Manufacturing and applications of screen-printed RFID tags on paper substrate”, in Proceedings of the Progress in Electromagnetics Research Symposium (PIERS), 12-15 August 2013, Stockholm, Sweden, pp. 562–566.

[Vir15] Virili, M., Roselli, L., Alimenti, F., Mezzanotte, P., Moscato, S., Silvestri, L., ... and Perregrini, L., “GRETA approach towards new green material technologies”, In Proceedings of 2015 International EURASIP Workshop on RFID Technology (EURFID), 22-23 October 2015, Rosenheim, Germany, pp. 9-15.

[Vou10] Voulodimos, A. S., Patrikakis, C. Z., Sideridis, A. B., Ntafis, V. A., and Xylouri, E. M. A., “Complete farm management system based on animal identification using RFID technology”, Computers and Electronics in Agriculture, Vol. 70, pp. 380-388, 2010.

[Vya09] Vyas, R., Lakafosis, V., Rida, A., Chaisilwattana, N., Travis, S., Pan, J., and Tenzeris, M. M., ”Paper-based RFID-enabled wireless platforms for sensing applications”, IEEE Transactions on Microwave Theory and Techniques, Vol. 57, No. 5, pp. 1370–1382, 2009.

[Wan06] Want, R., “An introduction to RFID technology”, IEEE Pervasive Computing, Vol. 5, No. 1, pp. 25–33, 2006.

[Wan15] Wang, S., Chong, N., Virkki, J., Björninen, T., Sydänheimo, L., and Ukkonen, L., “Towards washable electro-textile UHF RFID tags: reliability study of epoxy-coated copper fabric antennas”, International Journal of Antennas and Propagation. 2015.

[Wei05] Weinstein, R., "RFID: a technical overview and its application to the enterprise", IT professional 7.3 (2005): 27-33.

[Whi14] Whittow, W. G., Chauraya, A., Vardaxoglou, J. C., Li, Y., Torah, R., Yang, K., ... and Tudor, J., “Inkjet-printed microstrip patch antennas realized on textile for wearable applications”, IEEE Antennas and Wireless Propagation Letters, Vol. 13, pp. 71-74, 2014.

[Wyl06] Wyld, D. C., "RFID 101: the next big thing for management. Management Research News", Management Research News, Vol. 29, pp. 154-173, 2006.

[Zhe14] Zheng, Y.L., Ding, X.R., Poon, C.C.Y., Lo, B.P.L., Zhang, H., Zhou, X.L., and Zhang, Y.T., "Unobtrusive sensing and wearable devices for health informatics", IEEE Trans. Biomed. Eng. Vol. 61, pp. 1538–1554, 2014.

ORIGINAL PAPERS

Publication I

H. He, L. Sydänheimo, J. Virkki, and L. Ukkonen, “Experimental Study on Inkjet-Printed Passive UHF RFID Tags on Versatile Paper-Based Substrates’’, International Journal of Antennas and Propagation, Vol. 2016, Article ID 9265159, 8 pages, 2016, doi:10.1155/2016/9265159.

Hindawi Publishing Corporation
International Journal of Antennas and Propagation
Volume 2016, Article ID 9265159, 8 pages
http://dx.doi.org/10.1155/2016/9265159

Research Article

Experimental Study on Inkjet-Printed Passive UHF RFID Tags on Versatile Paper-Based Substrates

Han He, Lauri Sydänheimo, Johanna Virkki, and Leena Ukkonen

Department of Electronics and Communications Engineering, Tampere University of Technology, P.O. Box 692, 33101 Tampere, Finland

Correspondence should be addressed to Han He; han.he@tut.fi

Received 13 May 2016; Accepted 13 July 2016

Academic Editor: Rocco Guerriero

We present the possibilities and challenges of passive UHF RFID tag antennas manufactured by inkjet printing silver nanoparticle ink on versatile paper-based substrates. The most efficient manufacturing parameters, such as the pattern resolution, were determined and the optimal number of printed layers was evaluated for each substrate material. Next, inkjet-printed passive UHF RFID tags were fabricated on each substrate with the optimized parameters and number of layers. According to our measurements, the tags on different paper substrates showed peak read ranges of 4–6.5 meters and the tags on different cardboard substrates exhibited peak read ranges of 2–6 meters. Based on their wireless performance, these inkjet-printed paper-based passive UHF RFID tags are sufficient for many future wireless applications and comparable to tags fabricated on more traditional substrates, such as polyimide.

1. Introduction

The development of the Internet of Things has created a need for cost-effective wireless electronics on environmentally friendly substrates. Great potential lies especially in inkjet printing and inkjet-printed antennas [1–3]. Particularly RFID (radiofrequency identification) tag antennas printed on versatile substrates and the use of renewable substrate materials, such as paper and cardboard, provide endless opportunities. Paper and cardboard have a wide range of properties based on their composition; they can be flexible, rigid, soft, and coarse, and they may absorb or repel water. Paper and cardboard are also available with textured surfaces. These paper-based materials are indispensable materials in the packaging and graphics industry, which also makes them an interesting substrate material for printed RFID tag antennas [4–6]. However, the optimized printing parameters need to be studied first.

RFID technology is a wireless identification technology to automatically identify and track physical objects or people by using radiofrequency waves. When using RFID tags for identification, multiple devices can be read simultaneously and a line-of-sight is not necessary [7]. Passive UHF (ultra high frequency) RFID technology shows promise in embedded applications: passive tags require very little maintenance because no battery change is required. Also the read ranges of passive UHF RFID systems are longer compared to other RFID frequencies [8, 9]. The signal from the reader is necessary for a passive tag to power up the IC (integrated circuit) and reply to the reader.

The goal of this paper is to study the possibility of inkjet printing on various paper and cardboard substrates and to optimize the printing parameters in order to effectively fabricate passive UHF RFID tags on these substrates. The ready RFID tags are evaluated for their wireless performance and compared to tags fabricated on a more traditional polyimide substrate.

2. Manufacturing of Passive UHF RFID Tags

2.1. Material and Tools. The used ink was Harima NPS-JL silver nanoparticle ink [10] and the main specifications of the silver ink are shown in Table 1. In this study, the ink deposition was completed with Fujifilm Dimatix DMP-2831 material inkjet printer. A 10 pL volume cartridge,which has a

Table 1: Specifications of the utilized ink [10].

Ink	Ag NPS-JL NanoPaste®
Solid content (wt%)	52–57
Particle size (nm)	5–12
Average particle size (nm)	7
Resistivity ($\mu\Omega$·cm)	4–6
Viscosity (mPa·s)	11.5 (measured at 20°C and 60 rpm)
Recommended thermal curing	120–150°C for 60 minutes

Table 2: Substrate properties.

Substrate	Thickness	Speciation
Paper A	100 μm	Uncoated paper
Paper B	80 μm	Coated, calendered
Paper C	80 μm	Double coated: film + blade
Cardboard A	500 μm	Double coated: film + blade
Cardboard B	500 μm	Base board

snap-in replaceable print head with 16 nozzles, was applied for ejecting the drops.

The substrate material plays a big role in additive RFID tag manufacturing. Different substrate materials need different printing parameters, because they have different surface properties and morphologies. In [5] the dielectric characteristics of paper were investigated in the UHF range and the relative permittivity (3.2–3.5) and loss tangent (0.006–0.008) of commercial paper were studied by using a microstrip ring resonator. It should also be noted that the reported values are not constant and, in addition to frequency, they will vary with, for example, temperature and humidity. In this study, several types of paper and cardboard materials were selected for inkjet printing and the properties (calendered/noncalendered, coated/noncoated) of these substrates are shown in Table 2. Furthermore, calendaring is a process that uses series of hard pressure rollers to form or smooth a sheet of material, such as paper or cardboard. A coating is a covering that is applied to the surface of the paper or cardboard by the manufacturer. With a glossy or matte finish, a coated substrate generally has very smooth surface and the coating can restrict the amount of ink that is absorbed by the substrate material. The substrates used in this experiment are blade coated and/or film coated.

2.2. Printing Parameters. There are several parameters that can affect the printing quality, such as the jetting pulse shape, the jetting frequency, the jetting voltage, and the temperature of the ink cartridge, as well as the pattern resolution. The used jetting pulse shape is shown in Figure 1. In this research, three active nozzles were used for inkjet printing. To ensure that the ink droplets jetted to each substrate attach well on the substrate surface, without unnecessary spreading, we did preliminary tests on droplets. Normally, the drop spacing, which decides the printing resolution, is defined as the distance between the centers of two adjacent droplets. On this printer, the drop spacing must be equal on both the X and Y directions. On the X direction, the drop spacing is always set manually. On the Y direction, the drop spacing is defined by the cartridge tilt angle between the X direction (axe of displacement of the print carriage) and the axe of the nozzles, which are regularly spaced by 254 μm. An angle of 90° corresponds to the maximum achievable drop spacing (254 μm). Decreasing the drop spacing corresponds to increasing the pattern resolution. Depending on the interaction of the ink with the substrate, the drop size of the ink on different substrate materials can be different. Usually, the appropriate droplet spacing is equal to the radius of the drop, which can then decide the printing resolution. If the resolution is too low, the droplets may not overlap, while if the resolution is too high, overspreading of the ink might occur causing the loss of the pattern shape [11]. Figure 2 shows the microscope images of the silver nanoparticle ink droplets on all substrates, and the selected resolution of every substrate is listed in Table 3. In addition, Table 4 indicates the printing parameters, which were kept identical for all substrates.

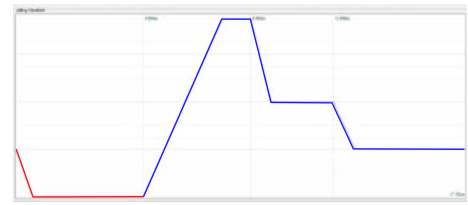

Figure 1: The used jetting pulse shape.

2.3. Number of Printed Layers. After finding the optimized printing parameters, simple lines with dimensions of 5 mm × 30 mm were printed on each substrate to study the optimal number of layers. In theory, when the antenna design and the substrate are the same, antennas with better conductivity (lower DC resistance) should have higher read ranges. Based on the datasheet of the ink, the sintering was done at 150°C for 60 minutes to maximize the conductivity of the printed layer [10]. The resistances of the lines were measured from corner to corner using Fluke 111 True RMS Multimeter. The measurement was repeated 4 times and then the average value was calculated. The measured resistances are presented in Table 5. In addition, Figure 3 shows the printed line patterns on all substrates and the surface magnified images from optical microscope can be seen in Figure 4.

One-layer lines were firstly printed on Cardboard A, and they showed no conductivity. But from Figure 4(a), it can be observed that the edge of line is metallic, while the central area of the line pattern is black. Next, lines with multiple layers were printed on this substrate as a comparison. A normal method for fabricating multilayer patterns is printing multiple layers directly before sintering. The two-layer lines on Cardboard A were also dielectric, but the metallic area increased. Figure 4(b) shows that the eight-layer lines on Cardboard A become more metallic and the resistance is correspondingly lower, around 14 Ω. Based on the analyses above, it is apparent to summarize that the metallic part increases with the number of printed layers.

Table 3: Printing resolution of every substrate.

Substrate	Average drop size (μm)	Angle (degree)	Resolution (dpi)
Paper A	110	11.4	508
Paper B	90	9.1	635
Paper C	95	10.2	564
Cardboard A	90	9.1	635
Cardboard B	105	11.4	508

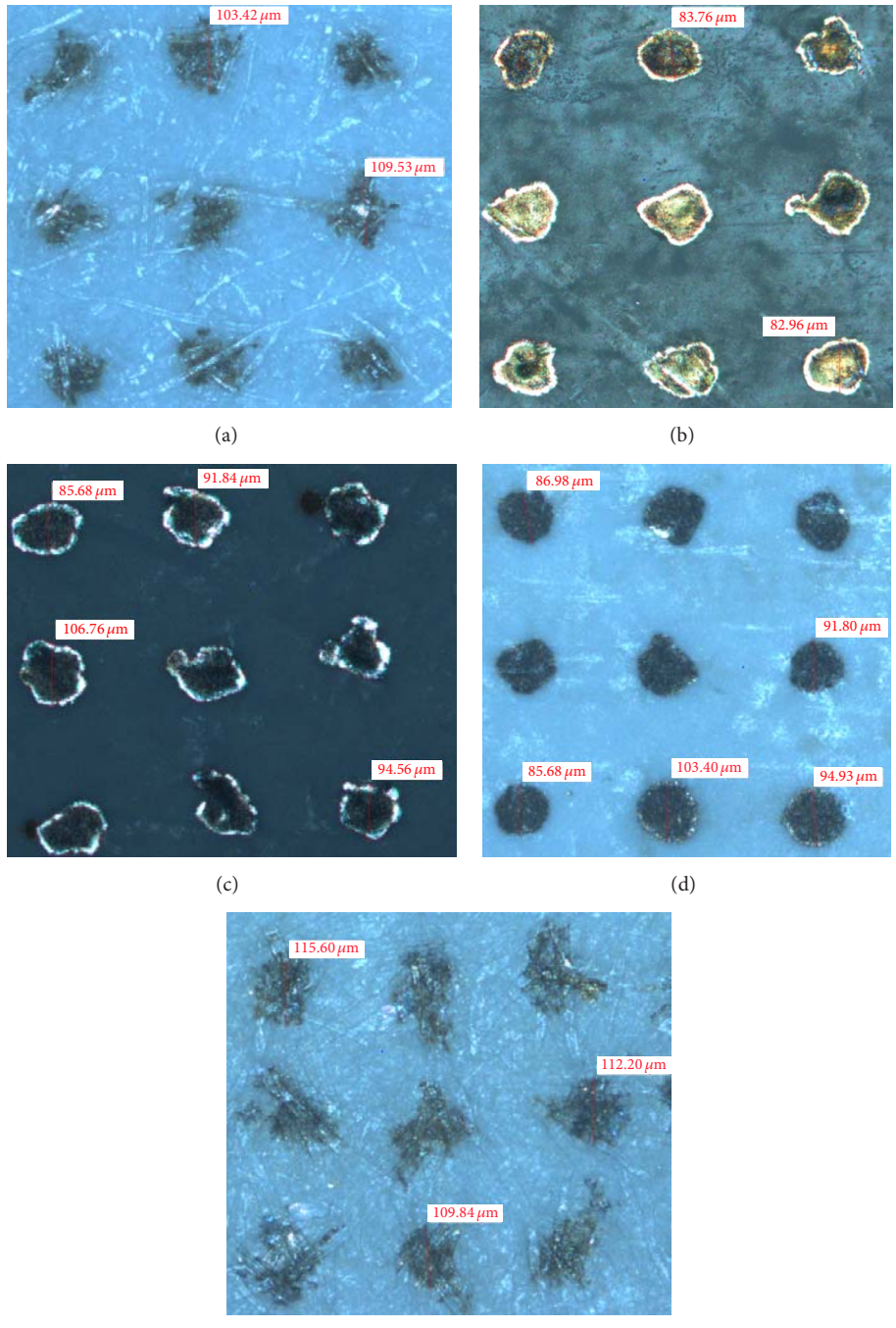

Figure 2: Droplet size test on all substrates: (a) droplets on Paper A, (b) droplets on Paper B, (c) droplets on Paper C, (d) droplets on Cardboard A, and (e) droplets on Cardboard B.

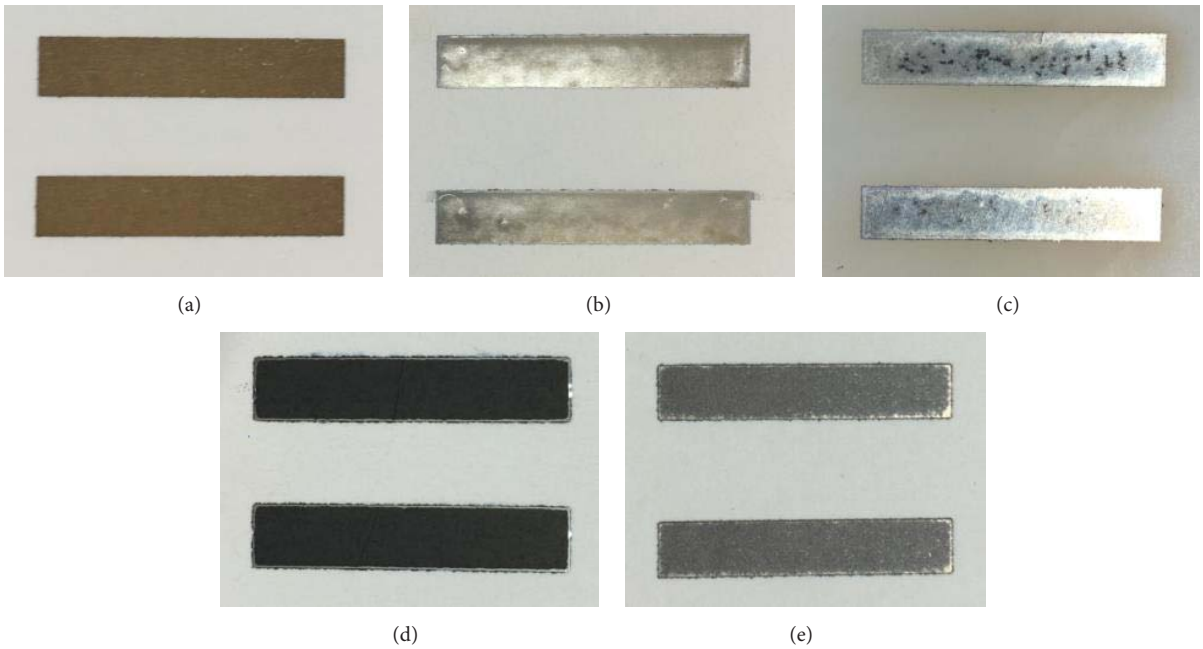

Figure 3: Inkjet-printed line patterns for fabrication optimization: (a) four-layer lines on Paper B, (b) four-layer lines on Paper A, (c) four-layer lines on Paper C, (d) four-layer lines on Cardboard A, and (e) four-layer lines on Cardboard B.

Table 4: Printing parameters.

Cartridge temperature (°C)	40
Platen temperature (°C)	50
Jetting voltage (V)	28
Jetting frequency (kHz)	23
Sintering time (minutes)	60
Sintering temperature (°C)	150

Another approach to manufacture the pattern with multiple layers is to repeat the process of printing and sintering. On this way, two printing-sintering rounds were carried out. At each turn, one-layer, two-layer, and four-layer lines were printed on Cardboard A and sintered in the oven. After that, the average resistance of those lines was measured, and they were found to be 5 Ω, 0.8 Ω, and 0.3 Ω, respectively. The major shortcoming of this method, along with the long manufacturing time, is that different layers are hard to be aligned perfectly.

The conductivity of the lines on Cardboard B was not good. The resistances of the four-layer lines and the eight-layer lines were found to be 2.5 MΩ and 161 Ω, respectively. Figure 4(c) shows the surface magnified image of the four-layer line, where the ink is absorbed by the substrate and the surface of the printed pattern is predominantly black with silver area inside. The metallic parts are not sufficient to form a good conductive trace, so the resistance is extremely high. Due to the poor performance, we chose not to try several printing-sintering rounds on Cardboard B.

On Paper A, the inkjet-printed lines showed no conductivity even with eight printed layers. The surface of the four-layer line is mostly black and no coherent metallic trace formed after sintering, which is shown in Figure 4(d) as an example. As with Cardboard B, due to the bad performance, we chose not to try several printing-sintering rounds.

On Paper B, the one-layer lines obtained good conductivity after sintering and the resistance was measured to be around 1.8 Ω. As shown in Figure 4(e), the surface is totally metallic although there are some small black holes and thin gaps. The possible reason is the inadequacy of the ink when only one layer is selected. As the number of the printed layers increases, the surface of the printed line becomes more homogenous. Thereby, the conductivity of the line increases with the number of layers. As the performance was excellent already after one layer, several printing-sintering rounds were not needed.

The two-layer lines on Paper C show tolerable conductivity as the average resistance is around 9.8 Ω, although the surface of the printed line is partially black, as shown in Figure 4(f). A continuous metallic pattern is formed when four layers and eight layers are applied. Again, multilayer printing brings much more ink and a greater thickness of silver film and therefore a lower resistance. As the performance was suitable already after four layers, several printing-sintering rounds were not needed.

2.4. Tag Fabrication Process. After finding the optimized printing parameters and the optimal number of layers, passive UHF RFID tag antennas were fabricated on Paper B, Paper C, Cardboard A, and Cardboard B. The tag antenna

Table 5: Resistances of printed lines on all substrates.

Substrate	Total layer(s)	Resistance (Ω)	Description
Paper A	2	∞	Not conductive, absorbed
	4	∞	Not conductive, absorbed
	8	∞	Not conductive, absorbed
Paper B	1	1.8	Good conductivity, totally metallic
	2	0.8	Good conductivity, totally metallic
	4	0.3	Good conductivity, totally metallic
Paper C	2	9.7	Good conductivity, mostly metallic
	4	2.8	Good conductivity, totally metallic
	6	2.1	Good conductivity, totally metallic
Cardboard A	1	∞	The edge of line is metallic, mostly black
	2	∞	The edge of line is metallic, mostly black
	4	79	The edge of line is metallic, mostly black
	6	14	The edge of line is metallic, mostly black
	8	1.3	The edge of line is metallic, partially black
	1-S-1	5	Totally silver, good conductivity
	2-S-2	0.8	Totally silver, good conductivity
	4-S-4	0.3	Totally silver, good conductivity
Cardboard B	2	∞	Not conductive
	4	2.5 M	Badly conductive
	8	161	Badly conductive

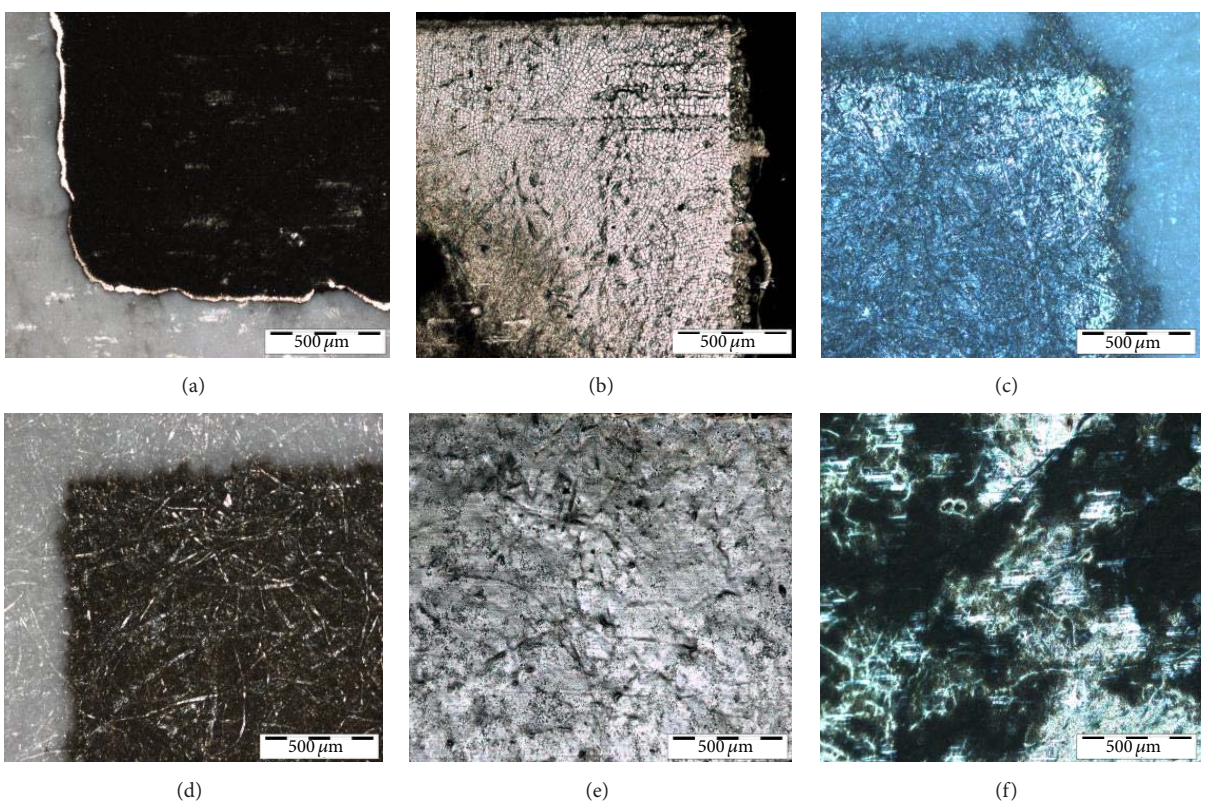

Figure 4: Microscopic images of the inkjet-printed layers: (a) surface of a one-layer line on Cardboard A, (b) surface of an eight-layer line on Cardboard A, (c) surface of a four-layer line on Cardboard B, (d) surface of a four-layer line on Paper A, (e) surface of a one-layer line on Paper B, and (f) surface of a two-layer line on Paper C.

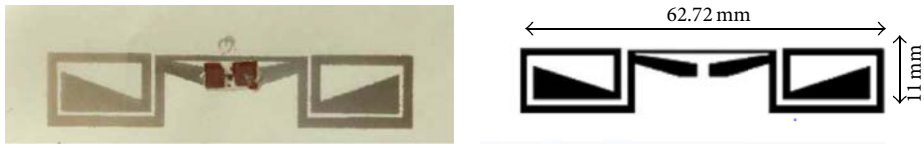

(a) (b)

Figure 5: (a) A ready inkjet-printed UHF RFID tag on Paper B. (b) The utilized tag antenna geometry.

structure applied in this study is shown with a manufactured tag in Figure 5. As a typical dipole antenna layout, this geometric construction has been already successfully used in [12]. The sintering was done at 150°C for 60 minutes.

The used tag IC was NXP UCODE G2iL series RFID IC [13], provided by the manufacturer in a fixture patterned from copper on a plastic film. We attached the $3 \times 3\,\text{mm}^2$ pads of the fixture to the printed antennas with CircuitWorks® Conductive Epoxy CW2400 [14], a highly reliable silver filled epoxy with a smooth, thixotropic consistency, and the IC-antenna joint was cured in 70°C for 20 minutes.

3. Measurements and Results

The wireless performance of the tags was evaluated with read range measurements using an RFID measurement unit. The tags were tested wirelessly using Voyantic Tagformance measurement system [15]. We conducted all the measurements with the tag suspended on a foam fixture in an anechoic chamber. The measurement equipment calculates the theoretical read range based on the measured path loss and the threshold power and computes the theoretical read range based on the relation given in

$$d = \frac{\lambda}{4\pi}\sqrt{\frac{\text{EIRP}}{P_{\text{th}}L_{\text{iso}}}}, \quad (1)$$

where λ is the wavelength transmitted from the reader antenna, P_{th} is the measured threshold power, L_{iso} is the measured path loss, and EIRP is the emission limit of an RFID reader given as equivalent isotropic radiated power. We present all the results corresponding to EIRP = 3.28 W, which is the emission limit, for instance, in European countries.

As expected based on the resistance measurements, Paper B was found to be the most suitable substrate. As can be seen from Figure 6(a), the peak read ranges of the tags with only one layer are around 4 meters, which is already suitable for many practical applications. In addition, more layers lead to longer read ranges, since more ink was deposited on the paper to form a thicker conductive pattern, which has lower losses and better radiation efficiency. The 12-layer tags have the longest read ranges, and the peak was measured to be about 6.5 meters at around 940 MHz.

Figure 6(b) shows the read ranges of the multilayer tags on Paper C. First it indicates the same tendency that the read ranges increase together with the number of layers. However, the read ranges of the 12-layer tags are lower than the 8-layer tags, which have the best performance.

Judging from the data in Figure 6(c), the 6-layer tags on Cardboard A have the best performance and the peak read ranges can reach about 6.1 meters. After that, when more layers are printed, the read range decreases inversely.

Thus, depositing multiple layers directly does not always correspond to a higher read range and the optimized number of layers for antennas on each substrate material needs to be studied separately. In case of the tags printed on Cardboard A and Paper C, which were both double coated materials, the double coating most probably causes the substrate not to absorb as much ink as the other substrates. Thus, twelve printed layers are too much on these coated substrate materials, causing the read ranges to decrease compared to tags with eight or six printed layers. On paper-based porous substrates, the substrate will absorb some of the deposited ink. When depositing too much ink on the substrate, most probably the conductive layers are not as uniformly connected. In addition, the ink can spread and destroy the shape of the printed pattern. Thus, the read range will decrease when too many layers are printed.

The resistances of the printed lines on Cardboard B were very high. Also the performance of the tags on this substrate is unsatisfying. The read ranges of the inkjet-printed tags on Cardboard B are shown in Figure 6(d). The four-layer tags were firstly fabricated and obtained no response when measured. In addition, the peak read range of the eight-layer tag is only 2 meters. Next, 12-layer tags were manufactured by repeating printing and sintering process two times, and 6 layers were deposited at each round. The peak read range can reach 4 meters, which is sufficient for many applications. However, the manufacturing process cannot be considered to be efficient.

Generally, the dielectric substrate affects the tag performance through its electrical properties, such as loss tangent and relative permittivity. Porous substrates like paper and cardboard also have an indirect effect on the tag through the ink film morphology [6, 16]. The achieved results are very comparable to the earlier results with the same antenna geometry and silver nanoparticle ink in [12], where the tag antennas were fabricated by inkjet printing on a polyimide substrate (Kapton 200 HN [17]). Kapton is a low-loss, polyimide film, which provides a smooth, heat-resistant surface for high precision inkjet printing. The peak read range of a three-layer tag on polyimide was measured to be about 5.8 meters [12]. Thus, the environmentally friendly

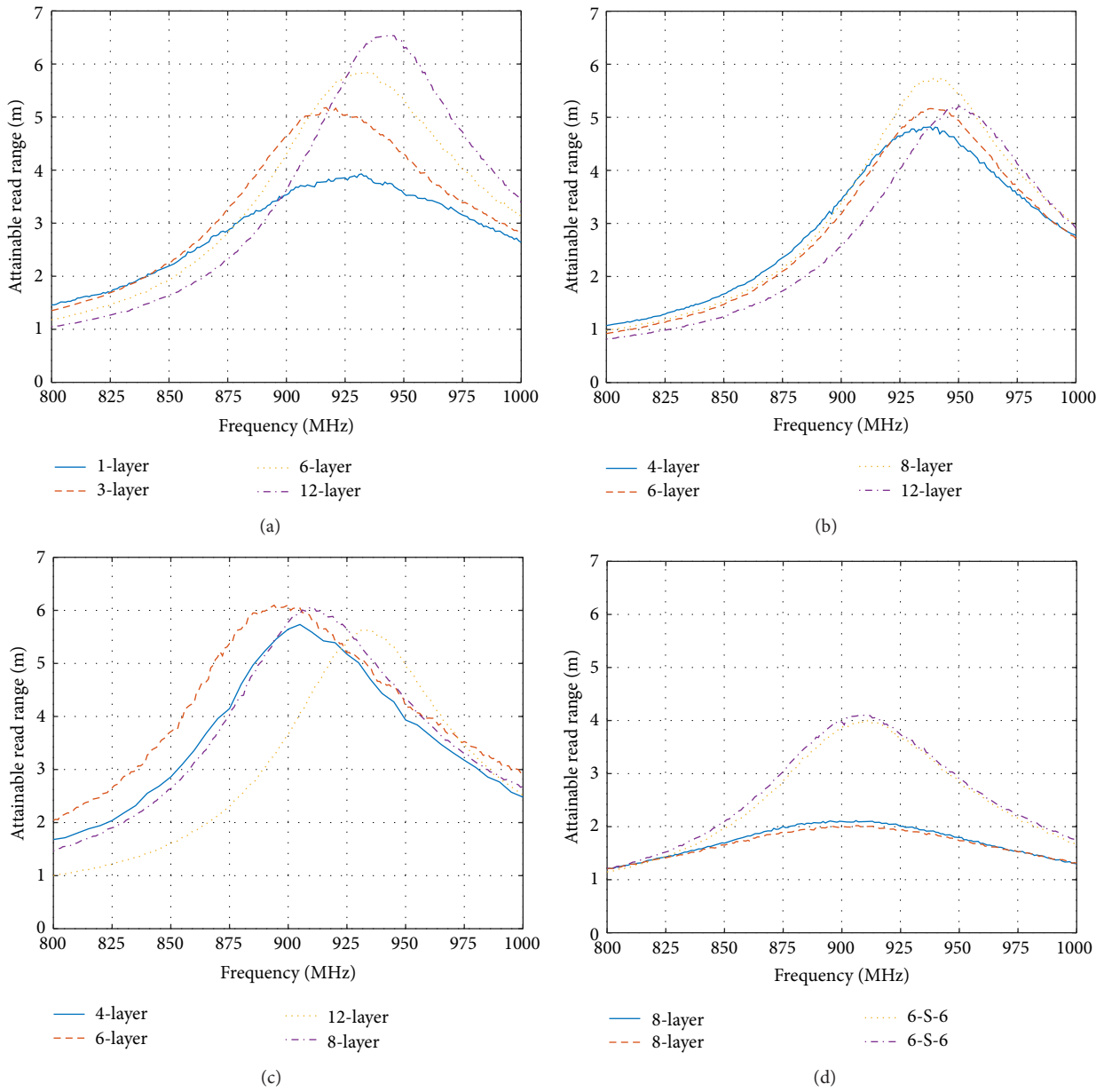

FIGURE 6: The measured read ranges of all tags: (a) the read ranges of tags on Paper B, (b) the read ranges of tags on Paper C, (c) the read ranges of tags on Cardboard A, and (d) the read ranges of tags on Cardboard B.

tags fabricated on these paper-based substrates in this study definitely have the potential to replace tags fabricated on traditionally used substrate materials and to be utilized in future wireless applications.

4. Conclusions

In this paper, the possibility of inkjet printing on versatile paper and cardboard substrates using silver nanoparticle ink was studied. The printing parameters were optimized for each substrate material in order to fabricate passive UHF RFID tags on these substrates. It was discovered that, in addition to the printing parameters, also the number of printed layers needs to be studied separately for each substrate material. The wireless performance of the fabricated tags was evaluated and the read ranges of the tags were found to be comparable to tags inkjet-printed on a polyimide substrate. In the future, the use of copper nanoparticle ink on these paper and cardboard substrates will be studied for potential cost reduction.

Competing Interests

The authors declare that there are no competing interests regarding the publication of this paper, and the mentioned received funding in Acknowledgments did not lead to any competing interests regarding its publication.

Acknowledgments

This research work was supported by the Academy of Finland and TEKES.

References

[1] G. Shaker, S. Safavi-Naeini, N. Sangary, and M. M. Tentzeris, "Inkjet printing of ultrawideband (UWB) antennas on paper-based substrates," *IEEE Antennas and Wireless Propagation Letters*, vol. 10, pp. 111–114, 2011.

[2] J. Virtanen, J. Virkki, L. Ukkonen, and L. Sydänheimo, "Inkjet-printed UHF RFID tags on renewable materials," *Advances in Internet Things*, vol. 2, no. 4, pp. 79–85, 2012.

[3] M. F. Farooqui and A. Shamim, "Dual band inkjet printed bow-tie slot antenna on leather," in *Proceedings of the 2013 7th European Conference on Antennas and Propagation (EuCAP '13)*, pp. 3287–3290, IEEE, Gothenburg, Sweden, April 2013.

[4] M. M. Tentzeris, L. Yang, A. Rida, A. Traille, R. Vyas, and T. Wu, "Inkjet-printed RFID tags on paper-based substrates for UHF 'cognitive intelligence' applications," in *Proceedings of the 18th Annual IEEE International Symposium on Personal, Indoor and Mobile Radio Communications (PIMRC '07)*, pp. 1–4, Athens, Greece, September 2007.

[5] L. Yang, A. Rida, R. Vyas, and M. M. Tentzeris, "RFID tag and RF structures on a paper substrate using inkjet-printing technology," *IEEE Transactions on Microwave Theory and Techniques*, vol. 55, no. 12, pp. 2894–2901, 2007.

[6] S. L. Merilampi, J. Virkki, L. Ukkonen, and L. Sydänheimo, "Testing the effects of temperature and humidity on printed passive UHF RFID tags on paper substrate," *International Journal of Electronics*, vol. 101, no. 5, pp. 711–730, 2014.

[7] R. Want, "An introduction to RFID technology," *IEEE Pervasive Computing*, vol. 5, no. 1, pp. 25–33, 2006.

[8] D. Dobkin, *The RF in RFID: Passive UHF RFID in Practice*, Elsevier, New York, NY, USA, 2007.

[9] N. C. Karmakar, Ed., *Handbook of Smart Antennas for RFID Systems*, John Wiley & Sons, Hoboken, NJ, USA, 2010.

[10] Harima Chemicals Group, "NPS-JL nanopaste, datasheet," http://www.harima.co.jp/en/products/.

[11] D. Soltman and V. Subramanian, "Inkjet-printed line morphologies and temperature control of the coffee ring effect," *Langmuir*, vol. 24, no. 5, pp. 2224–2231, 2008.

[12] J. Virtanen, J. Virkki, A. Z. Elsherbeni, L. Sydänheimo, and L. Ukkonen, "A selective ink deposition method for the cost-performance optimization of inkjet-printed UHF RFID tag antennas," *International Journal of Antennas and Propagation*, vol. 2012, Article ID 801014, 9 pages, 2012.

[13] NXP UCODE G2iL IC, Datasheet, http://www.nxp.com/documents/data_sheet/SL3S1203_1213.pdf.

[14] CircuitWorks® Conductive Epoxy, datasheet, https://www.chemtronics.com/descriptions/document/Cw2400tds.pdf.

[15] Voyantic Ltd, Tagformance, http://www.voyantic.com/tagformance.

[16] S. Merilampi, T. Björninen, A. Vuorimäki, L. Ukkonen, P. Ruuskanen, and L. Sydänheimo, "The effect of conductive ink layer thickness on the functioning of printed UHF RFID antennas," *Proceedings of the IEEE*, vol. 98, no. 9, pp. 1610–1619, 2010.

[17] DuPont HN Kapton, datasheet, http://www2.dupont.com/Kapton/en_US/assets/downloads/pdf/HN_datasheet.pdf.

Publication II

H. He, J. Tajima, L. Sydänheimo, H. Nishikawa, L. Ukkonen, and J. Virkki, “Inkjet-Printed Antenna-Electronics Interconnections in Passive UHF RFID Tags’’, in Proceedings of International Microwave Symposium , 4-9 June 2017, Honolulu, HI, USA, pp. 598-601.

Inkjet-Printed Antenna-Electronics Interconnections in Passive UHF RFID Tags

Han He[1], Tajima Jun[2], Lauri Sydänheimo[1], Hiroshi Nishikawa[2], Leena Ukkonen[1], and Johanna Virkki[1]

[1]BioMediTech Institute and Faculty of Biomedical Sciences and Engineering, Tampere University of Technology, Tampere, Finland

[2]Joining and Welding Research Institute, Osaka University, Osaka, Japan

***Abstract*—We outline the possibilities of inkjet printing in fabrication of passive UHF RFID tag antennas and antenna-electronics interconnections on paper and polyimide substrates. In our method, the silver nanoparticle tag antenna is deposited directly on top of the IC fixture, in order to simplify the manufacturing process by removing one step, i.e., the IC attachment with conductive glue. Our wireless measurement results confirm that the manufactured RFID tags with the printed antenna-IC interconnections achieve peak read ranges of 8.5-10 meters, which makes them comparable to traditional tags with epoxy-glued ICs.**

***Index Terms*—Antennas, inkjet printing, interconnections, nanotechnology, RFID tags, silver ink.**

I. Introduction

The development of the Internet of Things has created a need for versatile wireless electronics on environmentally friendly substrates, such as paper. The utilization of these wireless components requires fast but low-cost manufacturing methods. Inkjet printing is an additive manufacturing method with proven possibilities in antenna fabrication on versatile substrates [1-3]. However, it can be also extremely useful method for fabricating electric interconnections, as has been shown in recent studies [4-5].

In this paper, to the best of our knowledge, the possibilities of inkjet-printed antennas and antenna-IC (integrated circuit) interconnections are studied for the first time, in order to simplify the manufacturing process of passive UHF (ultra high frequency) RFID (radiofrequency identification) tags on an environmentally friendly paper and traditional polyimide substrates. By printing the antennas directly on top of IC fixture, there is no need for a separate IC attachment step, which means more cost- and time-effective fabrication of these wireless components.

II. Fabrication

Inkjet printing, which can create a specific pattern by dropping the ink directly from the aperture to the printing substrate, is applied in this work for simple and effective fabrication of passive UHF RFID tags. The used ink is Harima NPS-JL silver nanoparticle ink [6] and the ink deposition is completed with Fujifilm Dimatix DMP-2831 material inkjet printer. A 10pl volume cartridge, which has a snap-in replaceable print head with 16 nozzles, is applied for ejecting the drops. The used printing parameters are shown in Table I.

TABLE I. The inkjet printing parameters.

Parameter	
Cartridge temperature (˚C)	40
Platen temperature (˚C)	50
Jetting voltage (V)	28
Jetting frequency (kHz)	23
Pattern resolution (dpi)	635
Sintering temperature (˚C)	150
Sintering time (minutes)	60

Two different types of materials, commercial coated and calendered paper with a smooth surface (See Fig. 1 for a cross-section) and commonly used polyimide (Kapton), were selected as the substrates. The used tag IC is NXP UCODE G2iL series RFID IC, which has a wake-up power of 15.8 μW (−18 dBm). The IC is provided by the manufacturer in a fixture patterned from copper on a plastic film. See Fig. 2 where the IC strap structure is presented.

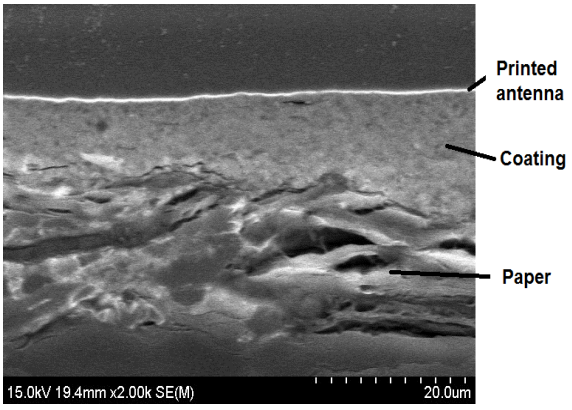

Fig. 1. The used paper substrate and the printed antenna.

Two different methods are studied for the antenna-IC interconnection. The first method is the tradition way, where the IC is attached on top of the printed and sintered antenna with conductive silver epoxy (Circuit Works CW2400). This method has been used, e.g., in [2] and [7]. In the second method, the

antenna is deposited on top of the IC fixture and thus the antenna-IC interconnection is sintered together with the antenna. This novel inkjet printing approach skips one process step and thus saves significant amounts of time and costs.

The tag antenna structure applied in this study is shown in Fig. 2. This dipole antenna is a very common type of antenna used in UHF RFID tags and has been previously, e.g., brush-painted on wood substrates with copper and silver nanoparticle inks [7]. The antenna is quite wide (2 cm), which reduces the impact of imperfections in the print outcome, and the length of the antenna (10 cm) is sufficient to avoid the weaknesses of electrically small antennas in the UHF frequencies from 800 MHz to 1000 MHz. In addition, the parts where the IC strap pads will be attached (See Fig. 2) are relatively large, which will be beneficial for the printed interconnections.

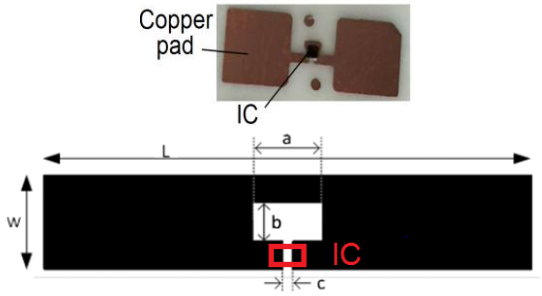

a (mm)	b (mm)	c (mm)	L (mm)	W (mm)
14.3	8.125	2	100	20

Fig. 2. The IC strap (top) and the tag antenna structure (bottom).

Firstly, it was discovered that for the printed antenna-IC interconnections, a better joint can be fabricated if the 3 mm × 3 mm IC fixture pads are cut to more narrow (2 mm x 1 mm) rectangles. Thus, these smaller pads were used for all IC attachments in this study. Also, unlike the paper substrate, the surface of the polyimide is extremely smooth, and the IC strap did not adhere to the substrate. Thus, a drop of Loctite® super glue was applied to improve the placement of the IC strap on the polyimide substrate, when the antennas were deposited on top of the IC directly. There was no need to add glue on the paper substrate as the IC strap was well adhered there.

Each tag was fabricated by printing four layers of ink and the subsequent sintering was done at 150 °C for 60 minutes. Four samples of each tag type were fabricated in order to also confirm the reproducibility. The ready tags with the inkjet-printed antenna-IC interconnections on paper and polyimide substrates are shown in Fig. 3 and Fig 4, respectively.

To further analyze the inkjet-printed antenna-IC joints, the resistances between the IC pads and the antennas were measured, and the average values were calculated. The connections between the ICs and the antennas showed reasonable conductivity, and the average resistance of the 4-layer tags on the paper and polyimide substrates were about 11.9 Ω and 12.2 Ω, respectively.

Fig. 3. Manufactured tag on paper and a magnification of the antenna-IC interconnection.

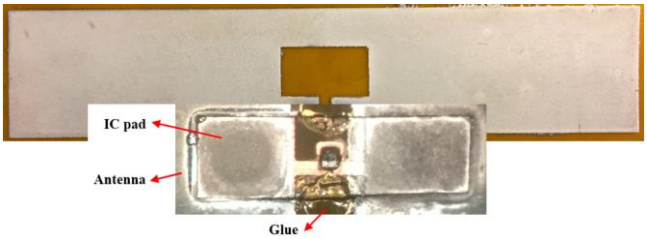

Fig. 4. Manufactured tag on polyimide and a magnification of the antenna-IC interconnection.

III. Measurements

The tags were tested wirelessly using Voyantic Tagformance measurement system [8]. It contains an RFID reader with an adjustable transmission frequency (0.8…1 GHz) and output power (up to 30 dBm) and provides the recording of the backscattered signal strength (down to −80 dBm) from the tag under test. During the test, we recorded the lowest continuous-wave transmission power (threshold power: Pth). Here we defined Pth as the lowest power at which a valid 16-bit random number from the tag is received as a response to the query command in ISO 18000-6C communication standard. In addition, the wireless channel from the reader antenna to the location of the tag under test was first characterized using a system reference tag with known properties. This enabled us to estimate the attainable read range of the tag (dt_{ag}) versus frequency from

$$d_{tag} = \frac{\lambda}{4\pi}\sqrt{\frac{EIRP}{\Lambda}\frac{P_{th*}}{P_{th}}}, \quad (1)$$

where λ is the wavelength transmitted from the reader antenna, Pth is the measured threshold power of the tag, Λ is a known constant describing the sensitivity of the system reference tag, and Pth* is the measured threshold power of the system reference tag. EIRP is the maximum equivalent isotropically radiated power allowed by local regulations. In this case EIRP = 3.28 W, which is the emission limit in European countries.

In addition, the realized gains of the tags were analyzed using the path-loss measurement data from the measurement unit. Realized gain takes into account the antenna–IC impedance matching and can be calculated as:

$$G_r = \frac{P_{IC,TS}}{L_{fwd} * P_{TS}} \quad (2)$$

where $P_{IC,TS}$ is the tag IC sensitivity, and P_{TS} and L_{fwd} are the

measured threshold power and forward losses, respectively. Fig. 5 shows the attainable read ranges of the inkjet-printed tags on paper and polyimide substrates. As can be seen, both types of tags on the polyimide substrate show peak read ranges of around 10 meters. The read ranges of the epoxy-glued tags are about 0.5 meters longer than the tags with the inkjet-printed interconnections. Thus, the inkjet-printed electric interconnection can be considered to be a good replacement for the epoxy-glued one on the polyimide substrate.

The attainable read ranges of the tags on the paper substrate have a more significant difference: the peak read ranges of the tags with inkjet-printed and epoxy-glued interconnections are around 8.5 and 10 meters, respectively. However, also read ranges of 8.5 meters can be considered more than suitable for versatile wireless identification and sensing applications. Also, unlike on the polyimide substrate, no pre-treatment, i.e., drop of glue to attach the IC strap to the substrate, was needed in case of the paper substrate.

The H-plane and E-plane realized gains were measured for the 4-layer tags with epoxy-glued and inkjet-printed antenna-IC interconnections on both substrates at 940 MHz, since all tags can reach their peak read range at this frequency. The radiation patterns can be seen in Fig. 6 and the results are in agreement with the read range results.

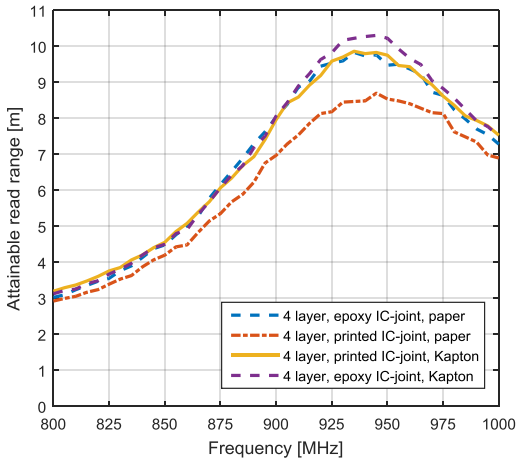

Fig. 5. The attainable read ranges of inkjet-printed tags on paper and polyimide (Kapton) substrates.

Based on these achieved results, inkjet-printed antenna-electronics interconnections can be considered to be promising replacements for the epoxy-glued ones in passive UHF RFID applications, and also in other wireless applications. However, more research is needed in order to study the effects of different substrate materials on the fabrication and reliability of the printed interconnections. Especially the effects of bending on the conductive pattern as well as on the IC attachment need to be studied next. Moreover, larger amounts of samples will be fabricated on different substrates to assure the repeatability of the fabrication method. Also, in addition to silver nanoparticle inks, more cost-effective solutions, such as copper nanoparticle inks, can provide even more possibilities for future cost- and time-effective RFID tag fabrication.

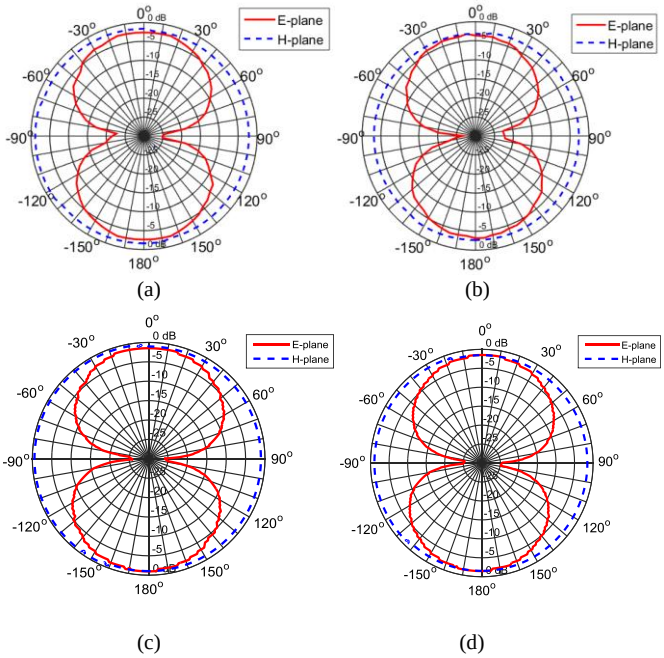

Fig. 6. The measured realized gains: (a) tag on paper, epoxy-glued antenna-IC joint. (b) tag on paper, printed antenna-IC joint. (c) tag on polyimide, epoxy-glued antenna-IC joint. (d) tag on polyimide, printed antenna-IC joint.

IV. Conclusion

In this paper, the possibility of applying inkjet printing to form the antenna-IC connection together with the antenna was studied for the first time, in order to simplify the manufacturing process of passive UHF RFID tags on paper and polyimide substrates. The results were compared to tags fabricated in a traditional way, with epoxy-glued ICs. Based on our results, the tags on both substrates showed excellent performance and supported the use of this novel fabrication method. In the future, in addition to the bending reliability and the use of other substrate materials, also the use of copper nanoparticle ink will be studied for potential cost reduction.

Acknowledgment

This research was done as part of the European Commission Marie Curie IRSES project "AdvIOT". The research work was supported by the Academy of Finland and TEKES.

References

[1] G. Shaker, S. Safavi-Naeini, and M.M. Tentzeris, “Inkjet printing of ultrawideband (UWB) antennas on paper-based substrates,” *IEEE AWPL*, vol. 10, 2011, pp. 111-114.

[2] J. Virtanen, J. Virkki, L. Ukkonen, L. Sydänheimo, “Inkjet-printed UHF RFID tags on renewable materials,” *Adv. IoT.*, vol. 2, no. 4, 2012, pp. 79-85.

[3] M.F. Farooqui and A. Shamim, “Dual band inkjet printed bow-tie slot antenna on leather,” in *EuCAP Dig.*, Gothenburg, Sweden, Apr. 2013, pp. 3287-3290.

[4] T. Falat, J. Felba, A. Moscicki and J. Borecki, “Nano-silver inkjet printed interconnections through the microvias for flexible electronics,” in *IEEE NANO Dig.*, Portland, OR, USA, Aug. 2011, pp. 473-477.

[5] N. B. Palacios-Aguilera et al., “Reliable inkjet-printed interconnections on foil-type Li-Ion batteries,” *IEEE Trans. Dev. Mat. Re.*, vol. 13, no. 1, 2013, pp. 136-145.

[6] Harima Chemicals Group, Inc., NPS-JL nanopaste datasheet. [Online]. Available: http://www.harima.co.jp/en

[7] E. Sipila, J. Virkki, L. Sydänheimo, L. Ukkonen, “Experimental study on brush-painted metallic nanoparticle UHF RFID tags on wood substrates,” *IEEE AWPL*, vol. 14, pp. 301–304, 2015.

[8] Voyantic Ltd. Tagformance. [Online]. Available: http://www.voyantic.com/tagformance.

Publication III

H. He, M. Akbari, X. Chen, A. Nommeots-Nomm, L. Chen, L. Ukkonen, and J. Virkki, “Fabrication and Performance Evaluation of 3D–Printed Graphene Passive UHF RFID Tags on Cardboard’’, in Proceedings of Progress in Electromagnetics Research Symposium, 22-25 May 2017, St Petersburg, Russia, pp. 1-5.

Fabrication and Performance Evaluation of 3D–Printed Graphene Passive UHF RFID Tags on Cardboard

Han He[1], Mitra Akbari[1], Xiaochen Chen[1], Amy Nommeots-Nomm[1], Liquan Chen[2], Leena Ukkonen[1], Johanna Virkki[1]

[1] BioMediTech Institute and Faculty of Biomedical Sciences and Engineering, Tampere University of Technology, Tampere, Finland

[2] School of Information Science and Engineering, Southeast University, Nanjing, China

***Abstract*—**This paper discusses the fabrication and wireless performance of 3D-printed graphene-based passive UHF (ultra high frequency) RFID (radiofrequency identification) tags on two different cardboard packaging substrates. Our results confirm that the low-cost and eco-friendly graphene-based RFID tags achieve high performance with attainable read ranges of 3.2-3.8 meters. These results are superior to those of previously reported RFID tags with graphene antennas.

Keywords—Antennas; 3D printing; cardboard; graphene; passive UHF RFID.

1. INTRODUCTION

The recent focus in additive antenna fabrication has been to use metallic components as the conductive element, which brings high material costs and usually requires high sintering temperatures or other sintering approaches [1][2]. An alternative to this could lie in the use of novel carbon-based materials, such as graphene. Graphene is an environmentally friendly and low-cost material, which can be used in additive manufacturing [3]-[6], it has the capacity to integrate with versatile materials, including porous substrates, such as cardboard and fabrics [5][6].

3D direct-write dispensing is a fast and low-cost additive manufacturing method, which enables the printing of complex geometries with micron resolution accuracy with limited wastage [1][7]. Graphene inks can be used as a conductor in printed antennas due to its suitability for printing, high electrical conductivity, and low material cost, combined with its unique mechanical properties.

In this paper, we present 3D-printed graphene-based passive UHF RFID tags on two cardboard packaging substrates: one has a rough, non-colored surface, while the other is smooth and colored white. The RFID tags were evaluated for their wireless performance and the results are compared to those of previously reported graphene-based RFID tags.

2. MANUFACTURING OF PASSIVE UHF RFID TAGS

In this work, 3D printing technique was utilized to fabricate graphene-based RFID tag antennas on cardboard substrates. A water-based graphene ink (HDPlas® IGSC02002) [8] was selected for this study. The 3D printing was completed by nScrypt tabletop series 3D direct write dispensing system, and the main manufacturing parameters are defined in Table 1.

Table 1. The used printing parameters.

3D dispensing parameters	
Material feed pressure	16.9 Psi
Printing spacing	125 microns
Printing angle	0°
Inner diameter of tip	125 microns

All fabricated antennas were sintered at 60 °C for 30 minutes as recommended by the ink datasheet [8]. The antenna geometry and dimensions are shown in Fig. 1 together with ready-made tags on both types of cardboard substrates.

The used IC (integrated circuit) was NXP UCODE G2iL series RFID IC with a wake-up power of −18 dBm (15.8 µW). The IC is provided by NXP Semiconductors in a carrier fixture patterned from copper on a plastic film. We attached the 3 x 3 mm^2 pads of the fixture to the antenna with conductive silver epoxy (Circuit Works CW2400).

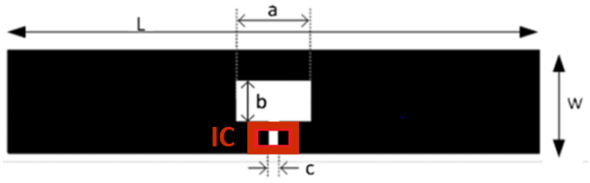

a (mm)	b (mm)	c (mm)	L (mm)	W (mm)
14.3	8.125	2	100	20

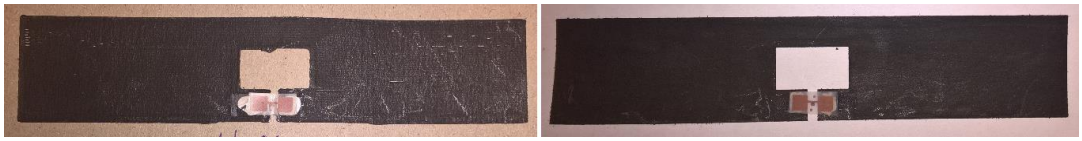

Fig. 1. The antenna geometry and dimensions (top) and fabricated graphene tags on the rough, non-colored (bottom, left) and smooth, white-colored (bottom, right) cardboard substrates.

3. Thickness Measurements and Wireless Performance

The wireless performance of the tags were evaluated by two key properties of passive UHF RFID tags: read range and realized gain. The tags were tested using Voyantic Tagformance measurement system [9]. All the measurements were conducted with the tag suspended on a foam fixture in an anechoic chamber.

The theoretical read range describes the maximal distance between the tag and reader antenna in free space, i.e., environment without reflections or external disturbances. The measurement equipment calculates the theoretical read range of the tag using its measured threshold power along with the measured forward losses. The forward loss from the transmit port to the tag, is first calculated using a reference tag. Theoretical read range was calculated assuming that the read range was limited by the maximum allowed transmitted power levels and can be therefore calculated using Equation 1:

$$d_{Tag} = \frac{\lambda}{4\pi}\sqrt{\frac{EIRP}{P_{TS}L_{fwd}}} \quad (1)$$

where λ is the wavelength transmitted from the reader antenna, EIRP is the maximum equivalent isotropically radiated power allowed by local regulations, P_{TS} and L_{fwd} are the measured threshold power and forward losses, respectively. We present all the results corresponding to EIRP = 3.28 W, which is the emission limit in European countries.

Fig. 2 presents the attainable read ranges of the fabricated tags on both cardboard types, and the cross-sections of the 3D-printed tag antennas are presented in Fig. 3. The peak read ranges of the 3D-printed tags on the smooth cardboard were around 3.8 meters, which is suitable for many practical applications, for example within the packaging industry. The cross-sections of this tag antenna shows an average thickness of around 85.73 µm. As a comparison, the average thickness of the tag antennas on the rough cardboard is 81.30 µm, which resulted in slightly shorter read ranges of around 3.2 meters. The peak read ranges together with the corresponding thicknesses and sheet resistances are shown in Table 2.

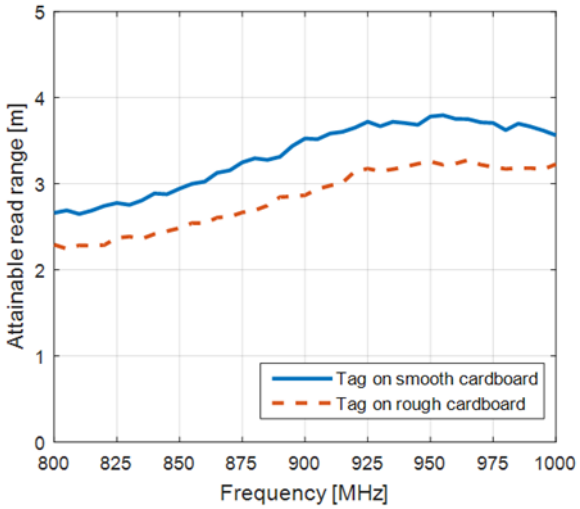

Fig. 2. The attainable read ranges of the fabricated tags.

Table 2. The peak read ranges together with the corresponding thickness and sheet resistance.

Substrate	Peak read range	Average thickness	Sheet resistance
Smooth cardboard	3.8 m	85.73 µm	8.7 Ω/sq
Rough cardboard	3.2 m	81.30 µm	18.6 Ω/sq

In addition, the H-plane and E-plane realized gains at 940 MHz, where both types of tags reach their peak read range, are presented in Fig. 4. The realized gain takes into account the antenna–IC impedance matching, and can be calculated as:

$$G_r = \frac{P_{IC,TS}}{L_{fwd} * P_{TS}} \qquad (2)$$

where $P_{IC,TS}$ is the tag IC sensitivity, and P_{TS} and L_{fwd} are as detailed in (1).

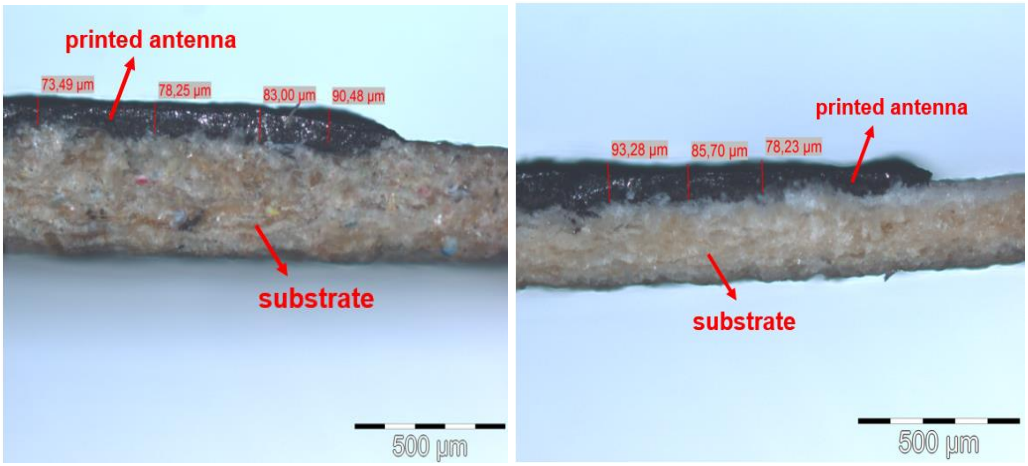

Fig. 3. Cross-sections of the tag antennas on the rough, non-colored cardboard (left) and smooth, white-colored cardboard (right).

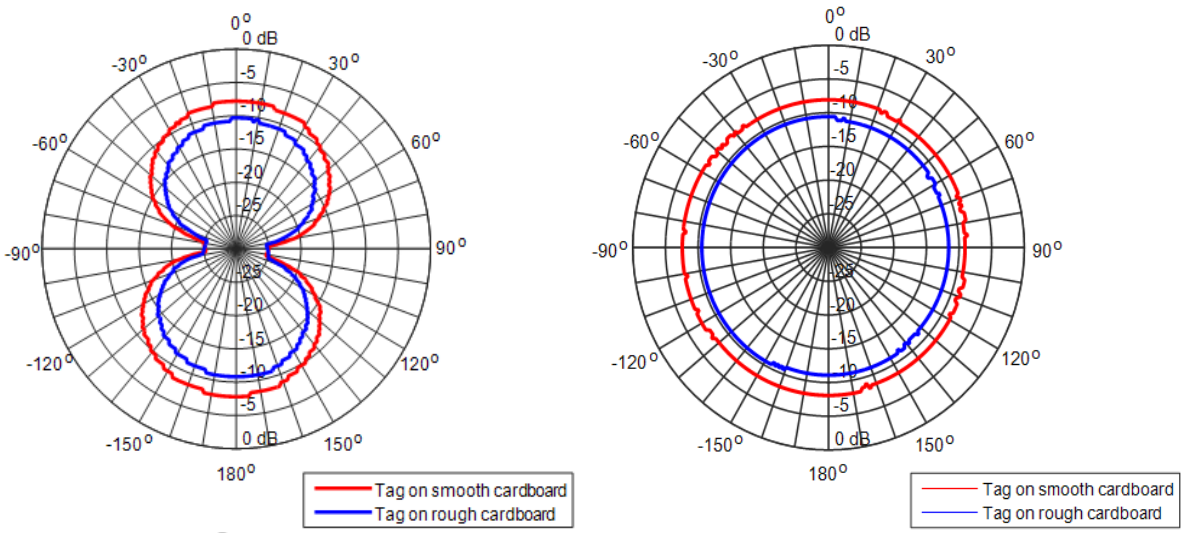

Fig. 4. The measured E-plane (left) and H-plane (right) realized gains at 940 MHz.

Next, the achieved read range results were compared to previously published results using the same antenna geometry and conductive ink, where the graphene tag antennas were fabricated by doctor-

blading on a cardboard [5] and fabric [6] substrates. These previously reported graphene tags achieved peak read ranges of 2.7 meters and 2 meters, on cardboard and fabric substrates, respectively. Thus, the antennas presented here, fabricated via direct-write dispensing, show superior performance compared to the earlier results. The results achieved in this study strongly support the 3D printing of graphene-based wireless electronics.

4. Conclusions

In this study, we presented 3D-printed passive UHF RFID graphene tags on two types of cardboard substrates. Based on our measurements, the tags show an excellent wireless performance and peak read ranges of 3.2-3.8 meters. By utilizing the direct-write dispensing manufacturing method, graphene antennas can be produced easily and reliably, with limited material waste, to a variety of different geometries and substrate roughness's. Thus, in the future, these 3D-printed graphene antennas could replace the significantly more expensive silver-based RFID antennas. The low-cost and eco-friendly graphene-based RFID tags have great possibilities in several application areas, such as the packaging industry.

Acknowledgements

This research was done as part of the European Commission Marie Curie IRSES project "AdvIOT". The research work was supported by the Academy of Finland and TEKES.

References

1. T. Björninen, J. Virkki, L. Sydänheimo, and L. Ukkonen: 'Possibilities of 3D direct write dispensing for textile UHF RFID tag manufacturing', IEEE International Symposium on Antennas and Propagation & USNC/URSI National Radio Science Meeting, 2015.
2. G. Xiaohui, et al.: 'Flexible and wearable 2.45 GHz CPW-fed antenna using inkjet-printing of silver nanoparticles on pet substrate', Microwave and Optical Technology Letters, vol. 59, no. 1, 2017, pp. 204-208.
3. P. Kopyt et al.: 'Graphene-based dipole antenna for a UHF RFID tag", IEEE Transactions on Antennas and Propagation, vol. 64, no. 7, 2015, pp. 2862-2868.
4. X. Huang, et al.: 'Binder-free highly conductive graphene laminate for low cost printed radio frequency applications', Applied Physics Letters, vol. 106, no. 20, 2015.
5. M. Akbari, J. Virkki, L. Sydänheimo, and L. Ukkonen 'The possibilities of graphene-based passive RFID tags in high humidity conditions', IEEE International Symposium on Antennas and Propagation & USNC/URSI National Radio Science Meeting, 2016.
6. M. Akbari, J. Virkki, L. Sydänheimo, and L. Ukkonen: 'Towards graphene-based passive UHF RFID textile tags: A reliability study', IEEE Transactions on Device and Materials Reliability, vol. 16, no. 3, 2016, pp. 429-431.
7. P. I. Deffenbaugh, T. M. Weller, and K. H. Church: 'Fabrication and microwave characterization of 3-D printed transmission lines', IEEE Microwave and Wireless Components Letters, vol. 25, no. 12, 2015, pp. 823-82.
8. Goodfellow USA: 'Screen printable functionalized graphene ink', http://www.goodfellowusa.com/news-article/screen-printable-functionalized-graphene-ink/, accessed on Jan. 2017.
9. Voyantic Ltd. Tagformance, http://www.voyantic.com/tagformance, accessed on Jan. 2017.

Publication IV

H. He, M. Akbari, L. Ukkonen, and J. Virkki, “Fabrication and Evaluation of 3D-Printed Heat and Photonic Cured Graphene RFID Tags on Veneer’’, in Proceedings of Applied Computational Electromagnetics Society Symposium, 1-4 Au-gust 2017, Suzhou, China, pp. 1-2.

Fabrication and Evaluation of 3D-Printed Heat and Photonic Cured Graphene RFID Tags on Veneer

Han He, Mitra Akbari, Leena Ukkonen, Johanna Virkki
BioMediTech Institute and Faculty of Biomedical Sciences and Engineering,
Tampere University of Technology, Tampere, Finland
Email: han.he@tut.fi , johanna.virkki@tut.fi

***Abstract*—We study 3D printing of graphene UHF RFID antennas on a thin wood veneer substrate, subsequently cured by heat in an oven or photonically by pulsed Xenon flash. We present the read range results of the tags and test the effects of moisture on the tag performance. Initially the peak read ranges of both types of tags are about 4.5 meters. The read range decreases about 50 cm when the tag antenna and wood substrate absorb moisture. However, after drying, the performance of the tag returns to normal.**

Keywords—3D printing; graphene antennas; heat curing; moisture; passive UHF RFID technology; photonic curing

I. INTRODUCTION

The use of metallic particles in additive antenna fabrication means high material costs and many non-environmentally friendly aspects. A potential solution lies in carbon-based materials, especially graphene [1]-[3], which is an environmentally friendly and low-cost material that has the capacity to integrate with versatile materials, including soft, porous, or stretchable materials, such as textiles and cardboard.

3D direct-write dispensing is an effective additive manufacturing method, which enables the printing of complex geometries with micron resolution accuracy [4]. Graphene ink can be used as a conductor in printed antennas due to its high electrical conductivity and low material cost, combined with its unique mechanical properties [2].

Passive ultra high freqcuency (UHF) radio-frequency identification (RFID) tags integrated into wood structures, which will be the focus of this paper, provide great possibilities especially for the construction and packaging industries. However, in case of a passive tag on wood, the response of the tag can change as a function of increased humidity. The moisture can change the permittivity of the wooden substrate, and the impedance of the antenna, which can create a mismatch between the tag antenna and the IC (integrated circuit). The increased moisture can also increase the losses in the wooden substrate, degrading the overall tag performance.

In this paper, we present 3D-printed graphene passive UHF RFID tags on wood veneer substrates. The printed antennas are cured by heat in a conventional oven or by photonic curing with a flash lamp. The ready RFID tags are evaluated for their wireless performance and also the effects of moisture are studied.

II. TAG FABRICATION

A water-based graphene ink (HDPlas® IGSC02002) [5] was used and the 3D printing was completed with nScrypt tabletop series 3D direct write dispensing system. By running a customizable computer-controlled valve open and close process, the printer can produce a controllable material flow. The antenna geometry was printed along the grain of the veneer and the main printing parameters are given in Table 1.

TABLE I. 3D PRINTING PARAMETERS

3D Printing Parameters	
Material feed pressure	16.9 Psi
Printing spacing	125 microns
Printing angle	0°
Inner diameter of tip	125 microns

The heat cured antennas were cured in an oven at 60℃ for 30 minutes, as presented in the ink datasheet. In photonic curing, the antennas were subjected to a series of flashes from a Xenon sintering system (Sinteron 2010-L, Xenon Corp.). The used operating mode was continuous mode, where three parameters are adjustable: high voltage value, pulse width, and period (pulse width + break between pulses). The used photonic curing parameters are listed in Table 2.

TABLE II. PHOTONIC CURING PARAMETERS

High voltage (V)	**Pulse width (μs)**	**Number of pulses**	**Period (ms)**	**Duration of whole curing process (s)**
1900	2100	6	1100	11

After tag antenna fabrication, NXP UCODE G2iL series RFID ICs with a wake-up power of −18 dBm (15.8 μW) were attached to the antennas. We attached the 3 x 3 mm^2 pads of the IC straps to the antennas with conductive silver epoxy (Circuit Works CW2400). A ready tag on a wood substrate is shown in Fig. 1.

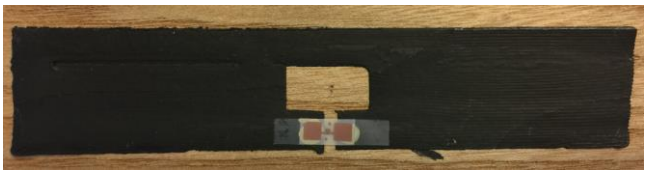

Fig, 1. Graphene RFID tag on wood veneer.

III. Wireless Measurements and Moisture Test

The tags were measured in the UHF frequency range of 800-1000 MHz with a Voyantic Tagformance RFID measurement system. It contains an RFID reader with an adjustable transmission frequency (0.8…1 GHz) and output power (up to 30 dBm), and provides the recording of the backscattered signal strength (down to −80 dBm) from the tag under test. The wireless channel from the reader antenna to the location of the tag under test is first characterized using a system reference tag with known properties. The system calculates the theoretical read range based on the measured path loss and the threshold power, as given in equation (1):

$$d_{Tag} = \frac{\lambda}{4\pi}\sqrt{\frac{EIRP}{P_{TS}\,L_{fwd}}} \qquad (1)$$

where λ is the wavelength transmitted from the reader antenna, P_{TS} and L_{fwd} are the measured threshold power and forward losses correspondingly, *EIRP* is the emission limit of an RFID reader given as equivalent isotropic radiated power. *EIRP* = 3.28 W, which is the emission limit in European countries.

Next, the effects of moisture on the tag performance were investigated. During the test, the tags were placed in tap water and wirelessly measured before the test and immediately after 1 minute in water. The tags were then left in room conditions to dry and were measured again after 1 hour. Finally, the tags were measured as dry again (after another 30 minutes in 60℃ in an oven).

IV. Results

The read ranges of the photonic cured and heat cured tags are shown in Fig. 2.

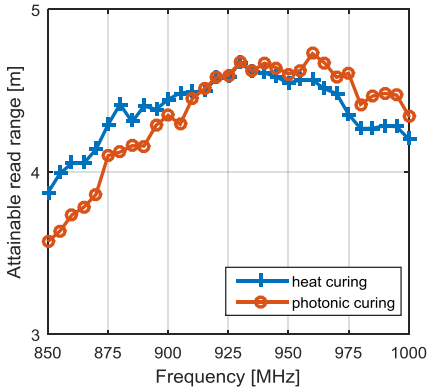

Fig. 2. Attainable read ranges of heat and photonic cured graphene tags on wood veneer.

As can be seen, the tags initially achieved peak read ranges of around 4.5 meters, which means that the heat and photonic cured tags showed similar performance.

Based on the measurement results, moisture did not have a significant instant effect on the tag performance. However, after 1 hour of drying in office conditions, the read ranges were about half a meter shorter than initially. This probably means that the moisture was absorbing deeper into to the antenna and wood substrate, after the tag was already in office conditions. After curing the tags again in the oven, the performance returned close to the initial performance.

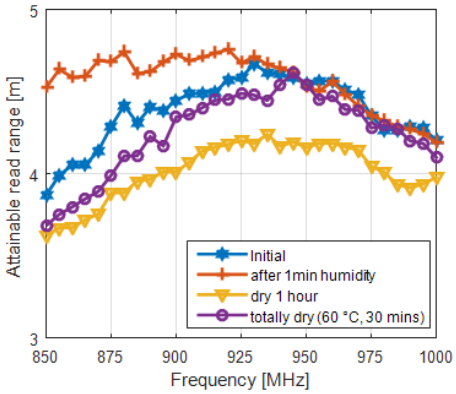

Fig. 3. Attainable read ranges of heat cured graphene tags as dry, wet, after drying for one hour, and after completely dry again.

V. Conclusions

We presented 3D-printed graphene passive UHF RFID tags on wood veneer substrates with read ranges of around 4.5 meters. Based on the achieved outcomes, photonic curing could replace the time-consuming curing in an oven, which could considerably cut down the manufacturing time. Based on the measurement results, moisture did not have a significant detrimental effect on the tag performance.

Acknowledgment

This research work was funded by the Academy of Finland and Tekes – the Finnish Funding Agency for Innovation.

References

[1] X. Huang, et al.: ‘Binder-free highly conductive graphene laminate for low cost printed radio frequency applications,’ Appl. Phys. Lett., vol. 106, 2015.

[2] M. Akbari, et al.; ‘Toward graphene-based passive UHF RFID textile tags: a reliability study,’ IEEE Trans. Device Mater. Rel., vol. 16, no. 3, pp. 429-431, 2016.

[3] P. Kopyt, et al.: ‘Graphene-based dipole antenna for a UHF RFID tag,‘ IEEE Trans. Antennas Propag., vol. 64, no. 7, pp. 2862-2868, 2016.

[4] T. Björninen, et al.; ‘Possibilities of 3D direct write dispensing for textile UHF RFID tag manufacturing,’ in Proc. IEEE AP-S Intl. Symp. Antennas Propag., pp. 1316–1317, 2015.

[5] Goodfellow USA: ‘Screen printable functionalized graphene ink’, http://www.goodfellowusa.com/news-article/screen-printable-functionalized-graphene-ink/, accessed on Jan. 2017

Publication V

H. He, M. Akbari, L. Sydänheimo, L. Ukkonen, and J. Virkki, “3D-Printed Graphene Antennas and Interconnections for Textile RFID Tags: Fabrication and Reliability towards Humidity”, International Journal of Antennas and Propagation, Vol. 2017, Article ID 1386017, 5 pages, 2017, doi:10.1155/2017/1386017.

Hindawi
International Journal of Antennas and Propagation
Volume 2017, Article ID 1386017, 5 pages
https://doi.org/10.1155/2017/1386017

Research Article

3D-Printed Graphene Antennas and Interconnections for Textile RFID Tags: Fabrication and Reliability towards Humidity

Han He, Mitra Akbari, Lauri Sydänheimo, Leena Ukkonen, and Johanna Virkki

BioMediTech Institute and Faculty of Biomedical Sciences and Engineering, Tampere University of Technology, P.O. Box 692, 33101 Tampere, Finland

Correspondence should be addressed to Han He; han.he@tut.fi

Received 7 April 2017; Accepted 15 May 2017; Published 5 June 2017

Academic Editor: Sanming Hu

We present the possibilities of 3D direct-write dispensing in the fabrication of passive UHF RFID graphene tags on a textile substrate. In our method, the graphene tag antenna is deposited directly on top of the IC strap, in order to simplify the manufacturing process by removing one step, that is, the IC attachment with conductive glue. Our wireless measurement results confirm that graphene RFID tags with printed antenna-IC interconnections achieve peak read ranges of 5.2 meters, which makes them comparable to graphene tags with epoxy-glued ICs. After keeping the tags in high humidity, the read ranges of the tags with epoxy-glued and printed antenna-IC interconnections decrease 0.8 meters and 0.5 meters, respectively. However, after drying, the performance of both types of tags returns back to normal.

1. Introduction

Graphene is an environmentally friendly and low-cost conductive material that has the capacity to integrate with challenging substrate materials, such as soft and stretchable textiles [1, 2]. For those reasons, and because of graphene's great electrical and mechanical properties, graphene-based conductive inks have the potential to revolutionize the area of printed electronics, by replacing traditional inks with metallic components.

3D direct-write dispensing is a fast and versatile additive manufacturing method, which enables the printing of complex geometries into textile materials with micron resolution accuracy [3]. Graphene ink can be used as a conductor in these printed structures, which opens novel possibilities for textile antenna and antenna-electronics interconnection fabrication. In particular, passive RFID (radio-frequency identification) tags integrated into textiles, which will be the focus of this paper, provide versatile wireless identification and sensing possibilities embedded into clothing [4–7] and are thus a great platform for this new fabrication method and material. In wearable systems, textile antennas can be used in a great variation of applications [8] and often they operate in an extremely challenging environment. Wearable applications require the antennas and interconnections to endure different environmental stresses, such as moisture and wetting [9, 10].

In this paper, the possibilities of 3D-printed graphene antennas and antenna-IC (integrated circuit) interconnections are studied, in order to simplify the manufacturing process of passive UHF (ultra high frequency) RFID tags on a traditional 100% cotton fabric. By printing the graphene antennas directly on top of IC fixture, there is no need for a separate IC attachment step, which means more cost- and time-effective fabrication of these wireless components. The wireless performance of these tags is evaluated in normal room conditions, as well as in high humidity conditions, and compared to tags were the IC is attached with conductive glue.

2. Manufacturing of Passive UHF RFID Tags

In this work, 3D-printing technique is used to fabricate graphene-based RFID tags on a 100% cotton fabric by using a water-based graphene ink (HDPlas® IGSC02002) [11]. The printing is done with nScrypt tabletop series 3D direct-write dispensing system, and the main manufacturing parameters are defined in Table 1. The printing spacing and angle can

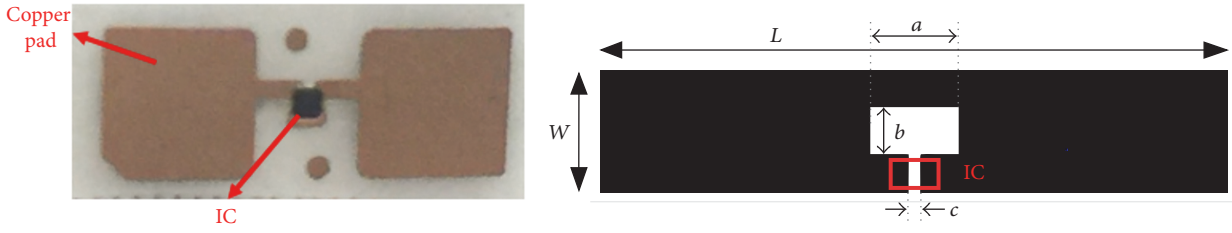

(a) (b)

a (mm)	b (mm)	c (mm)	L (mm)	W (mm)
14.3	8.125	2	100	20

Figure 1: The IC strap (a) and the tag antenna structure (b).

Table 1: The used 3D-printing and curing parameters.

Parameter	
Material feed pressure	16.9 Psi
Printing spacing	125 microns
Printing angle	0°
Inner diameter of tip	125 microns
Number of printed layers	1
Curing	60°C, 30 minutes

be defined when designing the printed pattern by a built-in software. The air pressure from a positive pressure pump is applied to the system, which pushes the ink into the main valve body and finally through the ceramic nozzle tip. By adjusting a constant material pressure, running a customizable computer-controlled valve open and close process, and selecting the ceramic nozzle tip with suitable size, the printing system can produce a controllable ink flow, precise starts and stops, and the ability to utilize a wide range of material viscosities [12].

Two different methods are studied for the antenna-IC interconnection. The first method is a previously reported way, where the IC is attached on top of the printed and cured antenna with conductive silver epoxy (Circuit Works CW2400). This method has been used, for example, in [2, 13]. In the second method, the antenna is deposited on top of the IC fixture, and thus the antenna-IC interconnection is cured together with the antenna. This 3D-printing approach skips one process step and thus saves significant amounts of time and costs. In both cases, only one layer of ink is printed. The curing of the antennas is done in 60°C for 30 minutes, as guided by the ink datasheet [11].

The utilized IC strap (NXP UCODE G2iL series RFID IC, provided by the manufacturer in a strap) and the tag antenna structure are shown in Figure 1. The antenna is quite wide (2 cm), which reduces the impact of imperfections in the print outcome, and the length of the antenna (10 cm) is sufficient to avoid the weaknesses of electrically small antennas in the UHF frequencies from 850 MHz to 1000 MHz. This antenna geometry has been previously used successfully on textile tags [2, 3]. The simulated current distribution on the dipole antenna at 915 MHz is shown in Figure 2.

For each tag type, three samples are fabricated to also evaluate the reproducibility. The surface of a 3D-printed and cured graphene antenna is shown in Figure 3. As can be seen, the graphene ink layer has a good adherence to the fabric substrate. Ready tags with epoxy-glued and 3D-printed antenna-IC interconnections on a cotton fabric are shown in Figures 4(a) and 4(b), respectively.

3. Measurements

The wireless performance of the fabricated tags is evaluated with a Tagformance RFID measurement system. All the measurements are conducted with the tag suspended on a foam fixture in an anechoic chamber. The measurements were obtained from a fixed angle (the angle of the highest read range) between the reader antenna and tag. In all measurements, the longer side of the antenna, where the IC was attached, was directly facing the reader antenna. During the test, we record the lowest continuous-wave transmission power (threshold power) at which the tag remains responsive. The forward loss from the transmit port to the tag is first attained using a reference tag with known properties. The measurement equipment calculates the theoretical read range of the tag using its measured threshold power along with the measured forward losses. The theoretical read range is based on the relation given in

$$d_{\text{Tag}} = \frac{\lambda}{4\pi}\sqrt{\frac{\text{EIRP}}{P_{\text{TS}}L_{\text{fwd}}}}, \quad (1)$$

where λ is the wavelength transmitted from the reader antenna, P_{TS} and L_{fwd} are the measured threshold power and forward losses, correspondingly, and EIRP is the emission limit of an RFID reader given as equivalent isotropic radiated power. All the results correspond to EIRP = 3.28 W, which is the emission limit in European countries.

Finally, the effects of moisture on the tags' wireless performance are investigated. During the moisture test, the tags (whole tag, including the IC) are placed in tap water and wirelessly measured before the test and immediately after 1

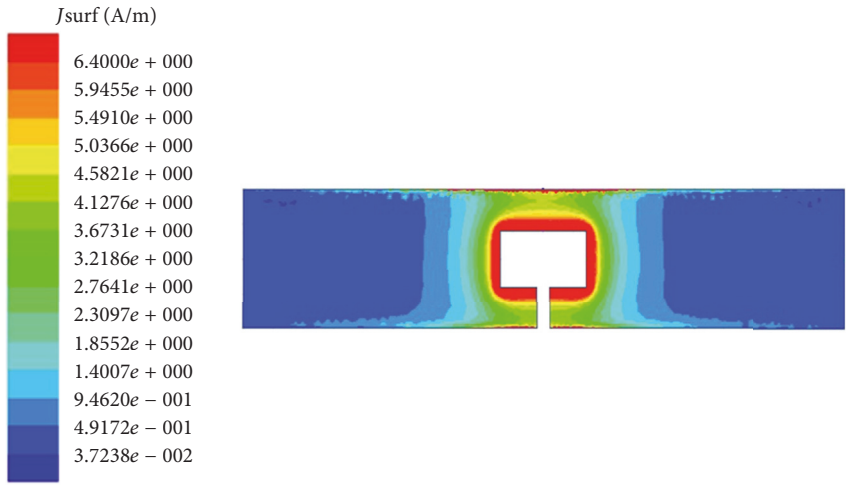

Figure 2: The simulated current distribution on the antenna at 915 MHz.

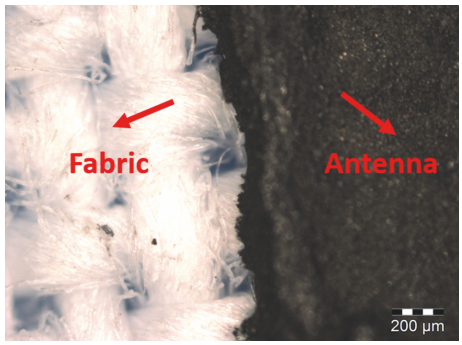

Figure 3: Optical microscopic image of a 3D-printed graphene antenna on cotton (magnification ×20).

minute in water. The tags are then left in room conditions to dry and are measured again after 1 hour, 1 day, and finally 1 week, when they are totally dry.

4. Achieved Results

On porous substrates, such as fabric, the ink is partially absorbed into the substrate and the average thickness of the printed layer depends thus on the substrate material. Figure 5 shows a microscopic image of a cross-section of a 3D-printed tag antenna together with the measured thickness. The average thickness of all fabricated antenna samples is 610.15 μm, while the standard deviation is 23.51 μm. Moreover, the average sheet resistances of all the fabricated antenna samples in room conditions and after 1 minute in water are 6.47 Ω/sq and 9.51 Ω/sq, respectively, while the corresponding standard deviations are 1.45 Ω/sq and 2.27 Ω/sq.

Figure 6 presents the attainable read ranges of the 3D-printed tags before and after the high humidity conditions. Despite the variation in the antenna thickness, all similarly fabricated tags showed similar performance. As can be seen, the peak read ranges of the tags with printed antenna-IC joints can achieve 5.2 meters, which is about 0.4 meters higher than the read ranges of the tags with epoxy-glued joints. Thus, the 3D-printed electric interconnection can be considered to be a good replacement for the epoxy-glued one. However, in order to draw further conclusions, the effects of antenna thickness variation on the tag read range should be studied with a significantly larger amount of antenna samples. Also, the contact resistances of the printed and glued IC attachments need to be investigated, and especially the variation of hand-made glue connections can affect the read ranges.

Both types of tags also show better performance than earlier published results using the same antenna geometry and conductive ink [2], where the graphene tag antennas were fabricated by doctor-blading on a cotton fabric substrate and the IC was attached with conductive epoxy. The same antenna geometry has been previously also reported to be 3D-printed using silver and copper inks [3]. The achieved peak read ranges for the copper- and silver-based tags were around 6 and 11 meters, respectively. Thus, the graphene ink cannot yet offer comparable read ranges to silver-based inks, but the achieved read ranges are suitable for many RFID identification and sensing applications. Also, it is interesting to study the effect of antenna thickness, for example, antennas with two or more layers of ink, on the tag performance.

Based on the moisture test, the read ranges of both types of tags decrease after 1 minute in high humidity conditions, which is also supported by the fact that the sheet resistances of the graphene antennas increase as the humidity level increases. After keeping the tags in high humidity, the read ranges of the tags with the epoxy-glued and printed antenna-IC interconnections decrease 0.8 meters and 0.5 meters, respectively. The effect of humidity on the tags with the epoxy-glued ICs is more significant, most probably due to the moisture absorption of the glue itself, which affects the antenna-IC impedance matching. This finding strongly supports the use of the printed antenna-IC joint. For the tags with the printed IC attachment, the read range in the frequency range of 850–900 MHz, after the humidity test, is better than that in the dry state. It could be true that despite

Figure 4: Ready 3D-printed passive UHF RFID tags and magnifications of the antenna-IC interconnections of (a) epoxy-glued joint and (b) printed joint.

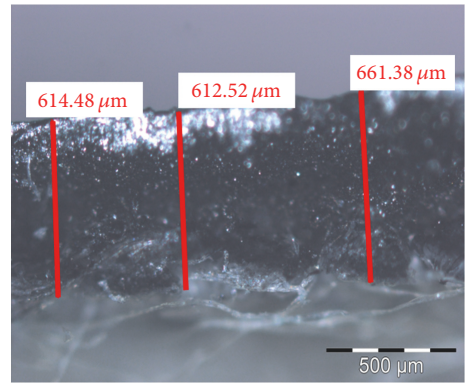

Figure 5: A cross-section of a printed antenna and its thickness.

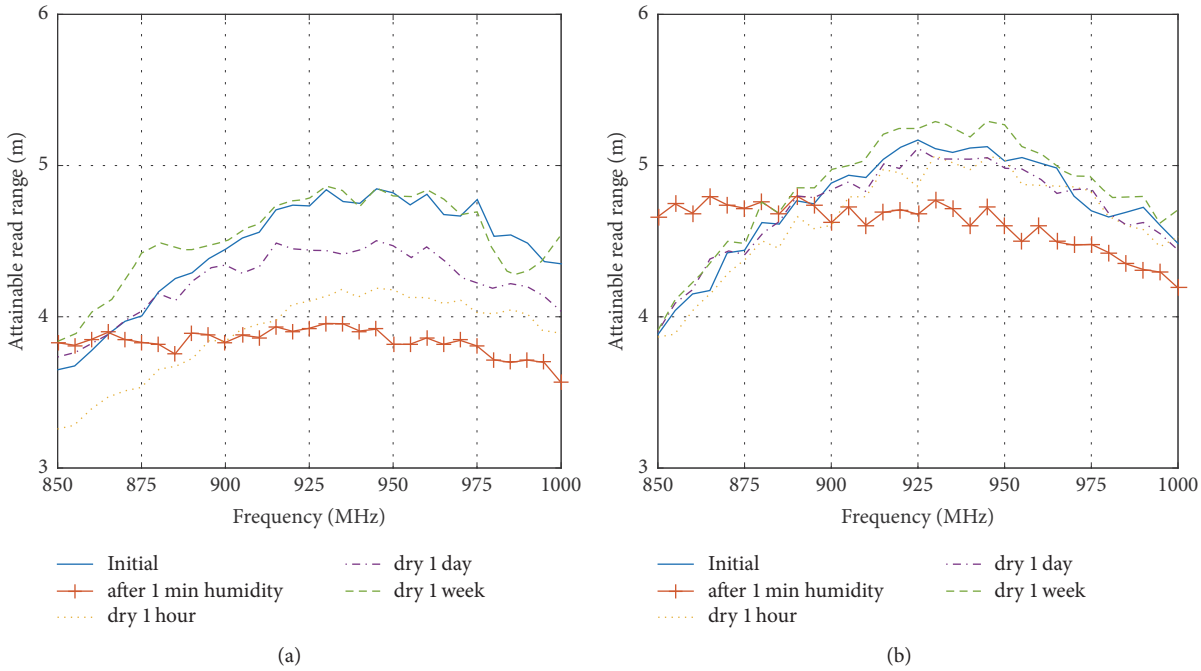

Figure 6: Read ranges of graphene RFID tags before and after high humidity conditions: (a) epoxy-glued IC attachment and (b) printed IC attachment.

the increased ohmic losses caused by the water, the read range in that frequency range increases due to the changed antenna impedance and power reflection from the antenna-IC interface. It should be noted that humidity can also have an effect on the fabric substrate. The moisture can affect the dielectric constant and loss tangent of the fabric, which can affect the wireless performance of the tags.

After drying for one hour in room conditions, the read ranges of both types of tags gradually increase back to normal. After 1 week, when the tags are totally dry, the performance of both types of tags has returned close to the initial performance. Thus, the harsh moisture test did not have a permanent effect on the performance of these tags.

5. Conclusions

In this paper, the possibility of applying 3D direct-write dispensing to form the antenna-IC connection together with the antenna was studied in order to simplify the manufacturing process of passive graphene UHF RFID tags on cotton fabric. The results were compared to tags fabricated with epoxy-glued ICs. Also, the effects of moisture on the tag performance were investigated. Based on our results, the tags with the 3D-printed antenna-IC interconnections showed excellent wireless performance and read ranges comparable to the tags with the epoxy-glued ICs. Moreover, moisture did not have a significant detrimental effect on either type of tags, and the slightly decreased performance returned back to normal when the tags were dry again. These findings support the use of 3D-printing in fabrication of graphene antennas and the use of the printed antenna-IC attachment method. However, more work needs to be done in order to draw more extensive conclusions.

Conflicts of Interest

The authors declare that there are no conflicts of interest regarding the publication of this paper and that the mentioned received funding in Acknowledgments did not lead to any conflicts of interest regarding the publication of this manuscript.

Acknowledgments

This research work was supported by the Jane and Aatos Erkko Foundation, Academy of Finland, and TEKES.

References

[1] X. Huang, T. Leng, X. Zhang et al., "Binder-free highly conductive graphene laminate for low cost printed radio frequency applications," *Applied Physics Letters*, vol. 106, no. 20, Article ID 203105, 2015.

[2] M. Akbari, J. Virkki, L. Sydanheimo, and L. Ukkonen, "Toward graphene-based passive UHF RFID textile tags: A Reliability Study," *IEEE Transactions on Device and Materials Reliability*, vol. 16, no. 3, pp. 429–431, 2016.

[3] T. Björninen, J. Virkki, L. Sydänheimo, and L. Ukkonen, "Possibilities of 3D direct write dispensing for textile UHF RFID tag manufacturing," in *Proceedings of the IEEE International Symposium on Antennas and Propagation & USNC/URSI National Radio Science Meeting*, pp. 1316-1317, Vancouver, BC, Canada, July 2015.

[4] C. Occhiuzzi, G. Contri, and G. Marrocco, "Reading range of wearable textile RFID tags in real configurations," in *Proceedings of the 5th European Conference on Antennas and Propagation (EUCAP '11)*, pp. 433–436, April 2011.

[5] R. Nayak, A. Singh, R. Padhye, and L. Wang, "RFID in textile and clothing manufacturing: technology and challenges," *Fashion and Textiles*, vol. 2, no. 1, 2015.

[6] D. Patron, W. Mongan, T. P. Kurzweg et al., "On the Use of Knitted Antennas and Inductively Coupled RFID Tags for Wearable Applications," *IEEE Transactions on Biomedical Circuits and Systems*, vol. 10, no. 6, pp. 1047–1057, 2016.

[7] L. Catarinucci, R. Colella, D. De Donno, and L. Tarricone, "Fully-passive devices for RFID smart sensing," in *Proceedings of the IEEE Antennas and Propagation Society International Symposium (APSURSI '13)*, pp. 2311-2312, IEEE, Orlando, Fla, USA, July 2013.

[8] M. Stoppa and A. Chiolerio, "Wearable electronics and smart textiles: a critical review," *Sensors*, vol. 14, no. 7, pp. 11957–11992, 2014.

[9] C. Hertleer, A. Van Laere, H. Rogier, and L. Van Langenhove, "Influence of relative humidity on textile antenna performance," *Textile Research Journal*, vol. 80, no. 2, pp. 177–183, 2010.

[10] R. Salvado, C. Loss, R. Gonçalves, and P. Pinho, "Textile materials for the design of wearable antennas: a survey," *Sensors*, vol. 12, no. 11, pp. 15841–15857, 2012.

[11] S. Goodfellow, "Screen printable functionalized graphene ink," 2017, http://www.goodfellowusa.com/news-article/screen-printable-functionalized-graphene-ink/.

[12] Nscrypt USA, "Smart Pump," 2017, http://www.nscrypt.com/wp-content/uploads/2017/02/2016-SmartPump-Gen2.pdf.

[13] J. Virtanen, J. Virkki, L. Ukkonen, and L. Sydänheimo, "Inkjet-printed UHF RFID tags on renewable materials," *Advances in Internet Things*, vol. 2, no. 4, pp. 79–85, 2012.

Publication VI

H. He, M. Akbari, L. Sydänheimo, L. Ukkonen, and J. Virkki, ‘‘3D-Printed Graphene and Stretchable Antennas for Wearable RFID Applications’’, in Proceedings of International Symposium on Antennas and Propagation, 30 Octorber-2 November 2017, Phuket, Thailand, pp. 1-2.

3D-Printed Graphene and Stretchable Antennas for Wearable RFID Applications

H. He, M. Akbari, L. Sydänheimo, L. Ukkonen, J. Virkki
BioMediTech Institute and Faculty of Biomedical Sciences and Engineering
Tampere University of Technology
Tampere, Finland

***Abstract*—This study presents the potentials of 3D printing in the utilization of passive RFID components on a cotton substrate. New types of 3D-printable conductive materials, graphene ink and stretchable silver conductor, are used in antenna fabrication. Our measurement results confirm that both types of wireless components reach high performance: the achievable read ranges of the graphene and stretchable tags are close to 5 and 11 meters, respectively. These results are well comparable to those of previously reported silver and copper textile RFID tags.**

Keywords—3D printing; graphene ink; RFID antennas; stretchable conductor, textiles; wearable electronics.

I. Introduction

Passive ultra high frequency (UHF) radio-frequency identification (RFID) components integrated into textiles, that are at the center of this study, offer versatile possibilities for wearable identification and sensing applications [1][2].

Metallic particles as the conductive antenna element bring high material costs. They also usually require high sintering temperatures or other sintering approaches [1][3]. An alternative could lie in carbon-based materials, such as graphene, which is an environmentally friendly and low-cost material [4][5]. In addition, in wearable applications, the antennas must be embedded as part of clothing, where they need to show high reliability in conditions of repeated mechanical stress. This leads to the task of realizing stretchable and bendable antennas [6].

In this paper, we present 3D-printed graphene and stretchable passive UHF RFID tags, and evaluate their wireless performance. The results are compared to those of previously published silver- and copper-based 3D-printed textile tags, as well as to previously reported graphene-based and stretchable RFID tags on textile materials.

II. Tag Fabrication

First, 3D direct-write dispensing was carried out to print graphene-based and stretchable antennas on a 100 % cotton fabric. HDPlas® IGSC02002, a water-based graphene ink, and a stretchable silver conductor, DuPont PE872, were selected as antenna materials.

The 3D printing was completed by nScrypt tabletop 3D direct-write dispensing system, and the main manufacturing parameters are defined in Table I. For each conductive ink, 3 antenna samples were fabricated, to also evaluate the reproducibility. After printing, the graphene-based tag antennas were cured at 60 °C for 30 min, while the stretchable antennas were cured at 110 °C for 15 min.

Finally, NXP UCODE G2iL series RFID ICs (integrated circuit), provided by the company in a strap, were attached to the antennas with silver epoxy (Circuit Works CW2400). Ready tags with their dimensions are shown in Fig. 1 and magnifications of 3D-printed antennas are presented in Fig. 2. As shown, both inks had good adherence to the fabric.

TABLE I. Main 3D Printing Parameters

3D printing parameters	
Material feed pressure	16.9 Psi
Printing spacing	125 microns
Printing angle	0°
Inner diameter of tip	125 microns

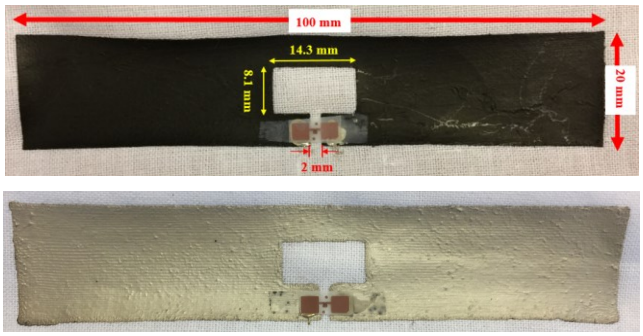

Fig. 1. Graphene (top) and stretchable (bottom) 3D-printed RFID tags.

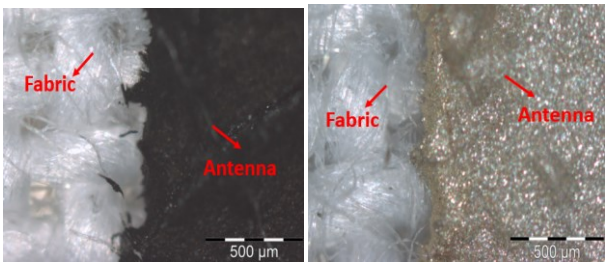

Fig. 2. Optical microscopic image of 3D-printed graphene ink (left) and stretchable conductor (right).

III. Measurements and Results

Voyantic Tagformance RFID measurement system was used to evaluate the fabricated components. The wireless channel from the reader antenna to the measurement location was firstly characterized with a reference tag. The theoretical read range is calculated based on the measured path loss and threshold power, and is based on the relationship given in (1).

$$d_{Tag} = \frac{\lambda}{4\pi}\sqrt{\frac{EIRP}{P_{TS}\,L_{fwd}}} \quad (1)$$

where λ is the wavelength transmitted from the reader antenna, P_{TS} and L_{fwd} are the measured threshold power and forward losses, correspondingly, and EIRP is the emission limit of an RFID reader, given as equivalent isotropic radiated power (3.28 W, which is the emission limit in European countries).

Fig. 3 shows the attainable read ranges of both types of fabricated tags. The peak read ranges of tags with graphene ink and stretchable conductor were 4.8 meters and 10.9 meters, respectively, which is in the range of many wearable identification and sensing applications. All three same type of tags showed similar wireless performance. The peak read ranges together with the corresponding measured thicknesses and sheet resistances are shown in Table II. Compared to the antennas fabricated from the stretchable conductor, the graphene antennas have a thicker conductive layer but higher sheet resistance.

The read range results of the graphene ink-based tags are superior to earlier published results using the same antenna design and the same antenna material [5], where the graphene antennas were utilized by doctor-blading on a cotton fabric substrate. These tags achieved read ranges of around 1.6-2 meters. The results of the stretchable ink tags are also superior to those of the same antenna and stretchable conductor [6], where tags fabricated by doctor-blading on a cotton substrate achieved maximum read ranges of around 9.5 meters. Thus, the antennas presented here, fabricated via 3D printing, show significantly superior performance compared to the earlier results.

The same tag design has been previously reported to be 3D-printed using silver and copper inks [1]. The achieved peak read ranges for the copper- and silver-based tags were around 6 and 11 meters, respectively. Therefore, in addition to the highly desired stretchability [6][7], the stretchable conductor material can offer comparable read ranges.

This work presents that 3D printing with graphene ink and stretchable conductor can be considered to be a solution for future cost- and time-effective textile antenna fabrication. We focused on evaluating the performance of the invented tags in air, without any environmental stresses or the effects of the closeness of the human body. The next step is to study the reliability of these wireless components in different environmental conditions. Especially the effects of humidity, together with bending and stretching, will be studied. The tags will also be tested attached to clothing, in order to study the effects of real body movements on the reliability of the clothing-integrated components.

TABLE II. Measured Antenna Properties

Used ink	Read range	Average thickness	Thickness standard deviation	Sheet resistance
Graphene	4.8 m	479.4 µm	23.8 µm	6.7 Ω/sq
Stretchable	10.9 m	402.7 µm	20.7 µm	0.2 Ω/sq

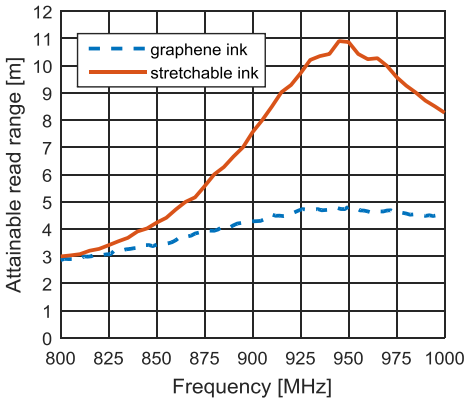

Fig. 3. Read ranges of graphene and stretchable tags.

IV. Conclusion

In this paper, we presented 3D-printed passive RFID tags on a cotton substrate, fabricated from graphene ink and stretchable silver conductor. Based on our measurements, the tags showed very good wireless performance, and achieved read ranges of 4.8 meters and 10.9 meters, respectively. By utilizing the direct-write dispensing manufacturing method, antennas can be produced efficiently and reliably, to a variety of different geometries. The next step is to study the reliability of the fabricated textile tags. Also tags designed to be used near the human body will be fabricated and their on-body reliability will be tested.

References

[1] T. Björninen, J. Virkki, L. Sydänheimo, and L. Ukkonen: 'Possibilities of 3D direct write dispensing for textile UHF RFID tag manufacturing', in IEEE APS/URSI, 2015.

[2] D. Patron, et al.: 'On the use of knitted antennas and inductively coupled RFID tags for wearable applications,' in IEEE Trans. Biomed. Circuits Syst., vol. 10, no. 6, pp. 1047-1057, 2016.

[3] G. Xiaohui, et al.: 'Flexible and wearable 2.45 GHz CPW-fed antenna using inkjet-printing of silver nanoparticles on pet substrate', in Microw Opt Technol Lett., vol. 59, no. 1, pp. 204-208, 2017.

[4] X. Huang, et al.; 'Binder-free highly conductive graphene laminate for low cost printed radio frequency applications', Appl. Phys. Lett., vol. 106, no. 20, 2015.

[5] M. Akbari, J. Virkki, L. Sydanheimo, and L. Ukkonen: 'Toward graphene-based passive UHF RFID textile tags: a reliability study,' IEEE Trans. Device Mater. Rel., pp. 429-431, 2016.

[6] J. Virkki, T. Björninen, M. Akbari, and L. Ukkonen: 'Strain reliability and substrate specific features of passive UHF RFID textile tag antennas', in IEEE ICECS, 2016.

[7] J. A. Rogers, T. Someya, Y. G. Huang 'Materials and mechanics for stretchable electronics,' Science, vol. 327, no. 5973, pp. 1603–1607, 2010.

Publication VII

H. He, X. Chen, L. Ukkonen, and J. Virkki, “Textile-Integrated Three-Dimensional Printed and Embroidered Structures for Wearable Wireless Platforms’’, Textile Research Journal, published online, doi: https://doi.org/10.1177/0040517517750649.

Textile-Integrated 3D-Printed and Embroidered Structures for Wearable Wireless Platforms

Abstract

In this paper, we present fabrication and performance evaluation of 3D-printed and embroidered textile-integrated passive ultra high frequency (UHF) radio frequency identification (RFID) platforms. The antennas were manufactured by 3D printing stretchable silver conductor directly on an elastic band. The electric and mechanical joint between the 3D-printed antennas and microchips was formed by gluing with conductive epoxy glue, by printing the antenna directly on top of the microchip structure, and by embroidering with conductive yarn. Initially, all types of fabricated RFID tags achieved read ranges of 8-9 meters. Next, the components were tested for wetting as well as for harsh cyclic strain and bending. The immersing and cyclic bending slightly effected the performance of the tags. However, they did not stop the tags from working in an acceptable way, nor did they have any permanent effect. The epoxy-glued or 3D-printed antenna-microchip interconnections were not able to endure harsh stretching. On the other hand, the tags with the embroidered antenna-microchip interconnections showed excellent wireless performance, both during and after a 100 strong stretching cycles. Thus, the novel approach of combining 3D printing and embroidery seems to be a promising way to fabricate textile-integrated wireless platforms.

Keywords

Antennas; embroidery; interconnections; passive UHF RFID; stretchable electronics; textile-integrated electronics; wearable platforms; 3D printing

Introduction

The growing interest towards wireless body area networks (WBAN), which will enable future body-centric wireless communication and sensing applications, has created a huge demand for textile-integrated electronics. The research and development work around WBAN technologies is currently very active [1-5].

One key technology in this interesting area is passive radio frequency identification (RFID) technology, which uses battery-free remotely addressable electronic tags, composed only of an antenna and a microchip [6][7]. The use of propagating electromagnetic waves in the ultra high frequency (UHF) frequency range for wirelessly powering and communicating with the passive tags enables rapid interrogation of a large number of tags. The communication with the tags is possible through various media, which means the components can e.g., be integrated into clothes. Thanks to the energy efficient mechanism of digitally modulated scattering utilized in the wireless communication between an RFID reader and tags, the data can be read from a distance of several meters. This makes the battery-free passive tags promising candidates as identification and sensing platforms as well as digital entities in future WBANs.

During actual use, these wearable wireless components have to endure many kinds on environmental stresses, such as harsh weather conditions and continuous washing [8]-[10]. Also mechanical stresses, including stretching and bending, are always involved in wearable

applications, and cause challenges for the design and manufacturing of wireless components [8][11][12]. One major reliability challenge lies in the electric and mechanical interconnections of wearable platforms [10][12].

3D direct-write dispensing is a fast and low-cost additive manufacturing method, which enables the printing of complex geometries with a high, micron resolution, accuracy. It has shown potential to be used for fabrication of conductors and antennas on textile substrates [13][14]. This 3D printing method has been recently proved to also be useful for fabrication of electric interconnections between microchips and antennas [14]. Embroidery is a simple but versatile fabrication method, with a great potential in conductor and antenna fabrication, when done using conductive yarn [5][12][15][16]. Further, embroidery has also been found to be a useful approach for embedding reliable electronic interconnections into textile materials [12][15][17]-[20]. In a word, these two techniques provide the foundation for integrating passive RFID platforms into textiles, which will be the focus of this study.

In this paper, we present the fabrication and wireless performance of textile-integrated stretchable passive UHF RFID tags, and evaluate their reliability in high moisture conditions, as well as during and after cycling bending and stretching. The tags have 3D-printed stretchable antennas, and antenna-microchip interconnections fabricated by three different ways: Firstly, by using previously commonly reported gluing with conductive silver epoxy; secondly, by utilizing a recently invented 3D-printed interconnection that is printed together with the antenna; and finally, by establishing a novel hybrid approach of 3D printing and embroidery, i.e., by sewing with conductive yarn on the printed antenna. In addition to the textile-integrated tag robustness, we evaluate the effects of the interconnection type on the tag performance and reliability.

3D printing of tag antennas

In this work, 3D direct-write dispensing was used to fabricate stretchable RFID tag antennas on a stretchable textile material, i.e., on an elastic band. A stretchable silver conductor (DuPont PE872) was selected as antenna material. The 3D printing was completed by nScrypt tabletop series 3D direct-write dispensing system; the main manufacturing parameters are defined in Table 1. The printing spacing and angle can be defined when designing the printed pattern, by a built-in software. The air pressure from a positive pressure pump is applied to the system, which pushes the ink into the main valve body, and finally through a ceramic nozzle tip. The printing system can produce a controllable ink flow, precise starts and stops, and the ability to utilize a wide range of material viscosities [21].

Table 1. 3D printing parameters.

Parameter	
Material feed pressure	16.9 Psi
Printing spacing	125 microns
Printing angle	0°
Inner diameter of tip	125 microns
Number of printed layers	1
Curing	110 °C, 15 minutes

Simple printed lines with dimension of 60 mm x 10 mm were studied first, instead of fully printed antennas, to understand the ink properties. Only one layer of ink was printed, and the lines were cured at 110 °C for 15 minutes. Fig. 1 presents the cross-section of the printed line, which shows the ink layer and the textile substrate. The conductive paste thickness measured from different parts is 555.4 µm, 529.8 µm, and 550.9 µm. Based on these three

values, the calculated average value of thickness is 545.3 µm. In addition, the ink is absorbed by the fabric substrate in some areas, which is also indicated in Fig. 1. Due to the absorption, the measured thickness in these parts is 801.3 µm.

The impact of stretching on the resistances of the printed lines was studied by stretching them from the initial length of 60 mm to 80 mm. The resistance measurements in this study were done using a Fluke 115 multimeter. The measurement probes were placed in the opposite corners of the printed lines, along longitudinal direction (60 mm).

The resistance results during strain are shown in Table 2. Then, as described in Table 3, the resistances of the printed lines were measured after 10, 20, 50, and 100 stretching cycles, where the lines were stretched from 60 mm to 80 mm and back. The frequency of the stretching cycles was 10 times / minute. The resistances were measured immediately after the stretching cycles.

The surface of a printed pattern before and during stretching is shown in Fig. 2. As can be seen, the ink layer had a good adherence to the fabric substrate before stretching. During stretching, there are some small cracks, which leads to the increase of the resistance, as presented Table 2. The increased resistances in Table 3, on the other hand, are caused by these small cracks not fully returning to their initial smooth structure immediately after strain.

Further, Table 4 shows the resistances of the lines measured immediately after the printed pattern was dipped in water for 1 minute and 10 minutes. It can be seen that wetting did not introduce any effect on the resistances of the printed patterns.

For both tests, immersing and stretching, two printed lines with the same dimension were utilized, to make sure the measurement were repeatable, and they had a similar performance in terms of resistance during the tests.

Next, the antenna design presented in Fig. 3. was printed on the stretchable textile, in order to utilize stretchable textile-integrated RFID components. The antenna is quite wide (2 cm), which reduces the impact of imperfections in the print outcome, and the length of the antenna (10 cm) is sufficient to avoid the weaknesses of electrically small antennas in the UHF frequencies from 800 MHz to 1000 MHz. Only one layer of ink was used, and also the antennas were cured at 110 °C for 15 minutes.

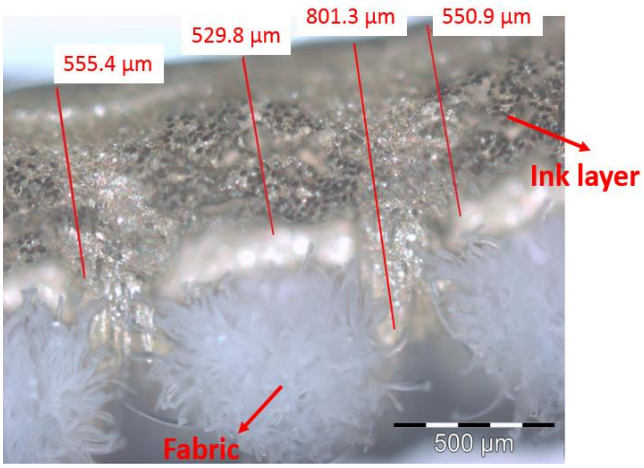

Fig. 1. Cross-section of a 3D-printed conductive line.

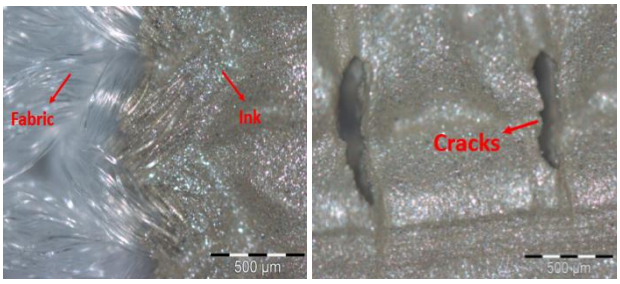

Fig. 2. Optical microscopic image of a 3D-printed line before stretching (left) and during stretching (right).

a (mm)	b (mm)	c (mm)	L (mm)	W (mm)
14.3	8.125	2	100	20

Fig. 3. A microchip strap (left) and the tag antenna structure (right).

Table 2. The resistance of the printed line during various strain positions.

Length (mm)	Resistance (Ω)
60 (initial)	0.7
70	9.2
80	21.5

Table 3. The resistance of the printed line after stretching cycles.

Stretching cycles	Resistance (Ω)
initial	0.7
10	2.3
20	5.5
50	22.4
100	66.7
After 1 week	1.9

Table 4. The resistance of the printed line in high humidity conditions.

Time in water (min)	Resistance (Ω)
initial	0.7
1	0.7
10	0.7

IC attachment methods

The used microchip, i.e., integrated circuit (IC) was NXP UCODE G2iL series RFID IC, provided by the manufacturer in a strap patterned from copper on a plastic film. The IC strap structure is shown in Fig. 3.

Three different methods were studied for the antenna-microchip interconnection: The first method was a commonly used way, where the IC is attached on top of the printed and cured antenna with conductive silver epoxy (Circuit Works CW2400). This method has been used, e.g., in [10][12][16]. It is proved that this epoxy glue shows good conductivity and establishes a well-working electric interconnection between antenna and IC. However, some challenges have been reported, such as reliability problems under mechanical stress and continuous washing [10][12].

In the second method, the antenna was deposited on top of the IC strap pads, and thus the antenna-IC interconnection was cured together with the antenna. Before printing, a reference point on the fabric substrate needs to be set using the built-in software of the 3D printer, in order to determine the position of the antenna. Then, IC strap is placed on the exact position on the substrate, and the antenna is printed on the substrate and on the IC strap copper pads. This recently invented 3D-printing approach skips one process step, and thus saves significant amounts of time and costs. This type of 3D-printed interconnection has showed suitable electric performance in recent studies, where graphene ink [14] and non-stretchable silver ink [13] have been used to fabricate RFID tags. However, no reliability evaluations have been reported.

In the third method, embroidery technique was utilized for attaching the IC on the printed antenna pattern. The IC strap copper pads were embroidered on the 3D-printed tag antenna using Husqvarna Viking embroidery machine and conductive yarn (Shieldex multifilament thread 110f34 dtex 2-ply HC). The DC linear resistivity of the thread is 500 ± 100 Ω/m, and the diameter is approximately 0.16 mm. We attached the IC strap copper pads to the 3D-printed antennas by embroidering a cross over them with conductive yarn, as shown in Fig 4. This type of attachment has been previously utilized with embroidered and electro-textile antennas [10][16].

To the best of our knowledge, this paper is the first presentation of combining embroidered and 3D-printed structures on textile-integrated RFID platforms.

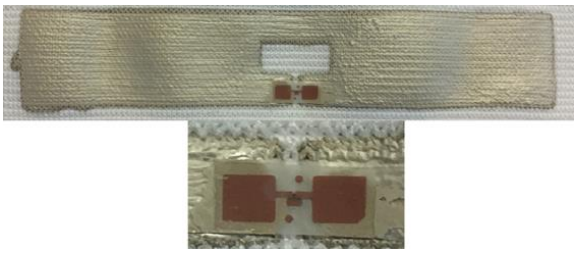

(a)

(b)

(c)

Fig. 4. Ready RFID tags and magnifications of the antenna-IC interconnections: (a) epoxy-glued joint, (b) 3D-printed joint, (c) embroidered joint.

For each tag type, two samples were fabricated to also evaluate the reproducibility. All three types of ready 3D-printed tags with different IC attachment methods and corresponding magnifications of the antenna-IC interconnections are shown in Fig. 4.

Wireless measurements

The tags were tested wirelessly using Voyantic Tagformance measurement system [22], which includes an RFID reader with an adjustable transmission frequency (0.8…1 GHz) and output power (up to 30 dBm), and provides the recording of the backscattered signal strength (down to −80 dBm) from the tag under test.

All the measurements were conducted with the tested tag suspended on a foam fixture in an anechoic chamber. The measurements were obtained from a fixed angle between the reader antenna and the tag, in order to achieve optimized performance and high read range. The angle was 0 degrees, which means the longer side of the antenna, where the IC was attached, was directly facing the reader antenna.

During the test, we recorded the lowest continuous-wave transmission power (threshold power: P_{th}) at which the tag remained responsive. Here we defined P_{th} as the lowest power at which a valid 16-bit random number from the tag is received as a response to the query command in ISO 18000-6C communication standard. In addition, the wireless channel from the reader antenna to the location of the tested tag was characterized using a system reference tag with known properties. As detailed in [23], this enabled the measurement device to estimate the attainable read range of the tag (d_{Tag}) from

$$d_{Tag} = \frac{\lambda}{4\pi}\sqrt{\frac{EIRP}{\Lambda}\frac{{P_{th}}^*}{P_{th}}},$$

where P_{th} is the measured threshold power of the tag, Λ is a known constant describing the sensitivity of the system reference tag, P_{th*} is the measured threshold power of the system reference tag, and EIRP is the emission limit of an RFID reader, given as equivalent isotropic radiated power. All results correspond to EIRP = 3.28 W, which is the emission limit in European countries.

Based on the calibration data provided by the manufacturer of the measurement system, we have estimated that the maximum variability in d_{Tag} due to variability in the system reference tag (Λ) and the output power meter of the reader (P_{th} and P_{th*}) is less than 5 % throughout the studied frequency range.

Measurement results

Fig. 5 shows the attainable read ranges of all types of fabricated tags. As can be seen, all these tags initially showed similar wireless performance and both "same type of tags" showed similar performance. The peak read ranges of the tags with epoxy-glued joint, 3D-printed joint, and embroidered joint were 8.8 meters, 9.6 meters, and 8.1 meters, respectively. These results are very promising when compared to earlier reported RFID tag results: The performance is similar or superior to 3D-printed silver and copper RFID tags, respectively [13], and significantly superior to 3D-printed graphene RFID tags [14] on textile substrates. Further, none of these previously reported 3D-printed RFID components has been stretchable.

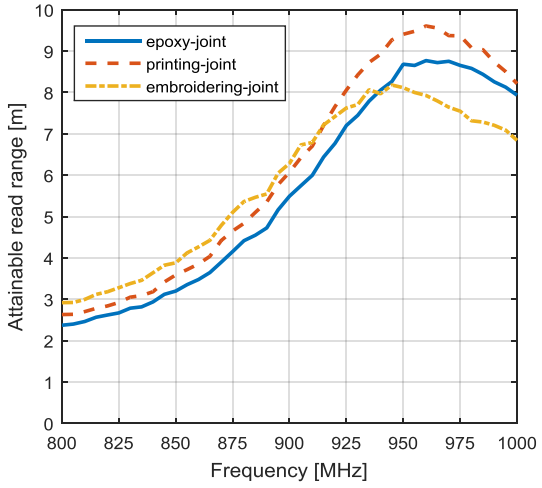

Fig. 5. Attainable read ranges of all types of stretchable tags in original state.

Next, three types of reliability evaluation tests, including an immersing test, a bending test, and a stretching test, were performed.

A. Immersing test

First, the effects of very high humidity and wetting on the tag performance were investigated. During the test, the tags were placed in tap water (pH = 6.5-7), as shown in Fig. 6, and wirelessly measured before the test and immediately after 1 minute in water. The tags were then left in room conditions to dry, and were measured again after 1 hour, and after 1 day. The wireless performance of the tags during and after the test are shown in Fig. 7.

Based on the measurement results, the read ranges of all types of tags decrease after 1 minute in water. The absorbed moisture affects the dielectric constant and loss tangent of the fabric substrate, which affects the performance of the antenna, as well as the antenna-IC impedance matching, and thus the wireless performance of the tags. After drying for one hour in room conditions, the read ranges of all types of tags have increased close to normal, but there is still a significant shift in the peak frequency range, caused by the absorbed moisture. After 1 day, when the tags are dry again, the wireless responses of all types of tags have returned to the initial performance. Thus, the harsh test did not have a permanent effect on the performance of these tags.

B. Bending test

In the bending test, the tags were bent over a 30 mm thick structure in Y-direction, as shown in Fig. 6. The wireless performance was measured at different steps: before bending, when bent, and in a non-bended state after up to 100 bending cycles. The frequency of the bending cycles was 10 times / minute. Fig. 8 shows the read ranges of all types of tags when testing the bending performance. As can be seen, the read ranges of all types of tags decrease about 2 meters during bending, but when measured in the non-bended state, the performance of these tags is stable even after a 100 times of bending.

C. Stretching test

In the stretching test, the performance of the tags was studied by stretching them from the initial length of 100 mm to 105 mm, 110 mm, and 115 mm. The stretching was done by attaching the tags to the foam structure with tape. The components were measured during each elongation. Based on the results, the tags with epoxy-glued IC attachment and 3D-printed IC attachment were not stretchable, since the antenna-IC interconnections of these tags were easily broken. See Fig. 9 for broken IC attachments. The attainable read ranges of the tags with embroidered antenna-IC interconnections under incremental strains from 0 % to 15 % are presented in Fig. 10 (a). In addition, Fig. 10 (b) shows the attainable read ranges in a non-stretched state after 20, 50, and 100 stretching cycles, where the tags were stretched from 100 mm to 115 mm each time. The frequency of the stretching cycles was 10 times / minute. After all stretching cycles, the tags recovered in room conditions for 5 days, and the performance was measured again.

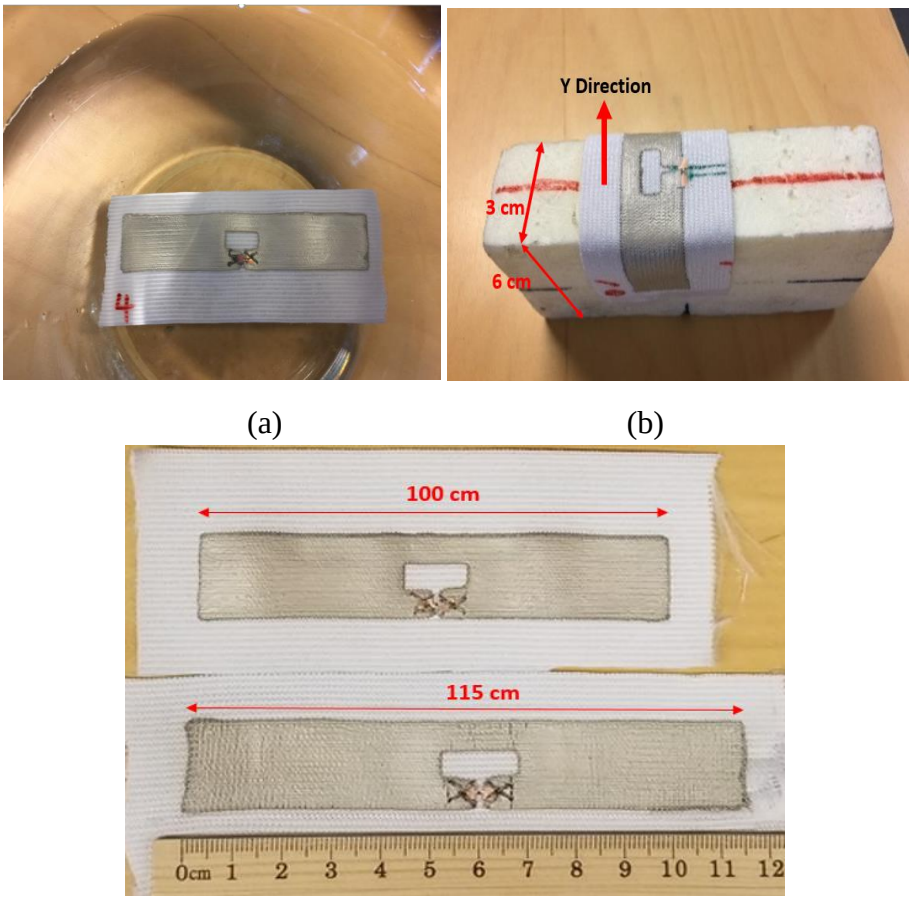

(a) (b)

(c)

Fig. 6. Reliability evaluations: (a) immersing test, (b) bending test, (c) stretching test.

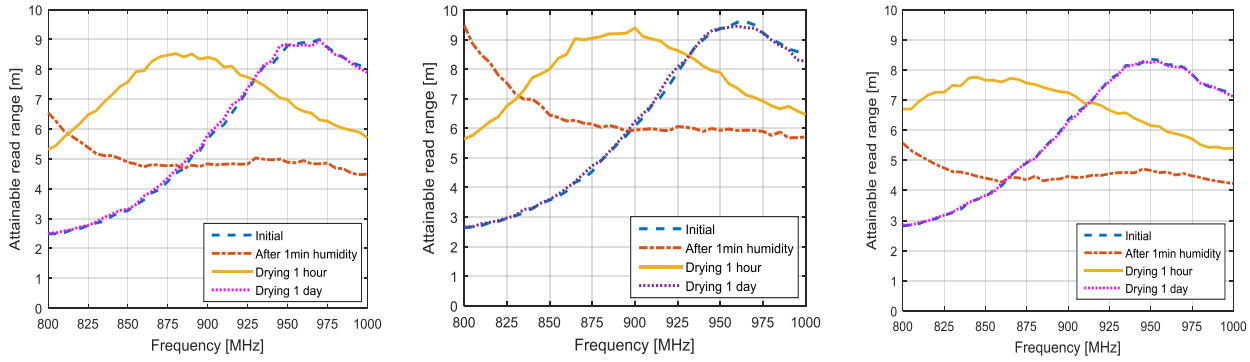

(a) (b) (c)

Fig. 7. Attainable read ranges of tags in the immersing reliability test: (a) tag with a glued antenna-IC joint, (b) tag with a 3D-printed antenna-IC joint, (c) tag with an embroidered antenna-IC joint.

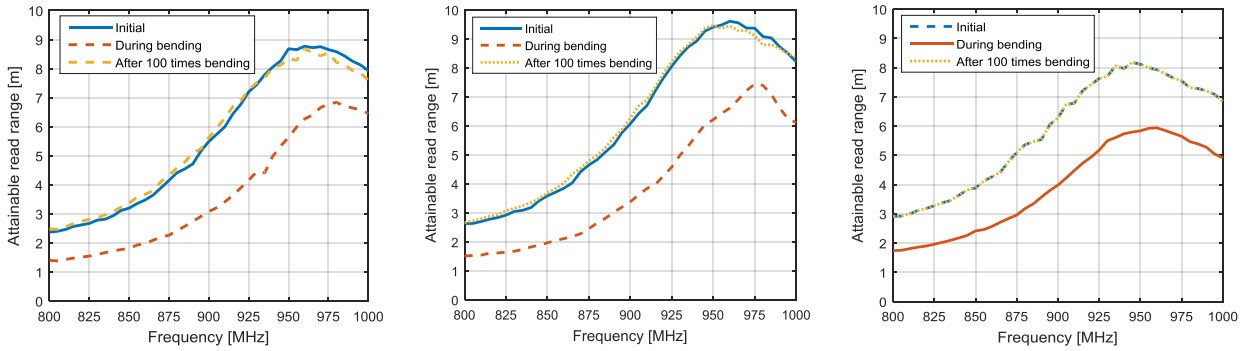

(a) (b) (c)

Fig. 8. Attainable read ranges of tags in bending reliability test: (a) tag with a glued antenna-IC joint, (b) tag with a 3D-printed antenna-IC joint, (c) tag with an embroidered antenna-IC joint.

The results in Fig. 10 (a) show that the tags with embroidered antenna-IC joints experienced a slight downward shift in the frequency of the peak read range when stretched increasingly. It is noticeable that the peak read range value was only slightly effected by the harsh strain, and the tags showed excellent read ranges of over 6 meters throughout the global UHF frequency band, even when stretched from 100 mm to 115 mm.

Moreover, as shown in Fig. 10 (b), after a 100 stretching cycles (stretched from 100 mm to 115 mm each time), the peak read range was still around 7 meters. It can be seen that the reduction in the performance of the non-stretched state tag also declined with the number of stretching cycles. After recovered 5 days in room conditions, the read range returned to 8 meters, which is only 0.8 meters less than the initial performance. It should also be noted a read range of 7 meters is still a very good result, especially since the tag is readable throughout the global UHF RFID band (860-960 MHz).

All the reliability evaluation tests and their results are summarized in Table 5.

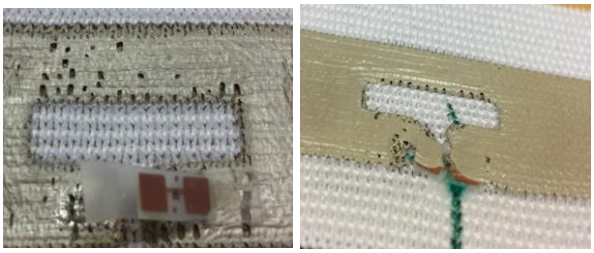

Fig. 9. Broken antenna-IC interconnections of epoxy-glued joint (left) and 3D-printed joint (right).

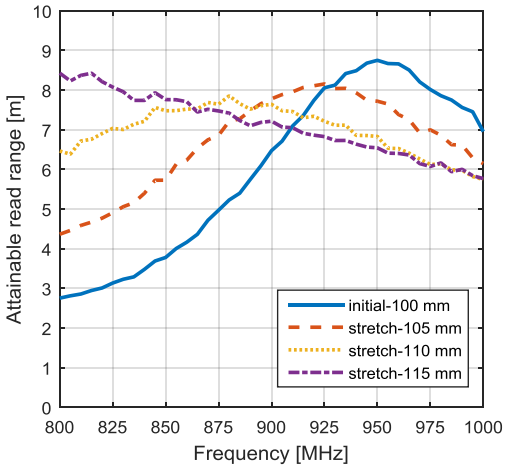

(a)

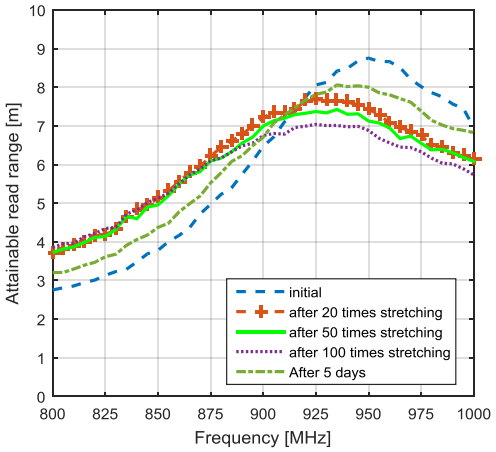

(b)

Fig. 10. Attainable read ranges of a tag with an embroidered antenna-IC joint: (a) during various elongations, (b) after multiple stretching cycles (stretched from 100 mm to 115 mm each time).

Table 5. Reliability evaluation results.

IC attachment method	Peak read range	Immersing test	Bending test	Stretching test
Epoxy-glued	8.8 m	good	good	fail
3D-printed	9.6 m	good	good	fail
Embroidered	8.2 m	good	good	good

Conclusions

In this paper, the possibility of 3D printing on a stretchable textile material using stretchable silver conductor was studied for RFID tag antenna fabrication. For microchip attachment, conductive epoxy glue, 3D printing, and embroidery were used, in order to find the most reliable methods to embed wireless platforms into textiles.

Initially, the tags with 3D-printed antenna-IC joints achieved the longest read ranges, which were around 0.8 meters and 1.6 meters better than the tags with epoxy-glued and embroidered joints, respectively.

Wetting and cyclic bending did not stop the tags from working in a suitable way, and they did not have any permanent effect on the tags' wireless performance. The results of the immersing test show the great potential of our wearable tags in a high humidity environment. These tags could work near a sweating body and even when dipped in water. Moreover, the bending test results indicate that the tags could be bended repeatedly while maintaining a stable performance, which is very important when integrating these platforms into clothing. The tags with embroidered antenna-IC attachment on a 3D-printed antenna showed the best reliability in continuous strain, as they were the only ones withstanding harsh stretching. Moving to stretchable antennas and interconnections will lead the way for practical integration of electronics into clothing. A combination of 3D printing and embroidery is a promising fabrication approach for solving the current reliability challenges in RFID antenna-IC interconnections and for taking the next steps in establishment of textile-integrated identification and sensing platforms. The next phase is to test the washing reliability of these fabricated tags, by combining mechanical stresses and moisture in a washing machine. This also means that suitable coating methods and materials need to be studied. In the future, we also plan to replace the stretchable silver conductor with a carbon-based stretchable conductor, which will offer a lower cost.

References

1. Van-Daele P, Moerman I and Demeester P. Wireless body area networks: status and opportunities. In: General Assembly and Scientific Symposium (URSI GASS), Beijing, China, 16-23 August 2014.
2. Zheng YL, Ding XR, Poon CCY, Lo BPL, Zhang H, Zhou XL and Zhang YT.

Unobtrusive sensing and wearable devices for health informatics. IEEE Trans. Biomed. Eng. 2014; 61.5: 1538–1554.
3. Kennedy T, Fink P, Chu A, Champagne N, Gregory Y, Lin G and Khayat M. Body-worn E-textile antennas: the good, the low-mass, and the conformal. IEEE Transactions on Antennas and Propagation 2009; 57.4: 910–918.
4. Manzari S, Occhiuzzi C and Marrocco G. Feasibility of body-centric systems using passive textile RFID tags. IEEE Antennas and Propagation Magazine 2012; 54.4: 49-62.
5. Kaufmann T, Fumeaux IM and Fumeaux C. Comparison of fabric and embroidered dipole antennas. In: European Conference on Antennas and Propagation, Gothenburg, Sweden, 8-12 April 2013, pp. 325–3255.
6. Want R. An introduction to RFID technology. IEEE Pervasive Computing 2006; 5: 25–33.
7. Dobkin D, The RF in RFID: passive UHF RFID in practice. Newnes-Elsevier, 2008.
8. Patron D, et al. On the use of knitted antennas and inductively coupled RFID tags for wearable applications. IEEE Trans. Biomed. Circuits Syst. 2016; 10.6: 1047-1057.
9. Nayak R, Singh A, Padhye R and Wang L, RFID in textile and clothing manufacturing: technology and challenges. Fashion and Textiles 2015; 2.1: 9.
10. Wang S, Chong N, Virkki J, Björninen T, Sydänheimo L and Ukkonen L. Towards washable electro-textile UHF RFID tags: reliability study of epoxy-coated copper fabric antennas. International Journal of Antennas and Propagation 2015.
11. Shao S, Kiourti A, Burkholder R, Volakis JL. Flexible and stretchable UHF RFID tag antennas for automotive tire sensing. In: Proc. Eur. Conf. Antennas Propag. (EuCAP), The Hague, Netherlands, 6-11 April 2014, pp. 2908-2910.
12. Chen X, Liu A, Wei Z, Ukkonen L and Virkki J. Experimental study on strain reliability of embroidered passive UHF RFID textile tag antennas and interconnections. Journal of Engineering 2017.
13. Björninen T, Virkki J, Sydänheimo L and Ukkonen L. Possibilities of 3D direct write dispensing for textile UHF RFID tag manufacturing. In: IEEE International Symposium on Antennas and Propagation & USNC/URSI National Radio Science Meeting, Vancouver, BC, Canada, 19-24 July 2015, IEEE, pp. 1316–1317.
14. He H, Akbari M, Sydänheimo L, Ukkonen L and Virkki J. 3D-Printed Graphene antennas and interconnections for textile RFID tags: fabrication and reliability towards humidity. International Journal of Antennas and Propagation 2017.
15. Ginestet G, Brechet N, Torres T, Moradi E, Ukkonen L, Bjorninen T and Virkki J. Embroidered antenna-microchip interconnections in passive UHF RFID textile tags, IEEE Antennas and Wireless Propagation Letters 2017; 16: 1205-1208.
16. Moradi E, Bjorninen T, Ukkonen L and Rahmat-Samii Y, Effects of sewing pattern on the performance of embroidered dipole-type RFID tag antennas, IEEE Antennas and Wireless Propagation Letters 2012; 11: 1482–1485.
17. Berglund ME, Duval J, Simon C and Dunne LE. Surface-mount component attachment for e-textiles. In: Proceedings of ACM International Symposium on Wearable Computers, Osaka, Japan, 7-11 September 2015, p. 65-66.
18. Post ER, Orth M, Russo PR and Gershenfeld N. E-broidery: design and fabrication of textile-based computing. IBM Syst. J. 2000; 39: 840–860.
19. Linz T, Kallmayer C, Aschenbrenner R and Reichl H. Embroidering electrical interconnects with conductive yarn for the integration of flexible electronic modules into fabric. In: Wearable Computers, Ninth IEEE International Symposium on, Osaka, Japan, 18-21 Octorber 2005, pp. 86-89.
20. Linz T, Vieroth R, Dils C, Koch M, Braun T, Becker KF, Kallmayer C and Hong SM. Embroidered interconnections and encapsulation for electronics in textiles for

wearable electronics applications. Adv. Sci. Technol. 2008; 60: 85–94.
21. Nscrypt USA, Smart Pump. http://www.nscrypt.com/wp-content/uploads/2017/02/2016-SmartPump-Gen2.pdf, accessed on Apr. 2017.
22. Voyantic Ltd. Tagformance. http://www.voyantic.com/tagformance, accessed on Apr. 2017.
23. Virkki J, Björninen T, Merilampi S, Sydänheimo L and Ukkonen L. The effects of recurrent stretching on the performance of electro-textile and screen-printed ultra-high-frequency radio-frequency identification tags. Text. Res. J. 2015; 85: 294–301.

Tampereen teknillinen yliopisto
PL 527
33101 Tampere

Tampere University of Technology
P.O.B. 527
FI-33101 Tampere, Finland

ISBN 978-952-15-4150-6
ISSN 1459-2045